

Fundamental Limits of Wideband Localization— Part I: A General Framework

Yuan Shen, *Student Member, IEEE*, and Moe Z. Win, *Fellow, IEEE*

Abstract—The availability of position information is of great importance in many commercial, public safety, and military applications. The coming years will see the emergence of location-aware networks with submeter accuracy, relying on accurate range measurements provided by wide bandwidth transmissions. In this two-part paper, we determine the fundamental limits of localization accuracy of wideband wireless networks in harsh multipath environments. We first develop a general framework to characterize the localization accuracy of a given node here and then extend our analysis to cooperative location-aware networks in Part II. In this paper, we characterize localization accuracy in terms of a performance measure called the squared position error bound (SPEB), and introduce the notion of equivalent Fisher information (EFI) to derive the SPEB in a succinct expression. This methodology provides insights into the essence of the localization problem by unifying localization information from individual anchors and that from *a priori* knowledge of the agent's position in a canonical form. Our analysis begins with the received waveforms themselves rather than utilizing only the signal metrics extracted from these waveforms, such as time-of-arrival and received signal strength. Hence, our framework exploits all the information inherent in the received waveforms, and the resulting SPEB serves as a fundamental limit of localization accuracy.

Index Terms—Cramér–Rao bound (CRB), equivalent Fisher information (EFI), information inequality, localization, ranging information (RI), squared position error bound (SPEB).

I. INTRODUCTION

LOCATION-AWARENESS plays a crucial role in many wireless network applications, such as localization services in next generation cellular networks [1], search-and-rescue operations [2], [3], logistics [4], and blue force tracking in battlefields [5]. The global positioning system (GPS) is the most important technology to provide location-awareness around the globe through a constellation of at least 24 satellites [6], [7]. However, the effectiveness of GPS is limited in harsh environments, such as in buildings, in urban

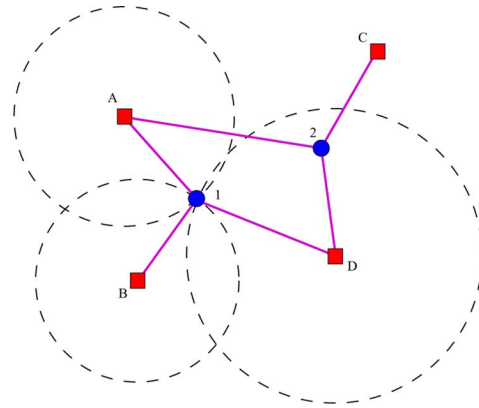


Fig. 1. Location-aware networks: the anchors (A, B, C, and D) communicate with the agents (1 and 2), and each edge denotes a connection link between anchor and agent.

canyons, under tree canopies, and in caves [8], [9], due to the inability of GPS signals to penetrate most obstacles. Hence, new localization techniques are required to meet the increasing need for accurate localization in such harsh environments [8], [9].

Wideband wireless networks are capable of providing accurate localization in GPS-denied environments [8]–[12]. Wide bandwidth or ultrawide bandwidth (UWB) signals are particularly well suited for localization, since they can provide accurate and reliable range (distance) measurements due to their fine delay resolution and robustness in harsh environments [13]–[20]. For more information about UWB, we refer the reader to [21]–[26].

Location-aware networks generally consist of two kinds of nodes: anchors and agents. Anchors have known positions (for example, through GPS or system design), while agents have unknown positions and attempt to determine their positions (see Fig. 1). Each node is equipped with a wideband transceiver, and localization is accomplished through the use of radio communications between agents and their neighboring anchors. Localizing an agent requires a number of signals transmitted from the anchors, and the relative position of the agent can be inferred from these received waveforms using a variety of signal metrics. Commonly used signal metrics include time-of-arrival (TOA) [8], [9], [17]–[20], [27]–[30], time-difference-of-arrival (TDOA) [31], [32], angle-of-arrival (AOA) [9], [33], and received signal strength (RSS) [9], [34], [35].

Time-based metrics, TOA and TDOA, are obtained by measuring the signal propagation time between nodes. In ideal scenarios, the estimated distance equals the product of the known propagation speed and the measured signal propagation time.

Manuscript received April 15, 2008; revised October 07, 2008. Date of current version September 15, 2010. This work was supported in part by the National Science Foundation under Grant ECCS-0901034, the Office of Naval Research Presidential Early Career Award for Scientists and Engineers (PECASE) N00014-09-1-0435, and the MIT Institute for Soldier Nanotechnologies. The material in this paper was presented in part at the IEEE Wireless Communications and Networking Conference, Hong Kong, March 2007.

The authors are with the Laboratory for Information and Decision Systems (LIDS), Massachusetts Institute of Technology, Cambridge, MA 02139 USA (e-mail: shenyuan@mit.edu; moewin@mit.edu).

Communicated by H. Boche, Associate Editor for Communications.

Color versions of one or more of the figures in this paper are available online at <http://ieeexplore.ieee.org>.

Digital Object Identifier 10.1109/TIT.2010.2060110

The TOA metric gives possible positions of an agent on a circle with the anchor at the center, and it can be obtained by either the one-way time-of-flight of a signal in a synchronized network [18], [19], [28], [29], or the round-trip time-of-flight in a nonsynchronized network [26], [36]. Alternatively, the TDOA metric provides possible positions of an agent on the hyperbola determined by the difference in the TOAs from two anchors located at the foci. Note that TDOA techniques require synchronization among anchors but not necessarily with the agent.

Another signal metric is AOA, the angle at which a signal arrives at the agent. The AOA metric can be obtained using an array of antennas, based on the signals' TOAs at different antennas.¹ The use of AOA for localization has been investigated, and many hybrid systems have been proposed, including hybrid TOA/AOA systems [30], [41], and hybrid TDOA/AOA systems [42]. However, some of these studies employ narrowband signal models, which are not applicable for wideband antenna arrays. Others are restricted to far-field scenarios or use far-field assumptions.

RSS is also a useful metric for estimating the propagation distance between nodes [9], [34], [36]. This metric can be measured during the data communications using low-complexity circuits. Although widely implemented, RSS has limited accuracy due to the difficulty in precisely modeling the relationship between the RSS and the propagation distance [4], [9].

Note that the signal metrics extracted from the received waveforms may discard relevant information for localization. Moreover, models for the signal metrics depend heavily on the specific measurement processes.² Therefore, in deriving the fundamental limits of localization accuracy, it is necessary to utilize the received waveforms rather than the signal metrics extracted from the waveforms [28], [29], [46], [47].

Since the received waveforms are affected by random phenomena such as noise, fading, shadowing, multipath, and nonline-of-sight (NLOS) propagations [48], [49], the agents' position estimates are subject to uncertainty. The Cramér–Rao bound (CRB) sets a lower bound on the variance of estimates for deterministic parameters [50], [51], and it has been used as a performance measure for localization accuracy [52]. However, relatively few studies have investigated the effect of multipath and NLOS propagations on localization accuracy. Multipath refers to a propagation phenomenon in which a transmitted signal reaches the receive antenna via multiple paths. The superposition of these arriving paths results in fading and interference. NLOS propagations, created by physical obstructions in the direct path, produce a positive bias in the propagation time and decrease the strength of the received signal, which can severely degrade the localization accuracy. Several types of methods have been proposed to deal with NLOS propagations: 1) treat NLOS biases as additive noise

¹The AOA metric can be obtained in two ways, directly through measurement by a directional antenna, or indirectly through TOA measurements using an antenna array [37]–[40]. Wideband directional antennas that satisfy size and cost requirements are difficult to implement, since they are required to perform across a large bandwidth [36]. As such, antenna arrays are more commonly used when angle measurement for wide bandwidth signals is necessary.

²For instance, the error of the TOA metric is commonly modeled as an additive Gaussian random variable [8], [30], [43]. This model contradicts the studies in [18]–[20], [44], and [45], and the experimental results in [8] and [16].

injected in the true propagation distances [8], [53], [54]³; 2) identify and weigh the importance of NLOS signals for localization [55]–[60]; or 3) consider NLOS biases as parameters to be estimated [27]–[30], [46], [47], [61], [62]. The authors in [8], [9], [28], and [29] showed that NLOS signals do not improve localization accuracy unless *a priori* knowledge of the NLOS biases is available, but their results were restricted to specific models or approximations. Moreover, detailed effects of multipath propagations on localization accuracy remains underexplored.

In this paper, we develop a general framework to determine the localization accuracy of wideband wireless networks.⁴ Our analysis begins with the received waveforms themselves rather than utilizing only signal metrics extracted from the waveforms, such as TOA, TDOA, AOA, and RSS. The main contributions of this paper are as follows.

- We derive the fundamental limits of localization accuracy for wideband wireless networks, in terms of a performance measure called the squared position error bound (SPEB), in the presence of multipath and NLOS propagation.
- We propose the notion of equivalent Fisher information (EFI) to derive the agent's localization information. This approach unifies such information from different anchors in a canonical form as a weighed sum of the direction matrix associated with individual anchors with the weights characterizing the information intensity.
- We quantify the contribution of the *a priori* knowledge of the channel parameters and agent's position to the agent's localization information, and show that NLOS components can be beneficial when *a priori* channel knowledge is available.
- We derive the performance limits for localization systems employing wideband antenna arrays. The AOA metrics obtained from antenna arrays are shown not to further improve the localization accuracy beyond that provided by TOA metric alone.
- We quantify the effect of clock asynchronism between anchors and agents on localization accuracy for networks where nodes employ a single antenna or an array of antennas.

The rest of the paper is organized as follows. Section II presents the system model, the notion of the SPEB, and the Fisher information matrix (FIM) for the SPEB. In Section III, we introduce the notion of EFI and show how it can help the derivation of the SPEB. In Section IV, we investigate the performance of localization systems employing wideband antenna arrays. Section V investigates the effect of clock asynchronism between anchors and agents. Discussions are provided in Section VI. Finally, numerical illustrations are given in Section VII, and conclusions are drawn in the last section.

Notations: The notation $\mathbb{E}_{\mathbf{z}}\{\cdot\}$ is the expectation operator with respect to the random vector \mathbf{z} ; $\mathbf{A} \succeq \mathbf{B}$ denotes that the

³In practice, however, an NLOS induced range bias can be as much as a few kilometers depending on the propagation environment [48], [55], and small perturbation may not compensate for NLOS induced error.

⁴In Part II [63], we extend our analysis to cooperative location-aware networks.

matrix $\mathbf{A} - \mathbf{B}$ is positive semidefinite; $\text{tr}\{\cdot\}$ is the trace of a square matrix; $[\cdot]_{n \times n}$ denotes the upper left $n \times n$ submatrix of its argument; $[\cdot]_{n,m}$ is the element at the n th row and m th column of its argument; $\|\cdot\|$ is the Euclidean norm of its argument; and the superscripts $[\cdot]^T$ represents the transpose of its argument. We denote by $f(\mathbf{x})$ the probability density function (pdf) $f_{\mathbf{X}}(\mathbf{x})$ of the random vector \mathbf{X} unless specified otherwise, and we also use in the paper the following function for the FIM:

$$\mathbf{F}_{\mathbf{z}}(\mathbf{w}; \mathbf{x}, \mathbf{y}) \triangleq \mathbb{E}_{\mathbf{z}} \left\{ \left[\frac{\partial}{\partial \mathbf{x}} \ln f(\mathbf{w}) \right] \left[\frac{\partial}{\partial \mathbf{y}} \ln f(\mathbf{w}) \right]^T \right\}$$

where \mathbf{w} can be either a vector or a symbol.⁵

II. SYSTEM MODEL

In this section, we describe the wideband channel model [14], [21], [24], [26], [64], formulate the problem, and briefly review the information inequality and Fisher information. We also introduce the SPEB, which is a fundamental limit of localization accuracy.

A. Signal Model

Consider a wireless network consisting of N_b anchors and multiple agents. Anchors have perfect knowledge of their positions, and each agent attempts to estimate its position based on the received waveforms from neighboring anchors (see Fig. 1).⁶ Wideband signals traveling from anchors to agents are subject to multipath propagation.

Let $\mathbf{p} \in \mathbb{R}^2$ denote the position of the agent,⁷ which is to be estimated. The set of anchors is denoted by $\mathcal{N}_b = \{1, 2, \dots, N_b\} \triangleq \mathcal{N}_L \cup \mathcal{N}_{NL}$, where \mathcal{N}_L denotes the set of anchors that provide line-of-sight (LOS) signals to the agent and \mathcal{N}_{NL} denotes the set of remaining anchors that provide NLOS signals to the agent. The position of anchor j is known and denoted by $\mathbf{p}_j \in \mathbb{R}^2 (j \in \mathcal{N}_b)$. Let ϕ_j denote the angle from anchor j to the agent, i.e.,

$$\phi_j = \tan^{-1} \frac{y - y_j}{x - x_j}$$

where $\mathbf{p} \triangleq [x \ y]^T$ and $\mathbf{p}_j \triangleq [x_j \ y_j]^T$.

The received waveform at the agent from anchor j can be written as

$$r_j(t) = \sum_{l=1}^{L_j} \alpha_j^{(l)} s(t - \tau_j^{(l)}) + z_j(t), \quad t \in [0, T_{\text{ob}}] \quad (1)$$

where $s(t)$ is a known wideband waveform whose Fourier transform is denoted by $S(f)$, $\alpha_j^{(l)}$ and $\tau_j^{(l)}$ are the amplitude and delay, respectively, of the l th path, L_j is the number of multipath components (MPCs), $z_j(t)$ represents the observation noise modeled as additive white Gaussian processes

⁵For example, \mathbf{w} is replaced by symbol $\mathbf{r}|\boldsymbol{\theta}$ in the case that $f(\cdot)$ is a conditional pdf of \mathbf{r} given $\boldsymbol{\theta}$.

⁶Agents estimate their positions independently, and hence without loss of generality, our analysis focuses on one agent.

⁷We first focus on 2-D cases and then extend the results to 3-D cases where $\mathbf{p} \in \mathbb{R}^3$.

with two-side power spectral density $N_0/2$, and $[0, T_{\text{ob}}]$ is the observation interval. The relationship between the agent's position and the delays of the propagation paths is

$$\tau_j^{(l)} = \frac{1}{c} \left[\|\mathbf{p} - \mathbf{p}_j\| + b_j^{(l)} \right] \quad (2)$$

where c is the propagation speed of the signal, and $b_j^{(l)} \geq 0$ is a range bias. The range bias $b_j^{(1)} = 0$ for LOS propagation, whereas $b_j^{(l)} > 0$ for NLOS propagation.⁸

B. Error Bounds on Position Estimation

Our analysis is based on the received waveforms given by (1), and hence the parameter vector $\boldsymbol{\theta}$ includes the agent's position and the nuisance multipath parameters [9], [62], i.e.,

$$\boldsymbol{\theta} = [\mathbf{p}^T \ \boldsymbol{\kappa}_1^T \ \boldsymbol{\kappa}_2^T \ \dots \ \boldsymbol{\kappa}_{N_b}^T]^T$$

where $\boldsymbol{\kappa}_j$ is the vector of the multipath parameters associated with $r_j(t)$, given by

$$\boldsymbol{\kappa}_j = \begin{cases} [\alpha_j^{(1)} \ b_j^{(2)} \ \alpha_j^{(2)} \ \dots \ b_j^{(L_j)} \ \alpha_j^{(L_j)}]^T, & j \in \mathcal{N}_L \\ [b_j^{(1)} \ \alpha_j^{(1)} \ b_j^{(2)} \ \alpha_j^{(2)} \ \dots \ b_j^{(L_j)} \ \alpha_j^{(L_j)}]^T, & j \in \mathcal{N}_{NL}. \end{cases}$$

Note that $b_j^{(1)} = 0$ for $j \in \mathcal{N}_L$ and is excluded from $\boldsymbol{\kappa}_j$.

We introduce \mathbf{r} as the vector representation of all the received waveforms $r_j(t)$, given by

$$\mathbf{r} = [\mathbf{r}_1^T \ \mathbf{r}_2^T \ \dots \ \mathbf{r}_{N_b}^T]^T$$

where \mathbf{r}_j is obtained from the Karhunen–Loeve expansion of $r_j(t)$ [50], [51]. Let $\hat{\boldsymbol{\theta}}$ denote an estimate of the parameter vector $\boldsymbol{\theta}$ based on observation \mathbf{r} . The mean squared error (MSE) matrix of $\hat{\boldsymbol{\theta}}$ satisfies the information inequality [50], [51], [65]

$$\mathbb{E}_{\mathbf{r}, \boldsymbol{\theta}} \{ (\hat{\boldsymbol{\theta}} - \boldsymbol{\theta})(\hat{\boldsymbol{\theta}} - \boldsymbol{\theta})^T \} \succeq \mathbf{J}_{\boldsymbol{\theta}}^{-1} \quad (3)$$

where $\mathbf{J}_{\boldsymbol{\theta}}$ is the FIM for the parameter vector $\boldsymbol{\theta}$.⁹ Let $\hat{\mathbf{p}}$ be an estimate of the agent's position, and it follows from (3) that¹⁰

$$\mathbb{E}_{\mathbf{r}, \boldsymbol{\theta}} \{ (\hat{\mathbf{p}} - \mathbf{p})(\hat{\mathbf{p}} - \mathbf{p})^T \} \succeq [\mathbf{J}_{\boldsymbol{\theta}}^{-1}]_{2 \times 2}$$

and hence

$$\mathbb{E}_{\mathbf{r}, \boldsymbol{\theta}} \{ \|\hat{\mathbf{p}} - \mathbf{p}\|^2 \} \geq \text{tr} \left\{ [\mathbf{J}_{\boldsymbol{\theta}}^{-1}]_{2 \times 2} \right\}. \quad (4)$$

⁸LOS propagation does not introduce a range bias because there is an unblocked direct path. NLOS propagation introduces a positive range bias because such signals either reflect off objects or penetrate through obstacles. In this paper, received signals whose first path undergoes LOS propagation are referred to as LOS signals, otherwise these signals are referred to as NLOS signals.

⁹When a subset of parameters is random, $\mathbf{J}_{\boldsymbol{\theta}}$ is called the Bayesian information matrix. Inequality (3) also holds under some regularity conditions and provides lower bound on the MSE matrix of any unbiased estimates of the deterministic parameters and any estimates of the random parameters [50], [65]. With a slight abuse of notation, $\mathbb{E}_{\mathbf{r}, \boldsymbol{\theta}} \{ \cdot \}$ will be used for deterministic, hybrid, and Bayesian cases with the understanding that the expectation operation is not performed over the deterministic components of $\boldsymbol{\theta}$.

¹⁰Note that for 3-D localization, we need to consider a 3×3 matrix $[\mathbf{J}_{\boldsymbol{\theta}}^{-1}]_{3 \times 3}$.

Therefore, we define the right-hand side of (4) as a measure to characterize the limits of localization accuracy as follows.

Definition 1 (SPEB): The SPEB is defined to be

$$\mathcal{P}(\mathbf{p}) \triangleq \text{tr} \left\{ [\mathbf{J}_\theta^{-1}]_{2 \times 2} \right\}.$$

C. Fisher Information Matrix

In this section, we derive the FIM for both deterministic and random parameter estimation to evaluate the SPEB.

1) *FIM Without a Priori Knowledge:* The FIM for the deterministic parameter vector $\boldsymbol{\theta}$ is given by [50]

$$\mathbf{J}_\theta = \mathbf{F}_r(\mathbf{r}|\boldsymbol{\theta}; \boldsymbol{\theta}) \quad (5)$$

where $f(\mathbf{r}|\boldsymbol{\theta})$ is the likelihood ratio of the random vector \mathbf{r} conditioned on $\boldsymbol{\theta}$. Since the received waveforms from different anchors are independent, the likelihood ratio can be written as [51]

$$f(\mathbf{r}|\boldsymbol{\theta}) = \prod_{j \in \mathcal{N}_b} f(\mathbf{r}_j|\boldsymbol{\theta}) \quad (6)$$

where

$$f(\mathbf{r}_j|\boldsymbol{\theta}) \propto \exp \left\{ \frac{2}{N_0} \int_0^{T_{\text{ob}}} r_j(t) \sum_{l=1}^{L_j} \alpha_j^{(l)} s(t - \tau_j^{(l)}) dt - \frac{1}{N_0} \int_0^{T_{\text{ob}}} \left[\sum_{l=1}^{L_j} \alpha_j^{(l)} s(t - \tau_j^{(l)}) \right]^2 dt \right\}.$$

Substituting (6) in (5), we have the FIM \mathbf{J}_θ as

$$\mathbf{J}_\theta = \frac{1}{c^2} \begin{bmatrix} \mathbf{T}_L \mathbf{\Lambda}_L \mathbf{T}_L^T + \mathbf{T}_{NL} \mathbf{\Lambda}_{NL} \mathbf{T}_{NL}^T & \mathbf{T}_{NL} \mathbf{\Lambda}_{NL} \\ \mathbf{\Lambda}_{NL} \mathbf{T}_{NL}^T & \mathbf{\Lambda}_{NL} \end{bmatrix} \quad (7)$$

where $\mathbf{\Lambda}_L$, \mathbf{T}_L , $\mathbf{\Lambda}_{NL}$, and \mathbf{T}_{NL} are given by (41) and (42). In the above matrices, $\mathbf{\Lambda}_L$ and \mathbf{T}_L are related to the LOS signals, and $\mathbf{\Lambda}_{NL}$ and \mathbf{T}_{NL} are related to the NLOS signals.

2) *FIM With a Priori Knowledge:* We now incorporate the *a priori* knowledge of the agent's position and channel parameters for localization. Since the multipath parameters $\boldsymbol{\kappa}_j$ are independent *a priori*, the pdf of $\boldsymbol{\theta}$ can be expressed as¹¹

$$f(\boldsymbol{\theta}) = f(\mathbf{p}) \prod_{j \in \mathcal{N}_b} f(\boldsymbol{\kappa}_j|\mathbf{p}) \quad (8)$$

where $f(\mathbf{p})$ is the pdf of the agent's position, and $f(\boldsymbol{\kappa}_j|\mathbf{p})$ is the joint pdf of the multipath parameter vector $\boldsymbol{\kappa}_j$ conditioned on the agent's position. Based on the models of wideband channels [36], [40], [64] and UWB channels [14], [21], [24], [26], [36], we derive $f(\boldsymbol{\kappa}_j|\mathbf{p})$ in (52) in Appendix II and show that

$$f(\boldsymbol{\kappa}_j|\mathbf{p}) = f(\boldsymbol{\kappa}_j|d_j) \quad (9)$$

where $d_j = \|\mathbf{p} - \mathbf{p}_j\|$.

The joint pdf of observation and parameters can be written as

$$f(\mathbf{r}, \boldsymbol{\theta}) = f(\mathbf{r}|\boldsymbol{\theta})f(\boldsymbol{\theta})$$

¹¹When a subset of parameters are deterministic, they are eliminated from $f(\boldsymbol{\theta})$.

where $f(\mathbf{r}|\boldsymbol{\theta})$ is given by (6), and hence the FIM becomes

$$\mathbf{J}_\theta = \mathbf{J}_w + \mathbf{J}_p \quad (10)$$

where $\mathbf{J}_w \triangleq \mathbf{F}_{r,\boldsymbol{\theta}}(\mathbf{r}|\boldsymbol{\theta}; \boldsymbol{\theta})$ and $\mathbf{J}_p \triangleq \mathbf{F}_\theta(\boldsymbol{\theta}; \boldsymbol{\theta}, \boldsymbol{\theta})$ are the FIMs from the observations and the *a priori* knowledge, respectively.¹² The FIM \mathbf{J}_w can be obtained by taking the expectation of \mathbf{J}_θ in (7) over the random parameter vector $\boldsymbol{\theta}$, and \mathbf{J}_p can be obtained by substituting (8) in (10) as

$$\mathbf{J}_p = \begin{bmatrix} \Xi_p + \sum_{j \in \mathcal{N}_b} \Xi_{p,p}^j & \Xi_{p,\boldsymbol{\kappa}}^1 & \cdots & \Xi_{p,\boldsymbol{\kappa}}^{N_b} \\ \left[\Xi_{p,\boldsymbol{\kappa}}^1 \right]^T & \Xi_{\boldsymbol{\kappa},\boldsymbol{\kappa}}^1 & & \mathbf{0} \\ \vdots & & \ddots & \\ \left[\Xi_{p,\boldsymbol{\kappa}}^{N_b} \right]^T & \mathbf{0} & & \Xi_{\boldsymbol{\kappa},\boldsymbol{\kappa}}^{N_b} \end{bmatrix} \quad (11)$$

where Ξ_p describes the FIM from the *a priori* knowledge of \mathbf{p} , given by

$$\Xi_p = \mathbf{F}_\theta(\mathbf{p}; \mathbf{p}, \mathbf{p})$$

and $\Xi_{\boldsymbol{\kappa},\boldsymbol{\kappa}}^j = \mathbf{F}_\theta(\boldsymbol{\kappa}_j|\mathbf{p}; \boldsymbol{\kappa}_j, \boldsymbol{\kappa}_j)$, $\Xi_{p,p}^j = \mathbf{F}_\theta(\boldsymbol{\kappa}_j|\mathbf{p}; \mathbf{p}, \mathbf{p})$, and $\Xi_{p,\boldsymbol{\kappa}}^j = \mathbf{F}_\theta(\boldsymbol{\kappa}_j|\mathbf{p}; \mathbf{p}, \boldsymbol{\kappa}_j)$ characterize the joint *a priori* knowledge of \mathbf{p} and $\boldsymbol{\kappa}_j$.

D. Equivalent Fisher Information Matrix

Determining the SPEB requires inverting the FIM \mathbf{J}_θ in (7) and (10). However, \mathbf{J}_θ is a matrix of high dimensions, while only a small submatrix $[\mathbf{J}_\theta^{-1}]_{2 \times 2}$ is of interest. To circumvent direction matrix inversion and gain insights into the localization problem, we first introduce the notions of EFI [46], [47].

Definition 2 (Equivalent Fisher Information Matrix): Given a parameter $\boldsymbol{\theta} = [\boldsymbol{\theta}_1^T \ \boldsymbol{\theta}_2^T]^T$ and the FIM \mathbf{J}_θ of the form

$$\mathbf{J}_\theta = \begin{bmatrix} \mathbf{A} & \mathbf{B} \\ \mathbf{B}^T & \mathbf{C} \end{bmatrix} \quad (12)$$

where $\boldsymbol{\theta} \in \mathbb{R}^N$, $\boldsymbol{\theta}_1 \in \mathbb{R}^n$, $\mathbf{A} \in \mathbb{R}^{n \times n}$, $\mathbf{B} \in \mathbb{R}^{n \times (N-n)}$, and $\mathbf{C} \in \mathbb{R}^{(N-n) \times (N-n)}$ with $n < N$, the equivalent Fisher information matrix (EFIM) for $\boldsymbol{\theta}_1$ is given by¹³

$$\mathbf{J}_e(\boldsymbol{\theta}_1) \triangleq \mathbf{A} - \mathbf{B}\mathbf{C}^{-1}\mathbf{B}^T. \quad (13)$$

Note that the EFIM retains all the necessary information to derive the information inequality for the parameter vector $\boldsymbol{\theta}_1$, since $[\mathbf{J}_\theta^{-1}]_{n \times n} = \mathbf{J}_e^{-1}(\boldsymbol{\theta}_1)$,¹⁴ and the MSE matrix of the estimates for $\boldsymbol{\theta}_1$ is bounded below by $\mathbf{J}_e^{-1}(\boldsymbol{\theta}_1)$. For 2-D localization ($n = 2$), we aim to reduce the dimension of the original FIM to the 2×2 EFIM.

¹²Note that \mathbf{J}_θ in (10) requires averaging over the random parameters, and hence does not depend on any particular value of $\boldsymbol{\theta}$. In contrast, \mathbf{J}_θ in (5) is a function of a particular value of the deterministic parameter vector $\boldsymbol{\theta}$.

¹³Note that $\mathbf{J}_e(\boldsymbol{\theta}_1)$ does not depend on any particular value of $\boldsymbol{\theta}_1$ for a random parameter vector $\boldsymbol{\theta}_1$, whereas it is a function of $\boldsymbol{\theta}_1$ for a deterministic parameter vector $\boldsymbol{\theta}_1$.

¹⁴The right-hand side of (13) is known as the Schur complement of the matrix \mathbf{C} [66].

III. EVALUATION OF EFIM

In this section, we apply the notion of EFI to derive the SPEB for both the case with and without *a priori* knowledge. We also introduce the notion of ranging information (RI), which turns out to be the basic component of the SPEB.

A. EFIM Without a Priori Knowledge

First consider a case in which *a priori* knowledge is unavailable. We apply the notion of EFI to reduce the dimension of the original FIM in (7), and the EFIM for the agent's position is presented in the following proposition.

Proposition 1: When *a priori* knowledge is unavailable, an EFIM for the agent's position is

$$\mathbf{J}_e(\mathbf{p}, \{\kappa_j : j \in \mathcal{N}_L\}) = \frac{1}{c^2} \mathbf{T}_L \mathbf{A}_L \mathbf{T}_L^T \quad (14)$$

where \mathbf{T}_L and \mathbf{A}_L are given by (41) and (42), respectively.

Proof: Let $\mathbf{A} = \mathbf{T}_{NL} \mathbf{A}_{NL} \mathbf{T}_{NL}^T + \mathbf{T}_L \mathbf{A}_L \mathbf{T}_L^T$, $\mathbf{B} = \mathbf{T}_{NL} \mathbf{A}_{NL}$, and $\mathbf{C} = \mathbf{A}_{NL}$ in (7). Applying the notion of EFI in (13) leads to the result. \square

Remark 1: When *a priori* knowledge is unavailable, NLOS signals do not contribute to the EFIM for the agent's position. Hence, we can eliminate these NLOS signals when analyzing localization accuracy. This observation agrees with the results of [29], but the amplitudes of the MPCs are assumed to be known in their model.

Note that the dimension of the EFIM in (14) is much larger than 2×2 . We will apply the notion of EFI again to further reduce the dimension of the EFIM in the following theorem. Before the theorem, we introduce the notion of the first contiguous cluster and RI.

Definition 3 (First Contiguous Cluster): The first contiguous cluster is defined to be the set of paths $\{1, 2, \dots, l\}$, such that $|\tau_i - \tau_{i+1}| < T_s$ for $i = 1, 2, \dots, l-1$, and $|\tau_l - \tau_{l+1}| > T_s$, where T_s is the duration of $s(t)$.

Definition 4 (RI): The RI is a 2×2 matrix of the form $\lambda \mathbf{J}_r(\phi)$, where λ is a nonnegative number called the ranging information intensity (RII), and $\mathbf{J}_r(\phi)$ a 2×2 matrix called the ranging direction matrix (RDM) with angle ϕ , given by

$$\mathbf{J}_r(\phi) \triangleq \begin{bmatrix} \cos^2 \phi & \cos \phi \sin \phi \\ \cos \phi \sin \phi & \sin^2 \phi \end{bmatrix}.$$

The first contiguous cluster is the first group of nondisjoint paths (see Fig. 2).¹⁵ The RDM is 1-D along the direction ϕ with unit intensity, i.e., $\mathbf{J}_r(\phi)$ has one (and only one) nonzero eigenvalue equal to 1 with corresponding eigenvector $\mathbf{q} = [\cos \phi \quad \sin \phi]^T$.

Theorem 1: When *a priori* knowledge is unavailable, the EFIM for the agent's position is a 2×2 matrix

$$\mathbf{J}_e(\mathbf{p}) = \sum_{j \in \mathcal{N}_L} \lambda_j \mathbf{J}_r(\phi_j) \quad (15)$$

¹⁵The first contiguous cluster, defined for general wideband received signals, may contain many MPCs. Two paths that arrive at time τ_i and $\tau_{i'}$ are called nondisjointed if $|\tau_i - \tau_{i'}| < T_s$.

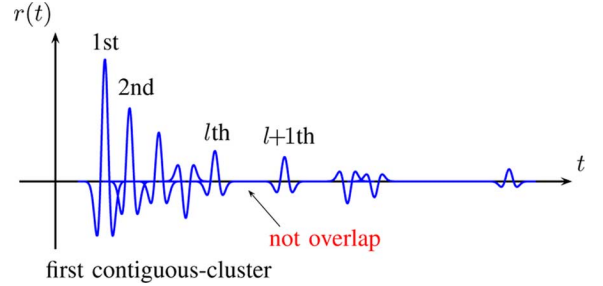


Fig. 2. An illustration of the first contiguous cluster (containing l paths) in a LOS signal.

where λ_j is the RII from anchor j , given by

$$\lambda_j = \frac{8\pi^2 \beta^2}{c^2} (1 - \chi_j) \text{SNR}_j^{(1)}. \quad (16)$$

In (16), $0 \leq \chi_j \leq 1$ is given by (59)

$$\beta \triangleq \left(\frac{\int_{-\infty}^{+\infty} f^2 |S(f)|^2 df}{\int_{-\infty}^{+\infty} |S(f)|^2 df} \right)^{1/2} \quad (17)$$

and

$$\text{SNR}_j^{(l)} \triangleq \frac{|\alpha_j^{(l)}|^2 \int_{-\infty}^{+\infty} |S(f)|^2 df}{N_0}. \quad (18)$$

Furthermore, only the first contiguous cluster of LOS signals contains information for localization.

Proof: See Appendix III-A. \square

Remark 2: In Theorem 1, β is known as the *effective bandwidth* [50], [67], χ_j is called path-overlap coefficient (POC) that characterizes the effect of multipath propagation for localization, and $\text{SNR}_j^{(l)}$ is the SNR of the l th path in $r_j(t)$. We draw the following observations from Theorem 1.

- The original FIM in (7) can be transformed into a simple 2×2 EFIM in a canonical form, given by (15), as a weighted sum of the RDM from individual anchors. Each anchor (e.g., anchor j) can provide only 1-D RI along the direction ϕ_j , from the anchor to the agent, with intensity λ_j .¹⁶
- The RII λ_j depends on the effective bandwidth of $s(t)$, the SNR of the first path, and the POC. Since $0 \leq \chi_j \leq 1$, path overlap in the first contiguous cluster will reduce the RII, thus leading to a higher SPEB, unless the signal via the first path does not overlap with others ($\chi_j = 0$).
- The POC χ_j in (59) is determined only by the waveform $s(t)$ and the NLOS biases of the MPCs in the first contiguous cluster. The independence of χ_j on the path amplitudes seems counterintuitive. However, this is due to the fact that, although large $\alpha_j^{(l)}$ causes severe interpath interference for estimating the TOA $\tau_j^{(l)}$, it increases the estimation accuracy for $\tau_j^{(l)}$, which in turn helps to mitigate the interpath interference.

We can specialize the above theorem into a case in which the first path in a LOS signal is completely resolvable, i.e., the first contiguous cluster contains only a single component.

¹⁶For notational convenience, we suppress the dependence of ϕ_j and λ_j on the agent's position \mathbf{p} throughout the paper.

Corollary 1: When *a priori* knowledge is unavailable and the first contiguous cluster of the received waveform from anchor j contains only the first path, the RII becomes

$$\lambda_j = \frac{8\pi^2\beta^2}{c^2} \text{SNR}_j^{(1)}. \quad (19)$$

Proof: See Appendix III-B. \square

Remark 3: When the first path is resolvable, $\chi_j = 0$ in (16) and hence λ_j attains its maximum value. However, when the signal via other paths overlap with the first one, these paths will degrade the estimation accuracy of the first path's arrival time and hence the RII. Corollary 1 is intuitive and important: the RII of a LOS signal depends only on the first path if the first path is resolvable. In such a case, all other paths can be eliminated, and the multipath signal is equivalent to a signal with only the first path for localization.

From Theorem 1, the SPEB can be derived in (20), shown at the bottom of the page. When the first paths are resolvable, by Corollary 1, we have all $\chi_j = 0$ in (20) and the corresponding $\mathcal{P}(\mathbf{p})$ becomes the same as those based on single-path signal models in [9], [29]. However, those results are not accurate when the first path is not resolvable.

B. EFIM With *a Priori* Knowledge

We now consider the case where there is *a priori* knowledge of the channel parameters, but not of the agent's position. In such cases, since \mathbf{p} is deterministic but unknown, $f(\mathbf{p})$ is eliminated in (8). Similar to the analysis in the previous section, we can derive the 2×2 EFIM for the corresponding FIM in (10).

Theorem 2: When *a priori* knowledge of the channel parameters is available and the sets of channel parameters corresponding to different anchors are mutually independent, the EFIM for the agent's position is a 2×2 matrix

$$\mathbf{J}_e(\mathbf{p}) = \sum_{j \in \mathcal{N}_L} \lambda_j \mathbf{J}_r(\phi_j) + \sum_{j \in \mathcal{N}_{NL}} \lambda_j \mathbf{J}_r(\phi_j) \quad (21)$$

where λ_j is given by (63a) for LOS signals and (63b) for NLOS signals.

Proof: See Appendix III-C. \square

Remark 4: Theorem 2 generalizes the result of Theorem 1 from deterministic to hybrid parameter estimation.¹⁷ In this case, the EFIM can still be expressed in a canonical form as a weighed sum of the RDMs from individual anchors. Note that due to the existence of *a priori* channel knowledge, the RII of NLOS signals can be positive, and hence these signals contribute to the EFIM as opposed to the case in Theorem 1.

Corollary 2: *A priori* channel knowledge increases the RII. In the absence of such knowledge, the expressions of RII in (63a)–(63b) reduce to (16) and zero, respectively.

¹⁷This is the case where the agent's position \mathbf{p} is deterministic and the channel parameters are random.

Proof: See Appendix III-D. \square

Corollary 3: LOS signals can be treated as NLOS signals with infinite *a priori* Fisher information of $b_j^{(1)}$, i.e., $b_j^{(1)}$ is known. Mathematically, (63a) is equivalent to (63b) with $\mathbf{F}_\theta(\boldsymbol{\theta}; b_j^{(1)}, b_j^{(1)}) \rightarrow \infty$.

Proof: See Appendix III-E. \square

Remark 5: Corollary 2 shows that Theorem 2 degenerates to Theorem 1 when *a priori* channel knowledge is unavailable. Moreover, Corollary 3 unifies the LOS and NLOS signals under the Bayesian estimation framework: the LOS biases $b_j^{(1)}$ ($j \in \mathcal{N}_L$) can be regarded as random parameters with infinite *a priori* Fisher information instead of being eliminated from $\boldsymbol{\theta}$ as in Section II-A. Hence, all of the signals can be modeled as NLOS, and infinite *a priori* Fisher information of $b_j^{(1)}$ will be assigned for LOS signals.

We next consider the case where *a priori* knowledge of the agent's position is available in addition to channel parameters. Note that the topology of the anchors and the agent changes with the position of the agent. The 2×2 EFIM is given in (65), which is more intricate than the previous two cases. To gain some insights, we consider a special case where¹⁸

$$\mathbb{E}_{\mathbf{p}}\{g(\mathbf{p})\} = g(\bar{\mathbf{p}}) \quad (22)$$

in which $\bar{\mathbf{p}} = \mathbb{E}_{\mathbf{p}}\{\mathbf{p}\}$ is the agent's expected position, for some function $g(\cdot)$ involved in the derivation of the EFIM (see Appendix III-F).

Proposition 2: When the *a priori* position distribution of the agent satisfies (22), and the sets of channel parameters corresponding to different anchors are mutually independent, the EFIM for the agent's position is a 2×2 matrix

$$\mathbf{J}_e(\mathbf{p}) = \sum_{j \in \mathcal{N}_b} \bar{\lambda}_j \mathbf{J}_r(\bar{\phi}_j) + \bar{\boldsymbol{\Xi}}_{\mathbf{p}} \quad (23)$$

where $\bar{\lambda}_j$ is given by (66), and $\bar{\phi}_j$ is the angle from anchor j to $\bar{\mathbf{p}}$.

Proof: See Appendix III-F. \square

Remark 6: The *a priori* knowledge of the agent's position is exploited, in addition to that of the channel parameters, for localization in Proposition 2. The expressions for the EFIM can be involved in general. Fortunately, if (22) is satisfied, the EFIM can be simply written as the sum of two parts as shown in (23): a weighted sum of the RDMs from individual anchors as in the previous two cases, and the EFIM from the *a priori* knowledge of the agent's position. This result unifies the contribution from anchors and that from the *a priori* knowledge of the agent's

¹⁸This occurs when the agent's *a priori* position distribution is concentrated in a small area relative to the distance between the agent and the anchors, so that $g(\mathbf{p})$ is flat in that area. For example, this condition is satisfied in far-field scenarios.

$$\mathcal{P}(\mathbf{p}) = \frac{c^2}{8\pi^2\beta^2} \frac{2 \sum_{j \in \mathcal{N}_L} (1 - \chi_j) \text{SNR}_j^{(1)}}{\sum_{j \in \mathcal{N}_L} \sum_{m \in \mathcal{N}_L} (1 - \chi_j)(1 - \chi_m) \text{SNR}_j^{(1)} \text{SNR}_m^{(1)} \sin^2(\phi_j - \phi_m)}. \quad (20)$$

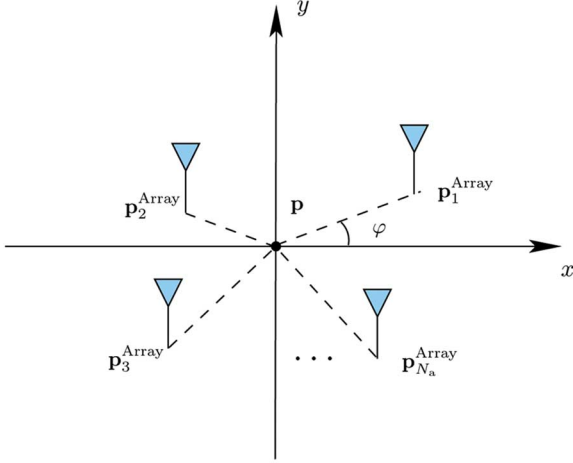


Fig. 3. An antenna array is described by the reference point \mathbf{p} , the orientation φ , and the relative positions of the antennas.

position into the EFIM. The concept of localization with *a priori* knowledge of the agent's position is useful for a wide range of applications such as successive localization or tracking.

IV. WIDEBAND LOCALIZATION WITH ANTENNA ARRAYS

In this section, we consider localization systems using wideband antenna arrays, which can perform both TOA and AOA measurements. Since the orientation of the array may be unknown, we propose a model to jointly estimate the agent's position and orientation, and derive the SPEB and the squared orientation error bound (SOEB).

A. System Model and SOEB

Consider a network where each agent is equipped with an N_a -antenna array,¹⁹ which can extract both the TOA and AOA information with respect to neighboring anchors. Let $\mathcal{N}_a = \{1, 2, \dots, N_a\}$ denote the set of antennas, and let $\mathbf{p}_k^{\text{Array}} \triangleq [x_k^{\text{Array}} \ y_k^{\text{Array}}]^T$ denote the position of the agent's k th antenna, which needs to be estimated. Let ϕ_{kj} denote the angle from anchor j to the agent's k th antenna, i.e.,

$$\phi_{kj} = \tan^{-1} \frac{y_k^{\text{Array}} - y_j}{x_k^{\text{Array}} - x_j}.$$

Since relative positions of the antennas in the array are usually known, if we denote $\mathbf{p} = [x \ y]^T$ as a reference point and φ as the orientation of the array,²⁰ then the position of the k th antenna in the array can be represented as (Fig. 3)

$$\mathbf{p}_k^{\text{Array}} = \mathbf{p} + \begin{bmatrix} \Delta x_k(\mathbf{p}, \varphi) \\ \Delta y_k(\mathbf{p}, \varphi) \end{bmatrix}, \quad k \in \mathcal{N}_a$$

where $\Delta x_k(\mathbf{p}, \varphi)$ and $\Delta y_k(\mathbf{p}, \varphi)$ denote the relative distance in x and y direction from the reference point to the k th antenna, respectively.

¹⁹Each anchor has only one antenna here. We will discuss the case of multiple antennas on anchors at the end of this section.

²⁰Note from geometry that the orientation φ is independent of the specific reference point.

Since the array orientation may be unknown, we classify the localization problem into *orientation-aware* and *orientation-unaware* cases, where φ can be thought of as a random parameter with infinite (orientation-aware) and zero (orientation-unaware) *a priori* Fisher information [46].

The received waveform at the agent's k th antenna from anchor j can be written as

$$r_{kj}(t) = \sum_{l=1}^{L_{kj}} \alpha_{kj}^{(l)} s(t - \tau_{kj}^{(l)}) + z_{kj}(t), \quad t \in [0, T_{\text{ob}})$$

where $\alpha_{kj}^{(l)}$ and $\tau_{kj}^{(l)}$ are the amplitude and delay, respectively, of the l th path, L_{kj} is the number of MPCs, and $z_{kj}(t)$ represents the observation noise modeled as additive white Gaussian processes with two-side power spectral density $N_0/2$. The relationship between the position of the k th antenna and the delay of the l th path is

$$\tau_{kj}^{(l)} = \frac{1}{c} \left[\|\mathbf{p}_k^{\text{Array}} - \mathbf{p}_j\| + b_{kj}^{(l)} \right]. \quad (24)$$

The parameters to be considered include the position of the reference point, the array orientation, and the nuisance multipath parameter as

$$\boldsymbol{\theta} = [\mathbf{p}^T \ \varphi \ \check{\boldsymbol{\kappa}}_1^T \ \check{\boldsymbol{\kappa}}_2^T \ \dots \ \check{\boldsymbol{\kappa}}_{N_a}^T]^T \quad (25)$$

where $\check{\boldsymbol{\kappa}}_k$ consists of the multipath parameters associated with the received waveforms from all anchors at the k th antenna

$$\check{\boldsymbol{\kappa}}_k = [\boldsymbol{\kappa}_{k,1}^T \ \boldsymbol{\kappa}_{k,2}^T \ \dots \ \boldsymbol{\kappa}_{k,N_b}^T]^T$$

and each $\boldsymbol{\kappa}_{kj}$ consists of the multipath parameters associated with $r_{kj}(t)$

$$\boldsymbol{\kappa}_{kj} = [b_{kj}^{(1)} \ \alpha_{kj}^{(1)} \ \dots \ b_{kj}^{(L_{kj})} \ \alpha_{kj}^{(L_{kj})}]^T.$$

Similar to Section II-B, the overall received waveforms at the antenna array can be represented, using the KL expansion, by $\mathbf{r} = [\mathbf{r}_1^T \ \mathbf{r}_2^T \ \dots \ \mathbf{r}_{N_a}^T]^T$, where

$$\mathbf{r}_k = [\mathbf{r}_{k,1}^T \ \mathbf{r}_{k,2}^T \ \dots \ \mathbf{r}_{k,N_b}^T]^T$$

in which \mathbf{r}_{kj} is obtained by the KL expansion of $r_{kj}(t)$.

Definition 5 (SOEB): The SOEB is defined to be

$$\mathcal{P}(\varphi) \triangleq [\mathbf{J}_{\boldsymbol{\theta}}^{-1}]_{3,3}.$$

B. EFIM Without a Priori Knowledge

We first consider scenarios in which *a priori* knowledge is unavailable. Following similar steps in Section III-B, we have the following theorem.

Theorem 3: When *a priori* knowledge is unavailable, the EFIMs for the position and the orientation, using an N_a -antenna array, are given respectively by

$$\mathbf{J}_e^{\text{Array}}(\mathbf{p}) = \sum_{k \in \mathcal{N}_a} \mathbf{J}_e(\mathbf{p}_k^{\text{Array}}) - \frac{1}{\sum_{k \in \mathcal{N}_a} \sum_{j \in \mathcal{N}_b} \lambda_{kj} h_{kj}^2} \mathbf{q} \mathbf{q}^T \quad (26)$$

and

$$\mathbf{J}_e^{\text{Array}}(\varphi) = \sum_{k \in \mathcal{N}_a} \sum_{j \in \mathcal{N}_b} \lambda_{kj} h_{kj}^2 - \mathbf{q}^T \left[\sum_{k \in \mathcal{N}_a} \mathbf{J}_e(\mathbf{p}_k^{\text{Array}}) \right]^{-1} \mathbf{q} \quad (27)$$

where λ_{kj} is given by (71), $\mathbf{q}_{kj} = [\cos \phi_{kj} \quad \sin \phi_{kj}]^T$, and

$$\begin{aligned} \mathbf{J}_e(\mathbf{p}_k^{\text{Array}}) &= \sum_{j \in \mathcal{N}_b} \lambda_{kj} \mathbf{J}_r(\phi_{kj}) \\ \mathbf{q} &= \sum_{k \in \mathcal{N}_a} \sum_{j \in \mathcal{N}_b} \lambda_{kj} h_{kj} \mathbf{q}_{kj} \end{aligned} \quad (28)$$

and

$$h_{kj} = \frac{d}{d\varphi} \Delta x_k(\mathbf{p}, \varphi) \cos \phi_{kj} + \frac{d}{d\varphi} \Delta y_k(\mathbf{p}, \varphi) \sin \phi_{kj}. \quad (29)$$

Proof: See Appendix IV-A. \square

Corollary 4: The EFIM for the position is given by

$$\mathbf{J}_e^{\text{Array}}(\mathbf{p}) = \sum_{k \in \mathcal{N}_a} \mathbf{J}_e(\mathbf{p}_k^{\text{Array}}) \quad (30)$$

for orientation-aware localization.

Proof: (Outline) In orientation-aware localization, the angle φ is known and hence excluded from the parameter vector $\boldsymbol{\theta}$ in (25). Consequently, the proof of this corollary is analogous to that of Theorem 3 except that the components corresponding to φ are eliminated from the FIM in (67) and (68). One can obtain (30) after some algebra. \square

Remark 7: The EFIM $\mathbf{J}_e(\mathbf{p}_k^{\text{Array}})$ in (26) and (30) corresponds to the localization information from the k th antenna. We draw the following observation from the above theorem.

- The EFIM $\mathbf{J}_e^{\text{Array}}(\mathbf{p})$ in (26) consists of two parts: 1) the sum of localization information obtained by individual antennas, and 2) the information reduction due to the uncertainty in the orientation estimate, which is subtracted from the first part.²¹ Since $\mathbf{q}\mathbf{q}^T$ in the second part is a positive-semidefinite 2×2 matrix and $\sum_{k \in \mathcal{N}_a} \sum_{j \in \mathcal{N}_b} \lambda_{kj} h_{kj}^2$ is always positive, we have the following inequality:

$$\mathbf{J}_e^{\text{Array}}(\mathbf{p}) \preceq \sum_{k \in \mathcal{N}_a} \mathbf{J}_e(\mathbf{p}_k^{\text{Array}}). \quad (31)$$

The inequality implies that the EFIM for the position, using antenna arrays, is bounded above by the sum of all EFIMs corresponding to individual antennas, since the uncertainty in the orientation estimate degrades the localization accuracy, except for $\mathbf{q} = \mathbf{0}$ or orientation-aware localization [i.e., (30)].

- The EFIM $\mathbf{J}_e^{\text{Array}}(\mathbf{p})$ and $J_e^{\text{Array}}(\varphi)$ depend only on the individual RI between each pair of anchors and antennas (through λ_{kj} 's and ϕ_{kj} 's), and the array geometry (through h_{kj} 's). Hence, it is not necessary to *jointly* consider the received waveforms at the N_a antennas, implying that AOA

²¹For notational convenience, we suppress the dependence of h_{kj} , λ_{kj} , and \mathbf{q} on the reference position \mathbf{p} .

obtained by antenna arrays does not increase position accuracy. Though counterintuitive at first, this finding should not be too surprising since AOA is obtained indirectly by the antenna array through TOA measurements, whereas the TOA information has already been fully utilized for localization by individual antennas.

- The gain of using antenna arrays for localization mainly comes from the multiple copies of the waveform received at the N_a antennas [see (26)],²² and its performance is similar to that of a single antenna with N_a measurements. The advantage of using antenna arrays lies in their ability of simultaneous measurements at the agent.

The equality in (31) is always achieved, independent of reference point, in orientation-aware localization. However, only a unique reference point achieves this equality in orientation-unaware localization. We define this unique point as the orientation center.

Definition 6 (Orientation Center): The orientation center is a reference point \mathbf{p}^* such that

$$\mathbf{J}_e^{\text{Array}}(\mathbf{p}^*) = \sum_{k \in \mathcal{N}_a} \mathbf{J}_e(\mathbf{p}_k^{\text{Array}}).$$

Proposition 3: Orientation center \mathbf{p}^* exists and is unique in orientation-unaware localization, and hence for any $\mathbf{p} \neq \mathbf{p}^*$

$$\mathbf{J}_e^{\text{Array}}(\mathbf{p}) \prec \mathbf{J}_e^{\text{Array}}(\mathbf{p}^*).$$

Proof: See Appendix IV-B. \square

Remark 8: The orientation center \mathbf{p}^* generally depends on the topology of the anchors and the agent, the properties of the received waveforms, the array geometry, and the array orientation. Since $\mathbf{q} = \mathbf{0}$ at the orientation center, the EFIMs for the array center and the orientation do not depend on each other, and hence the SPEB and SOEB can be calculated separately. The proposition also implies that the SPEB of reference points other than \mathbf{p}^* will be strictly larger than that of \mathbf{p}^* . The SPEB for any reference point is given in the next theorem.

Corollary 5: The SOEB $\mathcal{P}(\varphi)$ is independent of the reference point \mathbf{p} , and the SPEB is

$$\mathcal{P}(\mathbf{p}) = \mathcal{P}(\mathbf{p}^*) + \|\mathbf{p} - \mathbf{p}^*\|^2 \cdot \mathcal{P}(\varphi). \quad (32)$$

Proof: See Appendix IV-C. \square

Remark 9: The SOEB does not depend on the specific reference point, which was not apparent in (27). However, this is intuitive since different reference points only introduce different translations, but not rotations. On the other hand, different reference point \mathbf{p} results in different h_{kj} 's and hence different \mathbf{q} , which in turn gives different EFIM for position [see (26)]. We can interpret the relationship in (32) as follows: the SPEB of reference point \mathbf{p} is equal to that of the orientation center \mathbf{p}^* plus

²²In near-field scenarios where the antenna separation is on the order of the distances between the array and the anchors, additional gain that arises from the spatial diversity of the multiple antennas may be possible.

the orientation-induced position error, which is proportional to both the squared distance from \mathbf{p} to \mathbf{p}^* and the SOEB.

C. EFIM With a Priori Knowledge

We now consider a scenario in which the channel parameter vector $\boldsymbol{\kappa}_{k,j}$ independent for different k 's and j 's. The independence assumption serve as a reasonable approximation of many realistic scenarios, especially near-field cases. When the different sets of channel parameters are correlated, our results provide an upper bound for the EFIM.

Proposition 4: When *a priori* knowledge of channel parameters is available and the set of channel parameters corresponding to different anchors and antennas are mutually independent, the RII $\lambda_{k,j}$ becomes (70).

Proof: See Appendix IV-A. \square

We then consider the case where *a priori* knowledge of the agent's position and orientation is available in addition to channel knowledge. Note that the topology of the agent's antennas and anchors changes with the agent's positions and orientations. The expression of the EFIM can be derived analogous to (65), which is involved in general. Again to gain insights about the contribution of *a priori* position and orientation knowledge, we consider scenarios under condition

$$\mathbb{E}_{\mathbf{p},\varphi}\{g(\mathbf{p},\varphi)\} = g(\bar{\mathbf{p}},\bar{\varphi}) \quad (33)$$

where $\bar{\varphi} = \mathbb{E}_{\varphi}\{\varphi\}$, for some functions $g(\cdot)$ involved in the derivation of the EFIM.

Corollary 6: When *a priori* position and orientation distribution of the agent satisfies (33), and the sets of channel parameters corresponding to different anchors and antennas are mutually independent, the EFIMs for the position and the orientation, using an N_a -antenna array, are given, respectively, by

$$\mathbf{J}_e^{\text{Array}}(\mathbf{p}) = \Xi_{\mathbf{p}} + \sum_{k \in \mathcal{N}_a} \sum_{j \in \mathcal{N}_b} \bar{\lambda}_{k,j} \mathbf{J}_r(\bar{\phi}_{k,j}) - \frac{1}{\sum_{k \in \mathcal{N}_a} \sum_{j \in \mathcal{N}_b} \bar{\lambda}_{k,j} \bar{h}_{k,j}^2 + \Xi_{\varphi}} \bar{\mathbf{q}} \bar{\mathbf{q}}^T$$

and

$$J_e^{\text{Array}}(\varphi) = \Xi_{\varphi} + \sum_{k \in \mathcal{N}_a} \sum_{j \in \mathcal{N}_b} \bar{\lambda}_{k,j} \bar{h}_{k,j}^2 - \bar{\mathbf{q}}^T \left(\sum_{k \in \mathcal{N}_a} \sum_{j \in \mathcal{N}_b} \bar{\lambda}_{k,j} \mathbf{J}_r(\bar{\phi}_{k,j}) + \Xi_{\mathbf{p}} \right)^{-1} \bar{\mathbf{q}}$$

where $\bar{\lambda}_{k,j}$, $\bar{\phi}_{k,j}$, $\bar{h}_{k,j}$, and $\bar{\mathbf{q}}$ are corresponding functions in Theorem 3 of $\bar{\mathbf{p}}$ and $\bar{\varphi}$, respectively, and $\Xi_{\varphi} = \mathbf{F}_{\theta}(\varphi; \varphi, \varphi)$.

Proof: (Outline) The proof of this corollary is analogous to that of Theorem 3. Note that when condition (33) is satisfied, the *a priori* knowledge of position and orientation for localization can be characterized in the EFIM by using the approximation as in the proof of Proposition 2. \square

D. Discussions

1) *Far-Field Scenarios:* The antennas in the array are closely located in far-field scenarios, such that the received waveforms from each anchor experience statistically the same propagation channels. Hence, we have $\phi_{k,j} = \phi_j$ and $\lambda_{k,j} = \lambda_j$ for all k , leading to $\mathbf{J}_e(\mathbf{p}_k^{\text{Array}}) = \mathbf{J}_e(\mathbf{p})$. We define an important reference point as follows.

Definition 7 (Array Center): The array center is defined as the position \mathbf{p}_0 , satisfying

$$\sum_{k \in \mathcal{N}_a} \Delta x_k(\mathbf{p}_0, \varphi) = 0 \quad \text{and} \quad \sum_{k \in \mathcal{N}_a} \Delta y_k(\mathbf{p}_0, \varphi) = 0.$$

Proposition 5: The array center becomes the orientation center in far-field scenarios.

Proof: See Appendix IV-D. \square

Remark 10: Since the orientation center has the minimum SPEB, Proposition 5 implies that the array center always achieves the minimum SPEB in far-field scenarios. Hence, the array center is a well-suited choice for the reference point, since its position can be determined from the array geometry alone, without requiring the received waveforms and the knowledge of the anchor's topology.

In far-field scenarios, we choose the array center \mathbf{p}_0 as the reference point. The results of Theorem 3 become

$$\mathbf{J}_e^{\text{Array}}(\mathbf{p}_0) = N_a \sum_{j \in \mathcal{N}_b} \lambda_j \mathbf{J}_r(\phi_j)$$

and

$$J_e^{\text{Array}}(\varphi) = \sum_{k \in \mathcal{N}_a} \sum_{j \in \mathcal{N}_b} \lambda_j \bar{h}_{k,j}^2$$

where $\bar{h}_{k,j}$ is a function of \mathbf{p}_0 . Similarly, when the *a priori* position and orientation knowledge is available and condition (33) is satisfied, the results of Corollary 6 become

$$\mathbf{J}_e^{\text{Array}}(\mathbf{p}_0) = N_a \sum_{j \in \mathcal{N}_b} \bar{\lambda}_j \mathbf{J}_r(\bar{\phi}_j) + \Xi_{\mathbf{p}}$$

and

$$J_e^{\text{Array}}(\varphi) = \sum_{k \in \mathcal{N}_a} \sum_{j \in \mathcal{N}_b} \bar{\lambda}_j \bar{h}_{k,j}^2 + \Xi_{\varphi}$$

where $\bar{h}_{k,j}$ is a function of $\bar{\mathbf{p}}_0 = \mathbb{E}_{\mathbf{p}_0}\{\mathbf{p}_0\}$.

Note that the localization performance of an N_a -antenna array is equivalent to that of a single antenna with N_a measurements, regardless of the array geometry, in far-field scenarios.

2) *Multiple Antennas at Anchors:* When anchors are equipped with multiple antennas, each antenna can be viewed as an individual anchor. In this case, the agent's SPEB goes down with the number of the antennas at each anchor. Note that all the antennas of a given anchor provide RI approximately in the same direction with the same intensity, as they are closely located.

3) *Other Related Issues*: Other issues related to localization using wideband antenna arrays include the AOA estimation, the effect of multipath geometry, and the effect of array geometries. A more comprehensive performance analysis can be found in [11].

V. EFFECT OF CLOCK ASYNCHRONISM

In this section, we consider scenarios in which the clocks of all anchors are perfectly synchronized but the agent operates asynchronously with the anchors [68]. In such a scenario, the one-way time-of-flight measurement contains a time offset between the agent's clock and the anchors' clock.²³ Here, we investigate the effect of the time offset on localization accuracy.

A. Localization With a Single Antenna

Consider the scenario described in Section II, where each agent is equipped with a single antenna. When the agent operates asynchronously with the anchors, the relationship of (2) becomes

$$\tau_j^{(l)} = \frac{1}{c} \left[\|\mathbf{p} - \mathbf{p}_j\| + b_j^{(l)} + B \right]$$

where B is a random parameter that characterizes the time offset in terms of distance, and the corresponding parameter vector $\boldsymbol{\theta}$ becomes

$$\boldsymbol{\theta} = [\mathbf{p}^T \quad B \quad \boldsymbol{\kappa}_1^T \quad \boldsymbol{\kappa}_2^T \quad \cdots \quad \boldsymbol{\kappa}_{N_b}^T]^T.$$

Similar to Theorem 2, where \mathbf{p} is deterministic but unknown and the remaining parameters are random, we have the following result.

Theorem 4: When *a priori* knowledge of the channel parameters and the time offset is available, and the sets of channel parameters corresponding to different anchors are mutually independent, the EFIMs for the position and the time offset are given, respectively, by

$$\mathbf{J}_e^B(\mathbf{p}) = \sum_{j \in \mathcal{N}_b} \lambda_j \mathbf{J}_r(\phi_j) - \frac{1}{\sum_{j \in \mathcal{N}_b} \lambda_j + \Xi_B} \mathbf{q}_B \mathbf{q}_B^T \quad (34)$$

and

$$J_e(B) = \sum_{j \in \mathcal{N}_b} \lambda_j + \Xi_B - \mathbf{q}_B^T \left(\sum_{j \in \mathcal{N}_b} \lambda_j \mathbf{J}_r(\phi_j) \right)^{-1} \mathbf{q}_B \quad (35)$$

where λ_j is given by (63b), $\mathbf{q}_B = \sum_{j \in \mathcal{N}_b} \lambda_j \mathbf{q}_j$, and

$$\Xi_B \triangleq \mathbf{F}_\theta(B; B, B).$$

Proof: See Appendix V-A. \square

Remark 11: Since $\mathbf{q}_B \mathbf{q}_B^T$ is a positive-semidefinite matrix and $\sum_{j \in \mathcal{N}_b} \lambda_j$ is positive in (34), compare to Theorem 2, we always have the inequality

$$\mathbf{J}_e^B(\mathbf{p}) \preceq \mathbf{J}_e(\mathbf{p}) \quad (36)$$

²³We consider scenarios in which localization time is short relative to clock drifts, such that the time offset is the same for all measurements from the anchors.

where the equality in (36) is achieved for time-offset-known localization (i.e., $\Xi_B = \infty$), or time-offset-independent localization (i.e., $\mathbf{q}_B = \mathbf{0}$). The former corresponds to the case where accurate knowledge of the time offset is available, while the latter depends on the RII from each anchor, as well as the topology of the anchors and agent. The inequality of (36) results from the uncertainty in the additional parameter B , which degrades the localization accuracy. Hence, the SPEB in the presence of uncertain time offset is always larger than or equal to that without a offset or with a known offset.

We next consider the case where *a priori* knowledge of the agent's position is available. When the *a priori* position distribution of the agent satisfies (22), we have the following corollary.

Corollary 7: When the *a priori* position distribution of the agent satisfies (22), and the sets of channel parameters corresponding to different anchors are mutually independent, the EFIMs for the position and the time offset are given, respectively, by

$$\mathbf{J}_e^B(\mathbf{p}) = \sum_{j \in \mathcal{N}_b} \bar{\lambda}_j \mathbf{J}_r(\bar{\phi}_j) + \Xi_{\mathbf{p}} - \frac{1}{\sum_{j \in \mathcal{N}_b} \bar{\lambda}_j + \Xi_B} \bar{\mathbf{q}}_B \bar{\mathbf{q}}_B^T$$

and

$$J_e(B) = \sum_{j \in \mathcal{N}_b} \bar{\lambda}_j + \Xi_B - \bar{\mathbf{q}}_B^T \left(\Xi_{\mathbf{p}} + \sum_{j \in \mathcal{N}_b} \bar{\lambda}_j \mathbf{J}_r(\bar{\phi}_j) \right)^{-1} \bar{\mathbf{q}}_B$$

where $\bar{\phi}_j$ is the angle from anchor j to $\bar{\mathbf{p}}$, $\bar{\lambda}_j$ is given by (66), and $\bar{\mathbf{q}}_B$ is a function of $\bar{\mathbf{p}}$.

Proof: (Outline) Conditions in (22) hold in far-field scenarios, and we can approximate the expectation over random parameter vector \mathbf{p} using the average position $\bar{\mathbf{p}}$. By following the steps of Theorem 4 and Proposition 2, we can derive the theorem after some algebra. \square

B. Localization With Antenna Arrays

Consider the scenario describing in Section IV where each agent is equipped with an array of N_a antennas. Incorporating the time offset B , (24) becomes

$$\tau_{kj}^{(l)} = \frac{1}{c} \left[\|\mathbf{p}_k^{\text{Array}} - \mathbf{p}_j\| + b_{kj}^{(l)} + B \right]$$

and the corresponding parameter vector $\boldsymbol{\theta}$ becomes

$$\boldsymbol{\theta} = [\mathbf{p}^T \quad \varphi \quad B \quad \boldsymbol{\kappa}_1^T \quad \boldsymbol{\kappa}_2^T \quad \cdots \quad \boldsymbol{\kappa}_{N_a}^T]^T.$$

Similar to Theorem 3, where \mathbf{p} and φ are deterministic but unknown and the remaining parameters are random, we have the following theorem.

Theorem 5: When *a priori* knowledge of the channel parameters is available, and the sets of channel parameters corresponding to different anchors and antennas are mutually independent, the EFIM for the position, the orientation, and the time offset, using an N_a -antenna array, is given by (37) shown at the

bottom of the page, where $\Xi_\varphi = \infty$ and $\Xi_\varphi = 0$ correspond to orientation-aware and orientation-unaware localization, respectively, and λ_{kj} , \mathbf{q}_{kj} , and h_{kj} are given by (70), (28), and (29), respectively.

Proof: See Appendix V-B. \square

Remark 12: Theorem 5 gives the overall 4×4 EFIM for the position, the orientation, and the time offset, where individual EFIMs can be derived by applying the notion of EFI again.

We finally consider the case where *a priori* knowledge of the agent's position and orientation is available. The EFIM in far-field scenarios is given in the following corollary.

Corollary 8: When *a priori* knowledge of the agent's position, orientation, time offset, and the channel parameters is available, and the sets of channel parameters corresponding to different anchors and antennas are mutually independent, in far-field scenarios, the EFIMs for the position, the orientation, and the time offset, using an N_a -antenna array, are given, respectively, by

$$\mathbf{J}_e^{\text{Array-B}}(\mathbf{p}_0) = N_a \sum_{j \in \mathcal{N}_b} \bar{\lambda}_j \mathbf{J}_r(\bar{\phi}_j) + \Xi_{\mathbf{p}}$$

$$- \frac{1}{N_a \sum_{j \in \mathcal{N}_b} \bar{\lambda}_j + \Xi_B} \bar{\mathbf{q}}_B \bar{\mathbf{q}}_B^T$$

$$J_e^{\text{Array-B}}(\varphi) = \sum_{k \in \mathcal{N}_a} \sum_{j \in \mathcal{N}_b} \bar{\lambda}_j \bar{h}_{kj}^2 + \Xi_\varphi$$

and

$$J_e^{\text{Array-B}}(B) = N_a \sum_{j \in \mathcal{N}_b} \bar{\lambda}_j + \Xi_B$$

$$- \bar{\mathbf{q}}_B^T \left(N_a \sum_{j \in \mathcal{N}_b} \bar{\lambda}_j \mathbf{J}_r(\bar{\phi}_j) + \Xi_{\mathbf{p}} \right)^{-1} \bar{\mathbf{q}}_B$$

where $\bar{\mathbf{p}}_0$ is the expected position of the agent's array center, $\bar{\phi}_j$ is the angle from anchor j to $\bar{\mathbf{p}}_0$, and $\bar{\lambda}_j$, $\bar{\mathbf{q}}_B$, and \bar{h}_{kj} are functions of $\bar{\mathbf{p}}_0$.

Proof: See Appendix V-C. \square

VI. DISCUSSIONS

In this section, we will provide discussions on some related issues in the paper. It includes 1) the relations of our results to the bounds based on signal metrics, 2) the achievability of the SPEB, and 3) the extension of the results to 3-D localization.

A. Relation to Bounds Based on Signal Metrics

Analysis of localization performance in the literature mainly employs specific signal metrics, such as TOA, AOA, RSS, and TDOA, rather than utilizing the entire received waveforms. Our analysis is based on the received waveforms and exploits all the localization information inherent in these signal metrics, implicitly or explicitly. In particular, TOA and joint TOA/AOA metrics were incorporated in our analysis in Sections III and IV, respectively. Similarly, TDOA and joint TDOA/AOA metrics were included in the analysis of Section V, and the RSS metric has been implicitly exploited from *a priori* channel knowledge in Section II-C1.

B. Achievability of the SPEB

Maximum *a posteriori* (MAP) and maximum-likelihood (ML) estimates, respectively, achieve the CRB asymptotically in the high SNR regimes for both the case with and without *a priori* knowledge [50]. High SNR can be attained using sequences with good correlation properties [69]–[71], or simply repeated transmissions. Therefore, the SPEB is achievable.

C. Generalization to 3-D Localization

All results obtained thus far can be easily extended to 3-D case, i.e., $\mathbf{p} = [x \ y \ z]^T$ and the RDM becomes

$$\mathbf{J}_r(\varphi_j, \phi_j) = \mathbf{q}_j \mathbf{q}_j^T$$

where φ_j and ϕ_j are the angles in the coordinates, and

$$\mathbf{q}_j = [\cos \varphi_j \cos \phi_j \quad \sin \varphi_j \cos \phi_j \quad \sin \phi_j]^T.$$

Similarly, we can obtain a corresponding 3×3 EFIM in the form of (21).

VII. NUMERICAL RESULTS

In this section, we illustrate applications of our analytical results using numerical examples. We deliberately restrict our attention to a simple network to gain insights, although our analytical results are valid for arbitrary topology with any number of anchors and any number of MPCs in the received waveforms.

A. Effect of Path Overlap

We first investigate the effect of path overlap on the SPEB when *a priori* knowledge is unavailable. In particular, we compare the SPEB obtained by the *full-parameter model* proposed in this paper and that obtained by the *partial-parameter model* proposed in [28]. In the partial-parameter model, the amplitudes of MPCs are assumed to be known and hence excluded from the parameter vector.

$$\mathbf{J}_e^{\text{Array-B}} = \begin{bmatrix} \sum_{k \in \mathcal{N}_a} \sum_{j \in \mathcal{N}_b} \lambda_{kj} \mathbf{q}_{kj} \mathbf{q}_{kj}^T & \sum_{k \in \mathcal{N}_a} \sum_{j \in \mathcal{N}_b} h_{kj} \lambda_{kj} \mathbf{q}_{kj} & \sum_{k \in \mathcal{N}_a} \sum_{j \in \mathcal{N}_b} \lambda_{kj} \mathbf{q}_{kj} \\ \sum_{k \in \mathcal{N}_a} \sum_{j \in \mathcal{N}_b} h_{kj} \lambda_{kj} \mathbf{q}_{kj}^T & \sum_{k \in \mathcal{N}_a} \sum_{j \in \mathcal{N}_b} h_{kj}^2 \lambda_{kj} + \Xi_\varphi & \sum_{k \in \mathcal{N}_a} \sum_{j \in \mathcal{N}_b} h_{kj} \lambda_{kj} \\ \sum_{k \in \mathcal{N}_a} \sum_{j \in \mathcal{N}_b} \lambda_{kj} \mathbf{q}_{kj}^T & \sum_{k \in \mathcal{N}_a} \sum_{j \in \mathcal{N}_b} h_{kj} \lambda_{kj} & \sum_{k \in \mathcal{N}_a} \sum_{j \in \mathcal{N}_b} \lambda_{kj} + \Xi_B \end{bmatrix} \quad (37)$$

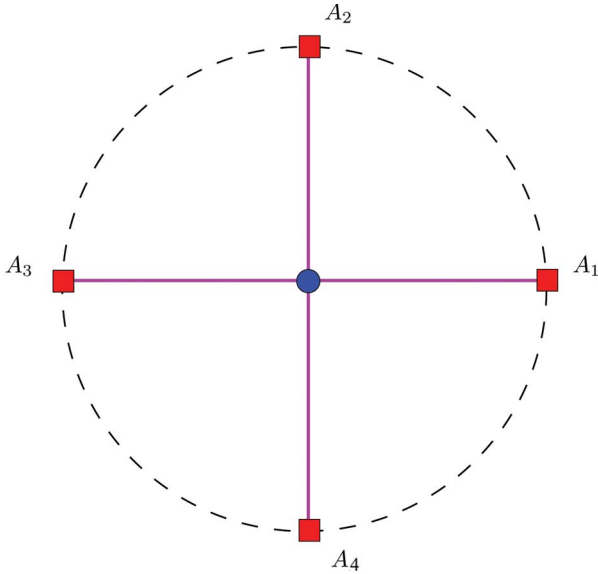


Fig. 4. Network topology: Four anchors are equally spaced on a circle with an agent at the center. All signals from the anchors to the agent are LOS.

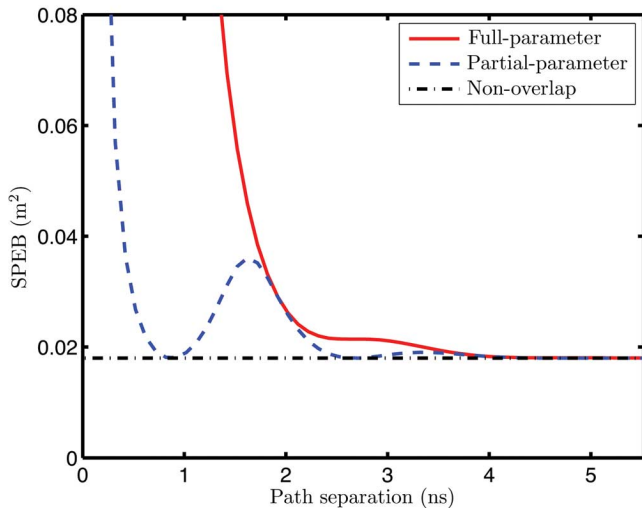


Fig. 5. SPEB as a function of path separation for the full-parameter, partial-parameter, and nonoverlap models, without *a priori* knowledge.

Consider a simple network with four anchors ($N_b = 4$) equally spaced on a circle and an agent at the center receiving all LOS signals (see Fig. 4). Each waveform consists of two paths: one LOS path ($\text{SNR}_j^{(1)} = 0$ dB) and one NLOS path ($\text{SNR}_j^{(2)} = -3$ dB), and the separations of the two paths $\tau_j^{(2)} - \tau_j^{(1)}$ are identical for all j . In addition, the transmitted waveform is a second derivative of Gaussian pulse with width approximately equal to 4 ns. Fig. 5 shows the SPEB as a function of path separation $\tau_j^{(2)} - \tau_j^{(1)}$ according to Theorem 1.

We can draw the following observations. First, path overlap increases the SPEB in both models, since it reduces the ability to estimate the first path and hence decreases the RII. Note that the shape of the curves depends on the autocorrelation function of the waveform $s(t)$ [47]. Second, when the path separation exceeds the pulse width (approximately 4 ns), the two models give the same SPEB, which equals the nonoverlapping case. In

such cases, the first contiguous cluster contains only the first path, and hence the RII is determined by this path. This agrees with the analysis in Section III. Third, excluding the amplitudes from the parameter vector incorrectly provides more RI when the two paths overlap, and hence the partial-parameter model results in a loose bound. This demonstrates the importance of using the full-parameter model.

B. Improvement From a Priori Channel Knowledge

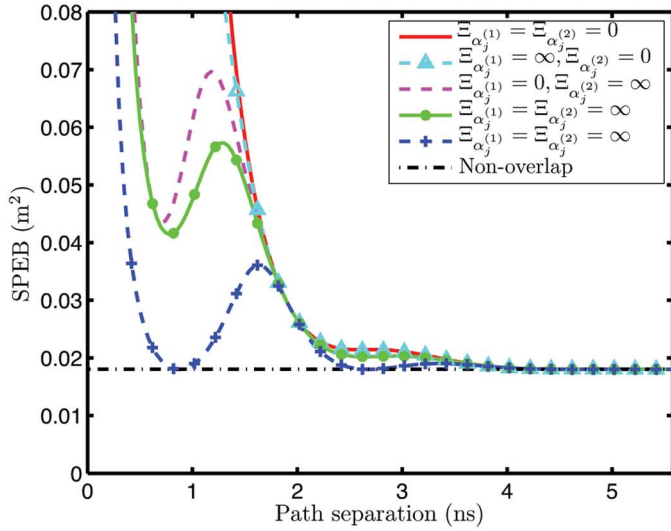
We then quantify the contribution of the *a priori* knowledge of channel parameters to the SPEB. The network topology and channel parameters are the same as those in Section VII-A, except *a priori* knowledge of $\alpha_j^{(1)}$, $\alpha_j^{(2)}$ and $b_j^{(2)}$ is now available. For simplicity, we consider these parameters to be independent *a priori* and denote the *a priori* Fisher information of parameter θ_1 by $\Xi_{\theta_1} = \mathbf{F}_{\theta}(\theta; \theta_1, \theta_1)$. In Fig. 6(a), the SPEBs are plotted as functions of the path separation for different *a priori* knowledge of $\alpha_j^{(1)}$ and $\alpha_j^{(2)}$ (no *a priori* knowledge of $b_j^{(2)}$); while in Fig. 6(b), the SPEBs are plotted for different *a priori* knowledge of $b_j^{(2)}$ (no *a priori* knowledge of $\alpha_j^{(1)}$ and $\alpha_j^{(2)}$).

We have the following observations. First, the SPEB decreases with the *a priori* knowledge of the amplitudes and the NLOS biases. This should be expected since *a priori* channel knowledge increases the RII and thus localization accuracy, as indicated in Corollary 2. Moreover, the NLOS components are shown to be beneficial for localization in the presence of *a priori* biases knowledge, as proven in Section III-B. Second, as the *a priori* knowledge of the amplitudes approaches infinity, the SPEB in Fig. 6(a) obtained using the full-parameter model converges to that in Fig. 5 obtained using the partial-parameter model. This is because the partial-parameter model excludes the amplitudes from the parameter vector, which is equivalent to assuming known amplitudes and hence infinite *a priori* Fisher information for the amplitudes ($\Xi_{\alpha_j^{(1)}} = \Xi_{\alpha_j^{(2)}} = \infty$). Third, it is surprising to observe that, when the *a priori* knowledge of the NLOS biases is available, path overlap can result in a lower SPEB compared to nonoverlapping scenarios. This occurs at certain regions of path separations, depending on the autocorrelation function of $s(t)$. Intuitively, path overlap can lead to a higher SNR compared to nonoverlapping cases, when *a priori* knowledge of the NLOS biases is available.

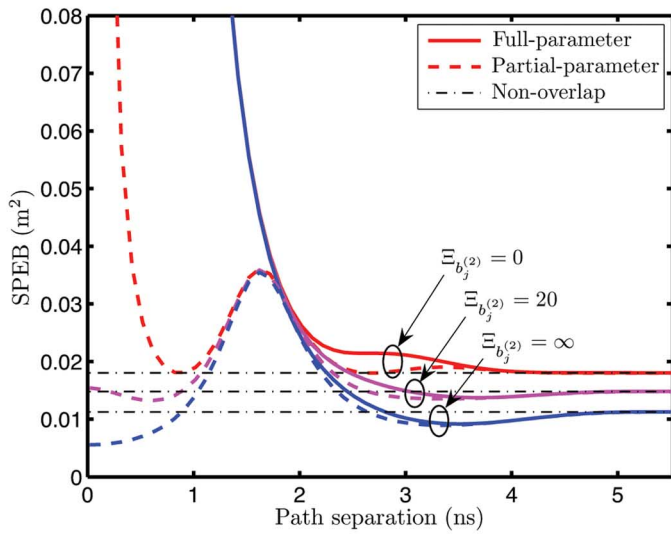
C. Path-Overlap Coefficient

We now investigate the dependence of POC χ on path arrival rate. We first generate channels with L MPCs according to a simple Poisson model with a fixed arrival rate ν , and then calculate χ according to (59). Fig. 7 shows the average path-overlap coefficient as a function of path interarrival rate ($1/\nu$) for different number of MPCs, where the averaging is obtained by Monte Carlo simulations.

We have the following observations. First, the POC χ is monotonically decreasing from 1 to 0 with $1/\nu$. This agrees with our intuition that denser multipath propagation causes more interference between the first path and other MPCs, and hence the received waveform provides less RII. Second, for a fixed ν , the POC increases with L . This should be expected as additional MPCs may interfere with earlier paths, which



(a)



(b)

Fig. 6. SPEB with *a priori* knowledge of the amplitudes and the NLOS biases as a function of path separation, respectively. (a) SPEB with *a priori* knowledge of $\alpha_j^{(1)}$ and $\alpha_j^{(2)}$, while $\Xi_{b_j^{(2)}} = 0$. (b) SPEB with *a priori* knowledge of $b_j^{(2)}$, while $\Xi_{\alpha_j^{(1)}} = \Xi_{\alpha_j^{(2)}} = 0$.

degrades the estimation accuracy of the first path and thus reduces the RII. Third, observe that beyond $L = 5$ paths, χ does not increase significantly. This indicates that the effects of additional MPCs beyond the fifth path on the RII is negligible, regardless of the power dispersion profile of the received waveforms.

D. Outage in Ranging Ability

We have observed that the channel quality for ranging is characterized by the POC. If the multipath propagation has a larger POC (close to 1), we may consider the channel in outage for ranging. We define the ranging ability outage (RAO) probability as

$$p_{\text{out}}(\chi_{\text{th}}) \triangleq \mathbb{P}\{\chi > \chi_{\text{th}}\}$$

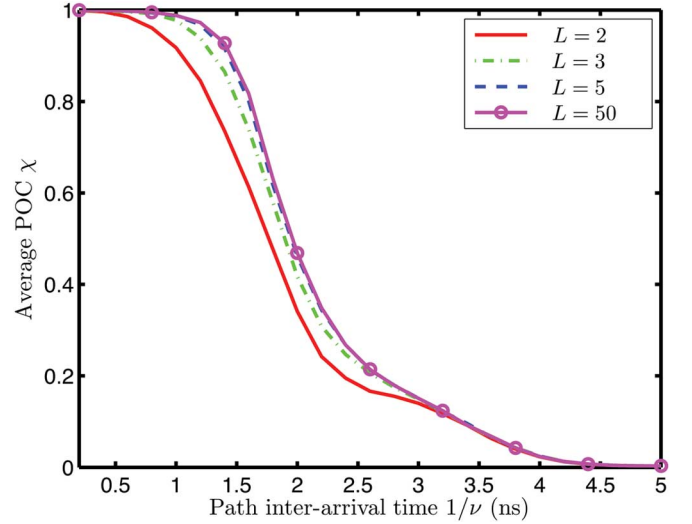


Fig. 7. POC as a function of the path interarrival time for different number of MPCs.

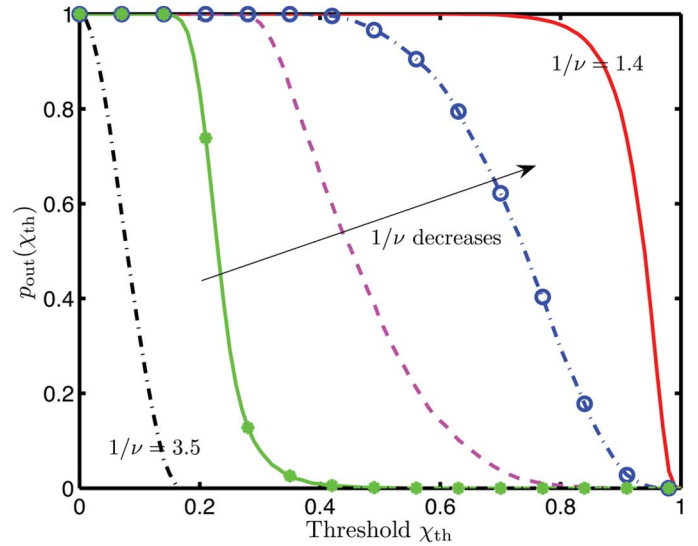


Fig. 8. RAO probability as a function of the threshold χ_{th} for different path interarrival time $1/\nu$ with $L = 50$. The five curves correspond to interarrival time $1/\nu = 3.5, 2.5, 2, 1.6, 1.4$ ns, respectively.

where χ_{th} is the threshold for the POC. The RAO probability tells us that with probability $p_{\text{out}}(\chi_{\text{th}})$, the propagation channel is unsatisfactory for ranging.

The RAO probability as a function of χ_{th} for different Poisson arrival rate is plotted in Fig. 8 for a channel with $L = 50$. The RAO probability decreases from 1 to 0, as the threshold χ_{th} increases or the path arrival rate ν decreases. This should be expected because the probability of path overlap decreases with the path arrival rate, and consequently decreases the RAO probability. The RAO probability can be used as a measure to quantify the channel quality for ranging and to guide the design of the optimal transmitted waveform for ranging.

E. SPEB and SOEB for Wideband Antenna Array Systems

We consider the SPEB and SOEB for different reference points of a uniform linear array (ULA). The numerical results

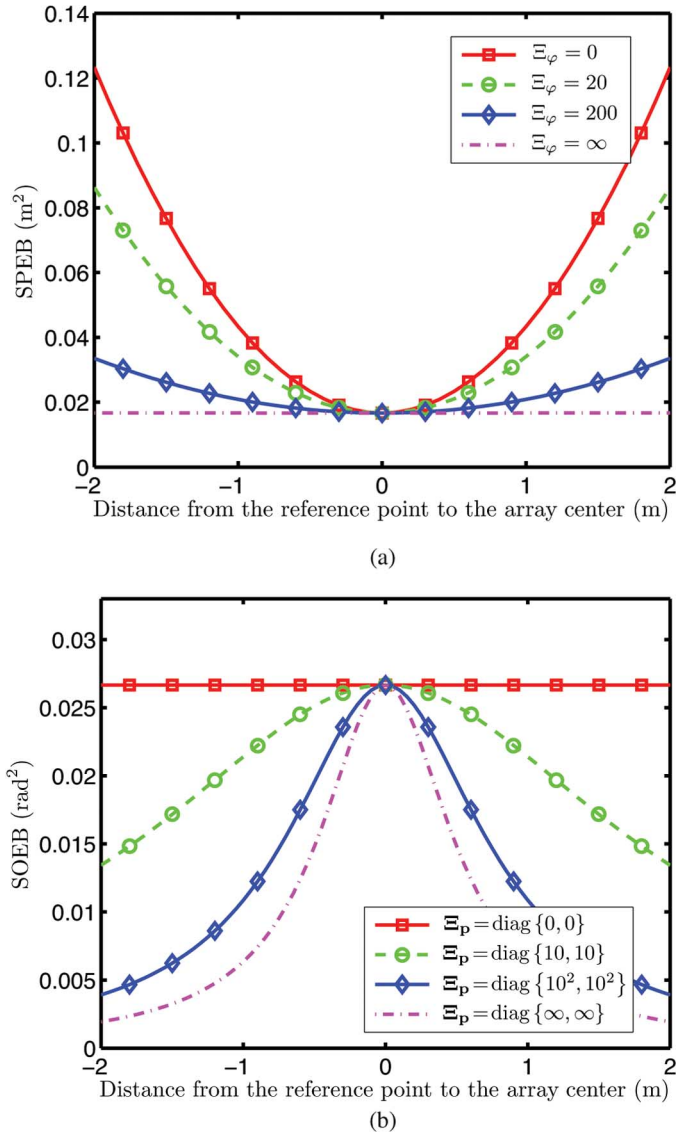


Fig. 9. SPEB and SOEB with different *a priori* knowledge of agent's position and orientation, respectively. (a) SPEB as a function of the reference point-to-array center distance. (b) SOEB as a function of the reference point-to-array center distance.

are based on a network with six equally spaced anchor nodes ($N_b = 6$) located on a circle with an agent in the center. The agent is equipped with a four-antenna array ($N_a = 4$) whose spacing is 0.5 m. In far-field scenarios, $\lambda_{kj} = \lambda_j = 10$ and $\phi_{kj} = \phi_j$. Fig. 9(a) and (b) shows the SPEB and the SOEB, respectively, as a function of different reference point along the ULA for different *a priori* knowledge of the orientation and reference point.

We have the following observations. First, *a priori* knowledge of the orientation improves the localization accuracy as the SPEB decreases with Ξ_φ . The curves for $\Xi_\varphi = 0$ and $\Xi_\varphi = \infty$ correspond to the orientation-unaware and orientation-aware cases, respectively. As a counterpart, *a priori* knowledge of the reference point improves the orientation accuracy as the SOEB decreases with Ξ_p . This agrees with both intuition and Theorem 3. Second, the array center has the best localization accuracy, and its SPEB does not depend on Ξ_φ , which

agrees with Theorem 3. On the other hand, the array center exhibits the worst orientation accuracy, and its SOEB does not depend on Ξ_p . This should be expected since the knowledge for the array center tells nothing about the array orientation. Third, the SPEB increases with both the distance from the reference point to the array center and the SOEB, as predicted by Corollary 5. On the contrary, the SOEB decreases as a function of the distance from the reference point to the array center if *a priori* knowledge of the reference point is available. This observation can be verified by Theorem 3. Last but not least, the SPEB is independent of specific reference point if $\Xi_\varphi = \infty$, as referred to orientation-aware localization, and the SOEB is independent of the specific reference point if $\Xi_p = \mathbf{0}$, as shown in Corollary 5.

F. SPEB With Time Offset and Squared Timing Error Bound

We finally investigate the effect of time offset on the SPEB and squared timing error bound (STEB) for the network illustrated in Fig. 4. The RII from each anchor $\lambda_j = 10$, $j \in \{1, 2, 3, 4\}$. Initially, four anchors are placed at $\phi_1 = 0$, $\phi_2 = \pi/2$, $\phi_3 = \pi$, and $\phi_4 = 3\pi/2$, respectively. We then vary the position of anchor A_1 counterclockwise along the circle. Fig. 10(a) and (b) shows the SPEB and the STEB, respectively, as functions of ϕ_1 for different *a priori* knowledge of the time offset.

We have the following observations. First, both the SPEB and the STEB decrease with the *a priori* knowledge of the time offset. The SPEB for the case $\Xi_B = \infty$ in Fig. 10(a), i.e., known time offset, is equal to that of a system without a time offset. On the other hand, when $\Xi_B = \infty$, the STEB in Fig. 10(b) is equal to zero regardless of ϕ_1 since the offset is completely known. Second, all the curves in Fig. 10(a) have the same value at $\phi_1 = 0$. The time offset has no effect on the SPEB at this point, since $\mathbf{q}_B = \mathbf{0}$, referred to as *time-offset-independent* localization. In this case, both the SPEB and the STEB achieve their minimum, implying that location and timing information of a network are closely related. Third, as ϕ_1 increases from 0 to π , all the curves in Fig. 10(a) first increase and then decrease, whereas all the curves in Fig. 10(b) increase monotonically. We give the following interpretations: the estimation error of time offset in Fig. 10(b) becomes larger when all the anchors tend to gather on one side of the agent (ϕ_1 increases from 0 to π). In Fig. 10(a), the SPEB first increases since both the localization information $\sum_{j \in \mathcal{N}_b} \lambda_j \mathbf{J}_r(\phi_j)$ in (34) and the information for the time offset becomes smaller. Then, the SPEB decreases since the localization information increases (when $\phi_1 > \pi/2$) faster compared to the decrease of the information for time offset. Note in Fig. 10(a) that although $\phi_1 = 0$ and $\phi_1 = \pi$ result in the same SPEB in the absence of time offset, $\phi_1 = 0$ gives a better performance in the presence of time offset.

VIII. CONCLUSION

In this paper, we developed a framework to study wideband wireless location-aware networks and determined their localization accuracy. In particular, we characterized the localization accuracy in terms of a performance measure called the SPEB, and derived the SPEB by applying the notion of EFI. This methodology provides insights into the essence of the localization problem by unifying the localization information from

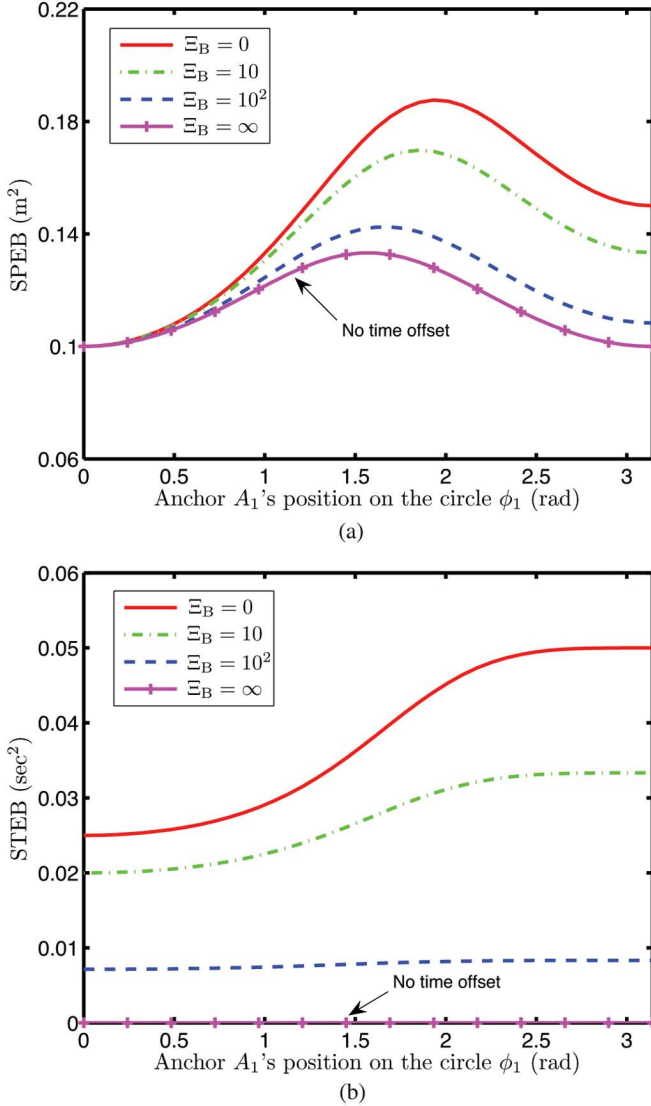


Fig. 10. SPEB and STEB with different *a priori* knowledge of the time offset, and $\Xi_B = 0, 10, 10^2, \infty$, respectively. (a) SPEB as a function of anchor A_1 's position. (b) STEB as a function of anchor A_1 's position.

the *a priori* knowledge of the agent's position and information from individual anchors. We showed that the contributions from anchors, incorporating both measurements and *a priori* channel knowledge, can be expressed in a canonical form as a weighted sum of the RDM. Our results are derived from the received waveforms themselves rather than the signal metrics extracted from the waveforms. Therefore, our framework exploits all the information inherent in the received waveforms, and consequently the results in this paper serve as fundamental limits of localization accuracy. These results can be used as guidelines for localization system design, as well as benchmarks for location-aware networks.

APPENDIX I FISHER INFORMATION MATRIX DERIVATION

To facilitate the analysis, we consider a mapping from θ into another parameter vector $\eta = [\eta_1^T \ \eta_2^T \ \cdots \ \eta_{N_b}^T]^T$, where $\eta_j = [\tau_j^{(1)} \ \tilde{\alpha}_j^{(1)} \ \cdots \ \tau_j^{(L_j)} \ \tilde{\alpha}_j^{(L_j)}]^T$ with $\tilde{\alpha}_j^{(l)} \triangleq \alpha_j^{(l)}/c$.

When the agent is localizable,²⁴ this mapping is a bijection and provides an alternative expression for the FIM as

$$\mathbf{J}_\theta = \mathbf{T} \mathbf{J}_\eta \mathbf{T}^T \quad (38)$$

where \mathbf{J}_η is the FIM for η , and \mathbf{T} is the Jacobian matrix for the transformation from θ to η , given, respectively, by

$$\mathbf{J}_\eta \triangleq \mathbf{F}_r(\mathbf{r}|\theta; \eta, \eta) = \begin{bmatrix} \Lambda_L & \mathbf{0} \\ \mathbf{0} & \Lambda_{NL} \end{bmatrix} \quad (39)$$

and

$$\mathbf{T} \triangleq \frac{\partial \eta}{\partial \theta} = \frac{1}{c} \begin{bmatrix} \mathbf{T}_L & \mathbf{T}_{NL} \\ \mathbf{0} & \mathbf{I} \end{bmatrix} \quad (40)$$

with $\mathbf{0}$ denoting a matrix of all zeros and \mathbf{I} denoting an identity matrix. The block matrices \mathbf{T}_L , \mathbf{T}_{NL} , Λ_L , and Λ_{NL} are given as follows:

$$\mathbf{T}_L = \begin{bmatrix} \mathbf{G}_1 & \mathbf{G}_2 & \cdots & \mathbf{G}_M \\ \mathbf{D}_1 & & & \mathbf{0} \\ & \mathbf{D}_2 & & \\ & & \ddots & \\ \mathbf{0} & & & \mathbf{D}_M \end{bmatrix}$$

$$\mathbf{T}_{NL} = \begin{bmatrix} \mathbf{G}_{M+1} & \cdots & \mathbf{G}_{N_b} \\ \mathbf{0} & \cdots & \mathbf{0} \end{bmatrix}$$

$$\Lambda_L = \text{diag} \{ \Psi_1, \Psi_2, \dots, \Psi_M \} \quad (41)$$

and

$$\Lambda_{NL} = \text{diag} \{ \Psi_{M+1}, \Psi_{M+2}, \dots, \Psi_{N_b} \} \quad (42)$$

where $\mathbf{D}_j = [\mathbf{0} \ \mathbf{I}_{2L_j-1}]$

$$\mathbf{G}_j = \mathbf{q}_j \mathbf{l}_j^T \quad \text{with} \quad \mathbf{l}_j = \underbrace{[1 \ 0 \ \cdots \ 1 \ 0]^T}_{2L_j \text{ components}} \quad (43)$$

$\mathbf{q}_j = [\cos \phi_j \ \sin \phi_j]^T$, and $\Psi_j \in \mathbb{R}^{2L_j \times 2L_j}$ is given by

$$\Psi_j \triangleq \mathbf{F}_r(\mathbf{r}|\theta; \eta_j, \eta_j). \quad (44)$$

Note that elements in Ψ_j can be expressed as

$$\begin{aligned} & \mathbb{E}_r \left\{ -\frac{\partial^2 \ln f(\mathbf{r}|\theta)}{\partial \tau_j^{(i)} \partial \tau_j^{(i')}} \right\} \\ &= \frac{2\alpha_j^{(i)} \alpha_j^{(i')}}{N_0} \int |2\pi f S(f)|^2 \left\{ -j2\pi f (\tau_j^{(i)} - \tau_j^{(i')}) \right\} df \\ &= \frac{2\alpha_j^{(i)} \alpha_j^{(i')}}{N_0} \frac{\partial^2}{\partial \tau_j^{(i)} \partial \tau_j^{(i')}} R_s (\tau_j^{(i)} - \tau_j^{(i')}) \\ & \mathbb{E}_r \left\{ -\frac{\partial^2 \ln f(\mathbf{r}|\theta)}{\partial \tau_j^{(i)} \partial \tilde{\alpha}_j^{(i')}} \right\} \\ &= \frac{2\alpha_j^{(i)} c}{N_0} \int j2\pi f |S(f)|^2 \exp \left\{ -j2\pi f (\tau_j^{(i)} - \tau_j^{(i')}) \right\} df \\ &= \frac{2\alpha_j^{(i)} c}{N_0} \frac{\partial}{\partial \tau_j^{(i)}} R_s (\tau_j^{(i)} - \tau_j^{(i')}) \end{aligned}$$

²⁴Note that an agent is said to be localizable if its position can be determined by the signal metrics extracted from the waveforms received from neighboring anchors, i.e., triangulation is possible. This is true when $M \geq 3$, or in some special cases when $M = 2$.

and

$$\begin{aligned} \mathbb{E}_{\mathbf{r}} \left\{ -\frac{\partial^2 \ln f(\mathbf{r}|\boldsymbol{\theta})}{\partial \tilde{\alpha}_j^{(i)} \partial \tilde{\alpha}_j^{(i')}} \right\} \\ = \frac{2c^2}{N_0} \int |S(f)|^2 \exp \left\{ -j2\pi f \left(\tau_j^{(i)} - \tau_j^{(i')} \right) \right\} df \\ = \frac{2c^2}{N_0} R_s \left(\tau_j^{(i)} - \tau_j^{(i')} \right) \end{aligned}$$

where $R_s(\tau) = \int s(t)s(t-\tau)dt$. In particular

$$[\Psi_j]_{1,1} = \mathbf{F}_{\mathbf{r}} \left(\mathbf{r}|\boldsymbol{\theta}; \tau_j^{(1)}, \tau_j^{(1)} \right) = 8\pi^2 \beta^2 \text{SNR}_j^{(1)} \quad (45)$$

where β and $\text{SNR}_j^{(l)}$ are given by (17) and (18), respectively. Substituting (39) and (40) into (38), we have the FIM $\mathbf{J}_{\boldsymbol{\theta}}$ in (7).

APPENDIX II

WIDEBAND CHANNEL MODEL AND A PRIORI CHANNEL KNOWLEDGE

Wideband channel measurements have shown that MPCs follow random arrival and their amplitudes are subject to path loss, large- and small-scale fading. While our discussion is valid for any wideband channels described by (1), we consider the model of IEEE 802.15.4a standard for exposition. Specifically, this standard uses Poisson arrivals, log-normal shadowing, Nakagami small-scale fading with exponential power dispersion profile (PDP) [26].

A. Path Arrival Time

The arrival time of MPCs is commonly modeled by a Poisson process [26], [64]. Given the path arrival rate ν , we have

$$g_{\tau_j} \left(\tau_j^{(l)} | \tau_j^{(l-1)} \right) = \nu \exp \left\{ -\nu \left(\tau_j^{(l)} - \tau_j^{(l-1)} \right) \right\}$$

for $\tau_j^{(l)} \geq \tau_j^{(l-1)}$ and $l \geq 2$. Using (2), we obtain

$$g_{b_j} \left(b_j^{(l)} | b_j^{(l-1)} \right) = \frac{\nu}{c} \exp \left\{ -\frac{\nu}{c} \left(b_j^{(l)} - b_j^{(l-1)} \right) \right\} \quad (46)$$

for $b_j^{(l)} \geq b_j^{(l-1)}$ and $l \geq 1$. Note that we let $b_j^{(0)} = 0$ for consistency.

B. Path Loss and Large-Scale Fading

The RSS in decibels at the distance d_j can be written as [26]

$$P_j = P_0 - 10\varrho \log_{10} \left(\frac{d_j}{d_0} \right) + w$$

where P_0 is the expected RSS at the reference distance d_0 , ϱ is the propagation (path gain) exponent, and w is a random variable (r.v.) that accounts for large-scale fading, or shadowing.

Shadowing is usually modeled with a log-normal distribution, such that w is a Gaussian r.v. with zero-mean and variance σ_S^2 , i.e., $w \sim N(0, \sigma_S^2)$.²⁵ The pdf of the RSS of $r_j(t)$ can then be written as

$$g_P(P_j | d_j) \propto \exp \left\{ -\frac{1}{2\sigma_S^2} \left[P_j - P_0 + 10\varrho \log_{10} \left(\frac{d_j}{d_0} \right) \right]^2 \right\} \quad (47)$$

where $d_j = \|\mathbf{p} - \mathbf{p}_j\|$, and P_j is given by

$$P_j = 10 \log_{10} \left[\sum_{l=1}^{L_j} \mathbb{E}_s \left\{ |\alpha_j^{(l)}|^2 \right\} \right]$$

with $\mathbb{E}_s\{\cdot\}$ denoting the average over small-scale fading.

C. Power Dispersion Profile and Small-Scale Fading

As in [24] and [26], we consider an exponential PDP given by²⁶

$$\mathbb{E}_s \left\{ |\alpha_j^{(l)}|^2 \right\} = Q_j \exp \left(-\frac{\tau_j^{(l)}}{\gamma_j} \right) \triangleq Q_j^{(l)} \quad (48)$$

where γ_j is the decay constant, and Q_j is a normalization coefficient such that

$$Q_j = \frac{10^{P_j/10}}{\sum_{l=0}^{L_j} \exp \left(-\tau_j^{(l)}/\gamma_j \right)} \quad (49)$$

In addition, $\alpha_j^{(l)}$ is a Nakagami r.v. with second moment given by (48). Specifically, we have

$$\begin{aligned} g_{\alpha_j} \left(\alpha_j^{(l)} | \mathbf{b}_j, d_j, P_j \right) &= g_{\alpha_j} \left(\alpha_j^{(l)} | \tau_j, P_j \right) \\ &= \frac{2}{\Gamma(m_l)} \left(\frac{m_l}{Q_j^{(l)}} \right)^{m_l} \left| \alpha_j^{(l)} \right|^{2m_l-1} \\ &\quad \times \exp \left(-\frac{m_l}{Q_j^{(l)}} \left| \alpha_j^{(l)} \right|^2 \right) \end{aligned} \quad (50)$$

where $\Gamma(m_l)$ is the gamma function and $m_l \geq 1/2$ is the Nakagami m -factor, which is a function of τ_j [26].

1) *A Priori PDF for Multipath Parameters:* The joint pdf of the multipath parameters and the RSS, conditioned on the distance from anchor j to the agent, can be derived as

$$\begin{aligned} f(\boldsymbol{\alpha}_j, \mathbf{b}_j, P_j | d_j) &= g_P(P_j | d_j) \prod_{l=1}^{L_j} g_{\alpha_j} \left(\alpha_j^{(l)} | \mathbf{b}_j, d_j, P_j \right) \\ &\quad \times \prod_{l=1}^{L_j} g_{b_j} \left(b_j^{(l)} | b_j^{(l-1)} \right). \end{aligned} \quad (51)$$

²⁵The standard deviation is typically 1–2 dB (LOS) and 2–6 dB (NLOS) [21] around the path gain.

²⁶Note that the first component of LOS signals can exhibit a stronger strength than (48) in some UWB measurement [72]. In such cases, (48) and (49) need to be modified, accordingly.

By integrating over P_j , we obtain the pdf of the multipath parameters of $r_j(t)$ as follows:

$$f(\boldsymbol{\kappa}_j|d_j) = f(\boldsymbol{\alpha}_j, \mathbf{b}_j|d_j) = \int_{-\infty}^{\infty} f(\boldsymbol{\alpha}_j, \mathbf{b}_j, P_j|d_j) dP_j. \quad (52)$$

Equation (52) characterizes the *a priori* knowledge of channel parameters, and can be obtained, for IEEE 802.15.4a standard, by substituting (46), (47), and (50) into (51) and (52). Note that since \mathbf{p}_j is known, d_j is a function of \mathbf{p} and hence we have (9).

APPENDIX III

PROOFS OF THE RESULTS IN SECTION III

A. Proof of Theorem 1

Proof: We first prove that $\mathbf{J}_e(\mathbf{p})$ is given by (15). We partition \mathbf{G}_j in (43) and $\check{\Psi}_j$ in (44) as

$$\mathbf{G}_j \triangleq [\mathbf{q}_j \quad \check{\mathbf{G}}_j] \quad \text{and} \quad \check{\Psi}_j = \begin{bmatrix} 8\pi^2\beta^2\text{SNR}_j^{(1)} & \mathbf{k}_j^T \\ \mathbf{k}_j & \check{\Psi}_j \end{bmatrix}$$

where $[\check{\Psi}_j]_{1,1}$ is obtained by (45), $\mathbf{k}_j \in \mathbb{R}^{2L_j-1}$, $\check{\Psi}_j \in \mathbb{R}^{(2L_j-1) \times (2L_j-1)}$, and

$$\check{\mathbf{G}}_j = \mathbf{q}_j \underbrace{[0 \quad 1 \quad 0 \quad \dots \quad 1 \quad 0]^T}_{2L_j-1 \text{ components}}.$$

Using these notations, we can write the EFIM given by (14) in Proposition 1, after some algebra, in the form of (12)

$$\mathbf{A} \triangleq 8\pi^2\beta^2 \sum_{j \in \mathcal{N}_L} \text{SNR}_j^{(1)} \mathbf{q}_j \mathbf{q}_j^T + \sum_{j \in \mathcal{N}_L} \left\{ \check{\mathbf{G}}_j \mathbf{k}_j \mathbf{q}_j^T + \mathbf{q}_j \mathbf{k}_j^T \check{\mathbf{G}}_j^T + \check{\mathbf{G}}_j \check{\Psi}_j \check{\mathbf{G}}_j^T \right\}$$

$$\mathbf{B} \triangleq [\mathbf{q}_1 \mathbf{k}_1^T + \check{\mathbf{G}}_1 \check{\Psi}_1 \quad \dots \quad \mathbf{q}_M \mathbf{k}_M^T + \check{\mathbf{G}}_M \check{\Psi}_M]$$

and

$$\mathbf{C} \triangleq \text{diag} \left\{ \check{\Psi}_1, \check{\Psi}_2, \dots, \check{\Psi}_M \right\}.$$

Applying the notion of EFI as in (13), we obtain the 2×2 $\mathbf{J}_e(\mathbf{p})$ as

$$\mathbf{J}_e(\mathbf{p}) = \frac{8\pi^2\beta^2}{c^2} \sum_{j \in \mathcal{N}_L} (1 - \chi_j) \text{SNR}_j^{(1)} \mathbf{q}_j \mathbf{q}_j^T \quad (53)$$

where the POC

$$\chi_j \triangleq \frac{\mathbf{k}_j^T \check{\Psi}_j^{-1} \mathbf{k}_j}{8\pi^2\beta^2 \text{SNR}_j^{(1)}}. \quad (54)$$

This completes the proof of (15).

Next, we show that only the first contiguous cluster contains information for localization. Let us focus on χ_j . Define the

following notations for convenience:

$$R_s(i, i') \triangleq R_s(t)|_{t=\tau_j^{(i)}-\tau_j^{(i')}}$$

$$\ddot{R}_s(i, i') \triangleq -\frac{\partial^2}{\partial t^2} R_s(t)|_{t=\tau_j^{(i)}-\tau_j^{(i')}}$$

and

$$\dot{R}_s(i, i') \triangleq \frac{\partial}{\partial t} R_s(t)|_{t=\tau_j^{(i)}-\tau_j^{(i')}} = -\dot{R}_s(i', i).$$

If the length of the first contiguous cluster in the received waveform is \tilde{L}_j where $1 \leq \tilde{L}_j \leq L_j$, then $\ddot{R}_s(i, i') = \dot{R}_s(i, i') = R_s(i, i') = 0$ for $i \in \{1, 2, \dots, \tilde{L}_j\}$ and $i' \in \{\tilde{L}_j + 1, \tilde{L}_j + 2, \dots, L_j\}$, and²⁷

$$\tilde{\mathbf{k}}_j \triangleq [\tilde{\mathbf{k}}_j^T \quad \mathbf{0}^T]^T \quad \text{and} \quad \check{\Psi}_j \triangleq \begin{bmatrix} \check{\Psi}_j & \mathbf{0} \\ \mathbf{0} & \boxtimes \end{bmatrix}$$

where $\tilde{\mathbf{k}}_j \in \mathbb{R}^{2\tilde{L}_j-1}$ and $\check{\Psi}_j \in \mathbb{R}^{(2\tilde{L}_j-1) \times (2\tilde{L}_j-1)}$. Hence, (54) becomes

$$\chi_j = \frac{\tilde{\mathbf{k}}_j^T \check{\Psi}_j^{-1} \tilde{\mathbf{k}}_j}{8\pi^2\beta^2 \text{SNR}_j^{(1)}} \quad (55)$$

which depends only on the first \tilde{L}_j paths, implying that only the first contiguous cluster of LOS signals contains information for localization.

Finally, we show that χ_j is independent of $\alpha_j^{(l)}$. Note that $\check{\Psi}_j$ and $\tilde{\mathbf{k}}_j$ can be written as

$$\check{\Psi}_j = \frac{2}{N_0} \text{diag} \left\{ c, \alpha_j^{(2)}, c, \dots, \alpha_j^{(L_j)}, c \right\} \boldsymbol{\Upsilon}_j \times \text{diag} \left\{ c, \alpha_j^{(2)}, c, \dots, \alpha_j^{(L_j)}, c \right\} \quad (56)$$

and

$$\tilde{\mathbf{k}}_j = \frac{2\alpha_j^{(1)}}{N_0} \text{diag} \left\{ c, \alpha_j^{(2)}, c, \dots, \alpha_j^{(L_j)}, c \right\} \mathbf{t}_j \quad (57)$$

where $\boldsymbol{\Upsilon}_j \in \mathbb{R}^{(2\tilde{L}_j-1) \times (2\tilde{L}_j-1)}$ and $\mathbf{t}_j \in \mathbb{R}^{2\tilde{L}_j-1}$ are given by the matrix partition in (58), shown at the bottom of the next page. Substituting (56) and (57) into (55), we obtain

$$\chi_j = \frac{1}{4\pi^2\beta^2} \mathbf{t}_j^T \boldsymbol{\Upsilon}_j^{-1} \mathbf{t}_j \quad (59)$$

which is independent of all the amplitudes.

Note that $0 \leq \chi_j \leq 1$: χ_j is nonnegative since it is a quadratic form and $\boldsymbol{\Upsilon}_j$ is a positive-semidefinite FIM (hence is $\boldsymbol{\Upsilon}_j^{-1}$); and $\chi_j \leq 1$ since the contribution from each anchor to the EFIM in (53) is nonnegative. \square

B. Proof of Corollary 1

Proof: This scenario can be thought of as a special case of Theorem 1 with $\tilde{L}_j = 1$, i.e., the first contiguous cluster contains only one path. In this case, (59) becomes

$$\chi_j = \frac{1}{4\pi^2\beta^2} \frac{\dot{R}_s^2(1, 1)}{R_s(1, 1)}.$$

²⁷ \boxtimes is a block matrix that is irrelevant to the rest of the derivation.

Since waveform $s(t)$ is continuous and time limited in realistic cases, we have

$$\dot{R}_s(1, 1) = \frac{\partial}{\partial \tau} R_s(\tau)|_{\tau=0} = 0$$

implying that $\chi_j = 0$, which leads to (19). \square

C. Proof of Theorem 2

Proof: When *a priori* channel knowledge of the channel is available, the FIM is

$$\mathbf{J}_\theta = \frac{1}{c^2} \begin{bmatrix} \mathbf{T}_{\text{NL}} \bar{\mathbf{A}}_{\text{NL}} \mathbf{T}_{\text{NL}}^T + \mathbf{T}_L \bar{\mathbf{A}}_L \mathbf{T}_L^T & \mathbf{T}_{\text{NL}} \bar{\mathbf{A}}_{\text{NL}} \\ \bar{\mathbf{A}}_{\text{NL}} \mathbf{T}_{\text{NL}}^T & \bar{\mathbf{A}}_{\text{NL}} \end{bmatrix} + \mathbf{J}_p$$

where $\bar{\mathbf{A}}_{\text{NL}} = \mathbb{E}_\theta \{\mathbf{A}_{\text{NL}}\} \triangleq \text{diag} \{ \bar{\Psi}_1, \bar{\Psi}_2, \dots, \bar{\Psi}_M \}$ and $\bar{\mathbf{A}}_L = \mathbb{E}_\theta \{\mathbf{A}_L\} \triangleq \text{diag} \{ \bar{\Psi}_{M+1}, \bar{\Psi}_{M+2}, \dots, \bar{\Psi}_{N_b} \}$. The FIM \mathbf{J}_θ can be partitioned as (12), where \mathbf{A} is given by (60), shown at the bottom of the page, and

$$\mathbf{B} \triangleq \begin{bmatrix} \mathbf{G}_{M+1} \bar{\Psi}_{M+1} + c^2 \Xi_{p,\kappa}^{M+1} & \dots & \mathbf{G}_{N_b} \bar{\Psi}_{N_b} + c^2 \Xi_{p,\kappa}^{N_b} \\ \mathbf{0} & \dots & \mathbf{0} \end{bmatrix}$$

and

$$\mathbf{C} \triangleq \text{diag} \{ \bar{\Psi}_{M+1} + c^2 \Xi_{\kappa,\kappa}^{M+1}, \dots, \bar{\Psi}_{N_b} + c^2 \Xi_{\kappa,\kappa}^{N_b} \}.$$

Applying the notion of EFI, we have the 2×2 EFIM, after some algebra, given by (61), shown at the bottom of the page. From (9), we can rewrite $\Xi_{p,p}^j$ and $\Xi_{p,\kappa}^j$ in (11) using chain rule as

$$\Xi_{p,p}^j = \mathbf{q}_j \Xi_{d,d}^j \mathbf{q}_j^T \quad \text{and} \quad \Xi_{p,\kappa}^j = \mathbf{q}_j \Xi_{d,\kappa}^j \quad (62)$$

where $\Xi_{d,d}^j = \mathbf{F}_\theta(\kappa_j | d_j; d_j, d_j)$ and $\Xi_{d,\kappa}^j = \mathbf{F}_\theta(\kappa_j | d_j; d_j, \kappa_j)$. Substituting (62) into (61) leads to (21), where λ_j is given by (63a)–(63b), shown at the bottom of the page, for LOS signals and NLOS signals, respectively. \square

D. Proof of Corollary 2

Proof: We first show that the *a priori* channel knowledge increases the RII. Consider λ_j in (63a). Let

$$\mathbf{F}_j \triangleq \frac{1}{c^2} \begin{bmatrix} \mathbf{I}_j^T \bar{\Psi}_j \mathbf{I}_j + c^2 \Xi_{d,d}^j & \mathbf{I}_j^T \bar{\Psi}_j \mathbf{D}_j^T + c^2 \Xi_{d,\kappa}^j \\ \mathbf{D}_j \bar{\Psi}_j \mathbf{I}_j + c^2 \Xi_{p,\kappa}^{jT} & \mathbf{D}_j \bar{\Psi}_j \mathbf{D}_j^T + c^2 \Xi_{\kappa,\kappa}^j \end{bmatrix}$$

and

$$\mathbf{E}_j \triangleq \frac{1}{c^2} \begin{bmatrix} \mathbf{I}_j^T \bar{\Psi}_j \mathbf{I}_j & \mathbf{I}_j^T \bar{\Psi}_j \mathbf{d}_j^T \\ \mathbf{D}_j \bar{\Psi}_j \mathbf{I}_j & \mathbf{D}_j \bar{\Psi}_j \mathbf{D}_j^T \end{bmatrix}.$$

$$\begin{bmatrix} \ddot{R}_s(1, 1) & \dot{R}_s(1, 1) & \ddot{R}_s(1, 2) & \dot{R}_s(1, 2) & \dots & \ddot{R}_s(1, \tilde{L}_j) & \dot{R}_s(1, \tilde{L}_j) \\ \dot{R}_s(1, 1) & R_s(1, 1) & -\dot{R}_s(1, 2) & R_s(1, 2) & \dots & -\dot{R}_s(1, \tilde{L}_j) & R_s(1, \tilde{L}_j) \\ \ddot{R}_s(1, 2) & -\dot{R}_s(1, 2) & & & & & \\ \dot{R}_s(1, 2) & R_s(1, 2) & & & & & \\ \vdots & \vdots & & & & & \\ \ddot{R}_s(1, \tilde{L}_j) & -\dot{R}_s(1, \tilde{L}_j) & \dots & & & \ddot{R}_s(\tilde{L}_j, \tilde{L}_j) & \dot{R}_s(\tilde{L}_j, \tilde{L}_j) \\ \dot{R}_s(1, \tilde{L}_j) & R_s(1, \tilde{L}_j) & \dots & & & \dot{R}_s(\tilde{L}_j, \tilde{L}_j) & R_s(\tilde{L}_j, \tilde{L}_j) \end{bmatrix} \quad (58)$$

$$\mathbf{A} \triangleq \begin{bmatrix} \sum_{j \in \mathcal{N}_b} \mathbf{G}_j \bar{\Psi}_j \mathbf{G}_j^T + c^2 \Xi_{p,p}^j & \mathbf{G}_1 \bar{\Psi}_1 \mathbf{D}_1^T + c^2 \Xi_{p,\kappa}^1 & \dots & \mathbf{G}_M \bar{\Psi}_M \mathbf{D}_M^T + c^2 \Xi_{p,\kappa}^M \\ \left(\mathbf{G}_1 \bar{\Psi}_1 \mathbf{D}_1^T + c^2 \Xi_{p,\kappa}^1 \right)^T & \mathbf{D}_1 \bar{\Psi}_1 \mathbf{D}_1^T + c^2 \Xi_{\kappa,\kappa}^1 & & \\ \vdots & & \ddots & \\ \left(\mathbf{G}_M \bar{\Psi}_M \mathbf{D}_M^T + c^2 \Xi_{p,\kappa}^M \right)^T & & & \mathbf{D}_M \bar{\Psi}_M \mathbf{D}_M^T + c^2 \Xi_{\kappa,\kappa}^M \end{bmatrix} \quad (60)$$

$$\mathbf{J}_e(\mathbf{p}) = \frac{1}{c^2} \left\{ \sum_{j \in \mathcal{N}_b} \left(\mathbf{G}_j \bar{\Psi}_j \mathbf{g}_j^T + c^2 \Xi_{p,p}^j \right) - \sum_{j \in \mathcal{N}_L} \left(\mathbf{G}_j \bar{\Psi}_j \mathbf{d}_j^T + c^2 \Xi_{p,\kappa}^j \right) \left(\mathbf{D}_j \bar{\Psi}_j \mathbf{D}_j^T + c^2 \Xi_{\kappa,\kappa}^j \right)^{-1} \left(\mathbf{G}_j \bar{\Psi}_j \mathbf{D}_j^T + c^2 \Xi_{p,\kappa}^j \right)^T \right. \\ \left. - \sum_{j \in \mathcal{N}_{\text{NL}}} \left(\mathbf{G}_j \bar{\Psi}_j + c^2 \Xi_{p,\kappa}^j \right) \left(\bar{\Psi}_j + c^2 \Xi_{\kappa,\kappa}^j \right)^{-1} \left(\mathbf{G}_j \bar{\Psi}_j + c^2 \Xi_{p,\kappa}^j \right)^T \right\}. \quad (61)$$

$$\lambda_j \triangleq \frac{1}{c^2} \left\{ \mathbf{I}_j^T \bar{\Psi}_j \mathbf{I}_j + c^2 \Xi_{d,d}^j - \left(\mathbf{I}_j^T \bar{\Psi}_j \mathbf{D}_j^T + c^2 \Xi_{d,\kappa}^j \right) \left(\mathbf{D}_j \bar{\Psi}_j \mathbf{D}_j^T + c^2 \Xi_{\kappa,\kappa}^j \right)^{-1} \left(\mathbf{I}_j^T \bar{\Psi}_j \mathbf{D}_j^T + c^2 \Xi_{d,\kappa}^j \right)^T \right\}, \quad j \in \mathcal{N}_L \quad (63a)$$

$$\lambda_j \triangleq \frac{1}{c^2} \left\{ \mathbf{I}_j^T \bar{\Psi}_j \mathbf{I}_j + c^2 \Xi_{d,d}^j - \left(\mathbf{I}_j^T \bar{\Psi}_j + c^2 \Xi_{d,\kappa}^j \right) \left(\bar{\Psi}_j + c^2 \Xi_{\kappa,\kappa}^j \right)^{-1} \left(\mathbf{I}_j^T \bar{\Psi}_j + c^2 \Xi_{d,\kappa}^j \right)^T \right\}, \quad j \in \mathcal{N}_{\text{NL}} \quad (63b)$$

We have $\mathbf{F}_j \succeq \mathbf{E}_j$, since

$$\mathbf{F}_j - \mathbf{E}_j = \begin{bmatrix} \Xi_{d,d}^j & \Xi_{d,\kappa}^j \\ \Xi_{p,\kappa}^j & \Xi_{\kappa,\kappa}^j \end{bmatrix} = \mathbf{F}_{\theta}(\kappa_j | d_j; \tilde{\theta}_j, \tilde{\theta}_j) \succeq \mathbf{0}$$

where $\tilde{\theta}_j = [d_j \ \kappa_j^T]^T$. Hence, we have $\lambda_j = 1/[\mathbf{F}_j^{-1}]_{1,1} \geq 1/[\mathbf{E}_j^{-1}]_{1,1}$, where $[\mathbf{E}_j^{-1}]_{1,1}$ equals (16). This implies that the *a priori* channel knowledge can increase the RII.

We next show that the RIIs in (63a)–(63b) reduce to (16) and zero, respectively, in the absence of a *a priori* channel knowledge.

When *a priori* channel knowledge is unavailable, $\Xi_{\kappa,\kappa}^j$, $\Xi_{p,\kappa}^j$, and $\Xi_{d,\kappa}^j$ all equal zero, and the corresponding RII λ_j in (63a)–(63b) becomes

$$\begin{aligned} \lambda_j &= \frac{1}{c^2} \left\{ \mathbf{1}_j^T \bar{\Psi}_j \mathbf{1}_j - (\mathbf{1}_j^T \bar{\Psi}_j \mathbf{D}_j^T) (\mathbf{D}_j \bar{\Psi}_j \mathbf{D}_j^T)^{-1} (\mathbf{D}_j \bar{\Psi}_j \mathbf{1}_j) \right\} \\ &= \frac{1}{c^2} \mathbf{1}_j^T \left\{ \begin{bmatrix} 8\pi^2 \beta^2 \text{SNR}_j^{(1)} & \mathbf{k}_j^T \\ \mathbf{k}_j & \check{\Psi}_j \end{bmatrix} - \begin{bmatrix} \mathbf{k}_j^T \\ \check{\Psi}_j \end{bmatrix} \check{\Psi}_j^{-1} \begin{bmatrix} \mathbf{k}_j & \check{\Psi}_j \end{bmatrix} \right\} \mathbf{1}_j \\ &= \frac{1}{c^2} \left\{ 8\pi^2 \beta^2 \text{SNR}_j^{(1)} - \mathbf{k}_j^T \check{\Psi}_j^{-1} \mathbf{k}_j \right\} \\ &= \frac{8\pi^2 \beta^2}{c^2} (1 - \chi_j) \text{SNR}_j^{(1)} \end{aligned}$$

for $j \in \mathcal{N}_L$, and

$$\lambda_j = \frac{1}{c^2} \left\{ \mathbf{1}_j^T \bar{\Psi}_j \mathbf{1}_j - \mathbf{1}_j^T \bar{\Psi}_j \bar{\Psi}_j^{-1} \bar{\Psi}_j \mathbf{1}_j \right\} = 0$$

for $j \in \mathcal{N}_{NL}$. \square

E. Proof of Corollary 3

Proof: The block matrices $\Xi_{\kappa,\kappa}^j$ and $\Xi_{d,\kappa}^j$ in (11) for NLOS signals can be written as

$$\Xi_{\kappa,\kappa}^j = \begin{bmatrix} t^2 & \mathbf{v}_j^T \\ \mathbf{v}_j & \check{\Xi}_{\kappa,\kappa}^j \end{bmatrix} \quad \text{and} \quad \Xi_{d,\kappa}^j = \begin{bmatrix} w & \check{\Xi}_{d,\kappa}^j \end{bmatrix}$$

where $\mathbf{v}_j, \check{\Xi}_{\kappa,\kappa}^j \in \mathbb{R}^{2L_j-1}$, and $\check{\Xi}_{d,\kappa}^j \in \mathbb{R}^{(2L_j-1) \times (2L_j-1)}$. Note that t^2 corresponds to the Fisher information of $b_j^{(1)}$. When the *a priori* knowledge of $b_j^{(1)}$ goes to ∞ , i.e., $g_b(b_j^{(1)}) \rightarrow \delta(b_j^{(1)})$, we claim that

$$\lim_{t^2 \rightarrow \infty} \left[\bar{\Psi}_j + c^2 \Xi_{\kappa,\kappa}^j \right]^{-1} = \begin{bmatrix} 0 & \mathbf{0}^T \\ \mathbf{0} & (\mathbf{D}_j \bar{\Psi}_j \mathbf{D}_j^T + c^2 \check{\Xi}_{\kappa,\kappa}^j)^{-1} \end{bmatrix}. \quad (64)$$

To show this, we partition $\bar{\Psi}_j$ as

$$\bar{\Psi}_j = \begin{bmatrix} u_j^2 & \mathbf{k}_j^T \\ \mathbf{k}_j & \check{\Psi}_j \end{bmatrix}$$

and then the left-hand side of (64) becomes

$$\begin{aligned} \text{LHS} &= \lim_{t^2 \rightarrow \infty} \begin{bmatrix} u_j^2 + c^2 t^2 & \mathbf{k}_j^T + c^2 \mathbf{v}_j^T \\ \mathbf{k}_j + c^2 \mathbf{v}_j & \check{\Psi}_j + c^2 \check{\Xi}_{\kappa,\kappa}^j \end{bmatrix}^{-1} \\ &= \lim_{t^2 \rightarrow \infty} \begin{bmatrix} A & B \\ B^T & C \end{bmatrix} \end{aligned}$$

where

$$A \triangleq \begin{bmatrix} u_j^2 + c^2 t^2 \\ -(\mathbf{k}_j + c^2 \mathbf{v}_j)^T (\check{\Psi}_j + c^2 \check{\Xi}_{\kappa,\kappa}^j)^{-1} (\mathbf{k}_j + c^2 \mathbf{v}_j) \end{bmatrix}^{-1}$$

$$B \triangleq -\frac{1}{u_j^2 + c^2 t^2} (\mathbf{k}_j + c^2 \mathbf{v}_j) \mathbf{C}^{-1}$$

and

$$C \triangleq \begin{bmatrix} \check{\Psi}_j + c^2 \check{\Xi}_{\kappa,\kappa}^j \\ -\frac{1}{u_j^2 + c^2 t^2} (\mathbf{k}_j + c^2 \mathbf{v}_j) (\mathbf{k}_j + c^2 \mathbf{v}_j)^T \end{bmatrix}^{-1}.$$

When $b_j^{(1)}$ is known, i.e., $t^2 \rightarrow \infty$, we have $\lim_{t^2 \rightarrow \infty} A = 0$, $\lim_{t^2 \rightarrow \infty} B = \mathbf{0}$, and $\lim_{t^2 \rightarrow \infty} C = \left[\check{\Psi}_j + c^2 \check{\Xi}_{\kappa,\kappa}^j \right]^{-1}$. Notice that $\check{\Psi}_j = \mathbf{D}_j \bar{\Psi}_j \mathbf{D}_j^T$. Hence, we proved our claim in (64).

Substituting (64) into (63b), we have

$$\begin{aligned} \lim_{t^2 \rightarrow \infty} \lambda_j &= \frac{1}{c^2} \left\{ \mathbf{1}_j^T \bar{\Psi}_j \mathbf{1}_j + c^2 \Xi_{d,d}^j - \left(\mathbf{1}_j^T \bar{\Psi}_j \mathbf{D}_j^T + c^2 \check{\Xi}_{d,\kappa}^j \right) \right. \\ &\quad \times \left(\mathbf{D}_j \bar{\Psi}_j \mathbf{D}_j^T + c^2 \check{\Xi}_{\kappa,\kappa}^j \right)^{-1} \\ &\quad \left. \times \left(\mathbf{1}_j^T \bar{\Psi}_j \mathbf{D}_j^T + c^2 \check{\Xi}_{d,\kappa}^j \right)^T \right\} \end{aligned}$$

for $j \in \mathcal{N}_{NL}$, which agrees with the RII of LOS signals in (63a).²⁸ Hence, LOS signals are equivalent to NLOS with infinite *a priori* knowledge of $b_j^{(1)}$ for localization. \square

F. Proof of Proposition 2

Proof: Note that $\mathbf{q}_j, \bar{\Psi}_j, \Xi_{p,p}^j, \Xi_{\kappa,\kappa}^j$, and $\Xi_{d,\kappa}^j$ are functions of \mathbf{p} when *a priori* knowledge of the agent's position is available. Hence, we need to take expectation of them over \mathbf{p} in (10). After some algebra, we have the EFIM for the agent's position as (65), shown at the bottom of the next page.

When the condition in (22) is satisfied for the functions $g(\mathbf{p})$'s: 1) $\mathbf{q}_j \Xi_{d,d}^j \mathbf{q}_j^T$, 2) $\mathbf{q}_j \mathbf{1}_j^T \bar{\Psi}_j \mathbf{1}_j \mathbf{q}_j^T$, 3) $\mathbf{q}_j \left(\mathbf{1}_j^T \bar{\Psi}_j + c^2 \Xi_{d,\kappa}^j \right)$, and 4) $\bar{\Psi}_j + \Xi_{\kappa,\kappa}^j$, we can approximate the expectation of each function over \mathbf{p} in (65) by the function value at the expected position $\bar{\mathbf{p}}$. Hence, the EFIM in (65) can be expressed as

$$\begin{aligned} \mathbf{J}_e(\mathbf{p}) &= \Xi_{\mathbf{p}} + \frac{1}{c^2} \sum_{j \in \mathcal{N}_b} \left\{ \mathbf{q}_j \left(\mathbf{1}_j^T \bar{\Psi}_j \mathbf{1}_j + c^2 \Xi_{d,d}^j \right) \mathbf{q}_j^T \right. \\ &\quad - \mathbf{q}_j \left(\mathbf{1}_j^T \bar{\Psi}_j + c^2 \Xi_{d,\kappa}^j \right) \left(\bar{\Psi}_j + \Xi_{\kappa,\kappa}^j \right)^{-1} \\ &\quad \left. \times \left(\mathbf{1}_j^T \bar{\Psi}_j + c^2 \Xi_{d,\kappa}^j \right)^T \mathbf{q}_j^T \right\} \\ &= \Xi_{\mathbf{p}} + \sum_{j \in \mathcal{N}_b} \bar{\lambda}_j \mathbf{J}_r(\bar{\phi}_j) \end{aligned}$$

²⁸Note that the size of $\Xi_{\kappa,\kappa}^j$ and $\Xi_{d,\kappa}^j$ for LOS signals and NLOS signals are different for the same L_j . Indeed, $\check{\Xi}_{\kappa,\kappa}^j$ and $\check{\Xi}_{d,\kappa}^j$ are not associated with $b_j^{(1)}$, and hence they are in the same form as $\Xi_{\kappa,\kappa}^j$ and $\Xi_{d,\kappa}^j$ for LOS signals in (63a).

where $\bar{\phi}_j$ is the angle from anchor j to $\bar{\mathbf{p}}$, and $\bar{\lambda}_j$ is given by (66), shown at the bottom of the page. Note that all functions are evaluated at $\bar{\mathbf{p}}$. \square

APPENDIX IV

PROOFS OF THE RESULTS IN SECTION IV

A. Proof of Theorem 3

Note that this proof also incorporates the *a priori* channel knowledge. In the absence of this knowledge, the corresponding results can be obtained by removing \mathbf{J}_p that characterizes the *a priori* channel knowledge.

Since \mathbf{p} and φ are deterministic but unknown, the joint likelihood function of the random vectors \mathbf{r} and $\boldsymbol{\theta}$ can be written as

$$f(\mathbf{r}, \boldsymbol{\theta}) = f(\mathbf{r}|\boldsymbol{\theta})f(\boldsymbol{\theta}) = \prod_{k \in \mathcal{N}_a} \prod_{j \in \mathcal{N}_b} f(\mathbf{r}_{kj}|\boldsymbol{\theta})f(\boldsymbol{\kappa}_{kj}|\mathbf{p}, \varphi).$$

Note that $f(\boldsymbol{\kappa}_{kj}|\mathbf{p}, \varphi) = f(\boldsymbol{\kappa}_{kj}|d_{kj})$, and the FIM \mathbf{J}_p from $f(\boldsymbol{\theta})$ can be expressed as (67), shown at the bottom of the page, where $\Xi_{\mathbf{p}, \mathbf{p}}^{kj} = \mathbf{q}_{kj} \Xi_{d,d}^{kj} \mathbf{q}_{kj}^T$, $\Xi_{\mathbf{p}, \varphi}^{kj} = \mathbf{q}_{kj} \Xi_{d,d}^{kj} h_{kj}$, and $\Xi_{\varphi, \varphi}^{kj} = h_{kj}^2 \Xi_{d,d}^{kj}$, in which

$$\Xi_{d,d}^{kj} \triangleq \mathbf{F}_{\boldsymbol{\theta}}(\mathbf{r}_{kj}|\boldsymbol{\theta}; d_{kj}, d_{kj}).$$

Block matrices $\Xi_{\mathbf{p}, k}$, $\Xi_{\varphi, k}$, and Ξ_k correspond to the k th antenna in the array, and they can be further decomposed into block matrices corresponding to each anchor

$$\begin{aligned} \Xi_{\mathbf{p}, k} &= \begin{bmatrix} \Xi_{\mathbf{p}, \boldsymbol{\kappa}}^{k,1} & \Xi_{\mathbf{p}, \boldsymbol{\kappa}}^{k,2} & \cdots & \Xi_{\mathbf{p}, \boldsymbol{\kappa}}^{k, N_b} \\ \Xi_{\varphi, \boldsymbol{\kappa}}^{k,1} & \Xi_{\varphi, \boldsymbol{\kappa}}^{k,2} & \cdots & \Xi_{\varphi, \boldsymbol{\kappa}}^{k, N_b} \end{bmatrix} \\ \Xi_{\varphi, k} &= \begin{bmatrix} \Xi_{\varphi, \boldsymbol{\kappa}}^{k,1} & \Xi_{\varphi, \boldsymbol{\kappa}}^{k,2} & \cdots & \Xi_{\varphi, \boldsymbol{\kappa}}^{k, N_b} \end{bmatrix} \end{aligned}$$

and

$$\Xi_k = \text{diag} \left\{ \Xi_{\boldsymbol{\kappa}, \boldsymbol{\kappa}}^{k,1}, \Xi_{\boldsymbol{\kappa}, \boldsymbol{\kappa}}^{k,2}, \dots, \Xi_{\boldsymbol{\kappa}, \boldsymbol{\kappa}}^{k, N_b} \right\}$$

where $\Xi_{\mathbf{p}, \boldsymbol{\kappa}}^{kj} = \mathbf{q}_{kj} \Xi_{d, \boldsymbol{\kappa}}^{kj}$ and $\Xi_{\varphi, \boldsymbol{\kappa}}^{kj} = h_{kj} \Xi_{d, \boldsymbol{\kappa}}^{kj}$, and $\Xi_{\boldsymbol{\kappa}, \boldsymbol{\kappa}}^{kj} = \mathbf{F}_{\boldsymbol{\theta}}(\boldsymbol{\kappa}_{kj}|\mathbf{p}, \varphi; \boldsymbol{\kappa}_{kj}, \boldsymbol{\kappa}_{kj})$, in which $\Xi_{d, \boldsymbol{\kappa}}^{kj} = \mathbf{F}_{\boldsymbol{\theta}}(\boldsymbol{\kappa}_{kj}|\mathbf{p}, \varphi; d_{kj}, \boldsymbol{\kappa}_{kj})$.

Similar to the proof of Theorem 2 in Appendix III-C, the FIM from observation can be obtained as (68), shown at the bottom of the page, where

$$\begin{aligned} \mathbf{G}_k &= [\mathbf{q}_{k,1} \mathbf{1}_{k,1}^T \quad \mathbf{q}_{k,2} \mathbf{1}_{k,2}^T \quad \cdots \quad \mathbf{q}_{k, N_b} \mathbf{1}_{k, N_b}^T] \\ \mathbf{h}_k &= [h_{k,1} \mathbf{1}_{k,1}^T \quad h_{k,2} \mathbf{1}_{k,2}^T \quad \cdots \quad h_{k, N_b} \mathbf{1}_{k, N_b}^T] \end{aligned}$$

and

$$\bar{\boldsymbol{\Lambda}}_k = \text{diag} \left\{ \bar{\boldsymbol{\Psi}}_{k,1}, \bar{\boldsymbol{\Psi}}_{k,2}, \dots, \bar{\boldsymbol{\Psi}}_{k, N_b} \right\}$$

correspond to the k th antenna as defined in (44).

$$\begin{aligned} \mathbf{J}_c(\mathbf{p}) &= \Xi_{\mathbf{p}} + \sum_{j \in \mathcal{N}_b} \left\{ \mathbb{E}_{\mathbf{p}} \left\{ \mathbf{q}_j \Xi_{d,d}^j \mathbf{q}_j^T \right\} + \frac{1}{c^2} \mathbb{E}_{\mathbf{p}} \left\{ \mathbf{q}_j \mathbf{1}_j^T \bar{\boldsymbol{\Psi}}_j \mathbf{1}_j \mathbf{q}_j^T \right\} \right. \\ &\quad \left. - \frac{1}{c^2} \mathbb{E}_{\mathbf{p}} \left\{ \mathbf{q}_j \left(\mathbf{1}_j^T \bar{\boldsymbol{\Psi}}_j + c^2 \Xi_{d, \boldsymbol{\kappa}}^j \right) \right\} \mathbb{E}_{\mathbf{p}} \left\{ \bar{\boldsymbol{\Psi}}_j + \Xi_{\boldsymbol{\kappa}, \boldsymbol{\kappa}}^j \right\}^{-1} \mathbb{E}_{\mathbf{p}} \left\{ \left(\mathbf{1}_j^T \bar{\boldsymbol{\Psi}}_j + c^2 \Xi_{d, \boldsymbol{\kappa}}^j \right)^T \mathbf{q}_j^T \right\} \right\}. \end{aligned} \quad (65)$$

$$\bar{\lambda}_j \triangleq \frac{1}{c^2} \left\{ \mathbf{1}_j^T \bar{\boldsymbol{\Psi}}_j \mathbf{1}_j + c^2 \Xi_{d,d}^j - \left(\mathbf{1}_j^T \bar{\boldsymbol{\Psi}}_j + c^2 \Xi_{d, \boldsymbol{\kappa}}^j \right) \left(\bar{\boldsymbol{\Psi}}_j + c^2 \Xi_{\boldsymbol{\kappa}, \boldsymbol{\kappa}}^j \right)^{-1} \left(\mathbf{1}_j^T \bar{\boldsymbol{\Psi}}_j + c^2 \Xi_{d, \boldsymbol{\kappa}}^j \right)^T \right\}. \quad (66)$$

$$\mathbf{J}_p = \begin{bmatrix} \sum_{k \in \mathcal{N}_a} \sum_{j \in \mathcal{N}_b} \Xi_{\mathbf{p}, \mathbf{p}}^{kj} & \sum_{k \in \mathcal{N}_a} \sum_{j \in \mathcal{N}_b} \Xi_{\mathbf{p}, \varphi}^{kj} & \Xi_{\mathbf{p}, 1} & \cdots & \Xi_{\mathbf{p}, N_a} \\ \sum_{k \in \mathcal{N}_a} \sum_{j \in \mathcal{N}_b} \Xi_{\mathbf{p}, \varphi}^{kjT} & \sum_{k \in \mathcal{N}_a} \sum_{j \in \mathcal{N}_b} \Xi_{\varphi, \varphi}^{kj} & \Xi_{\varphi, 1} & \cdots & \Xi_{\varphi, N_a} \\ \Xi_{\mathbf{p}, 1}^T & \Xi_{\varphi, 1}^T & \Xi_1 & & \\ \vdots & \vdots & & \ddots & \\ \Xi_{\mathbf{p}, N_a}^T & \Xi_{\varphi, N_a}^T & & & \Xi_{N_a} \end{bmatrix} \quad (67)$$

$$\mathbf{J}_w = \frac{1}{c^2} \begin{bmatrix} \sum_{k \in \mathcal{N}_a} \mathbf{G}_k \bar{\boldsymbol{\Lambda}}_k \mathbf{G}_k^T & \sum_{k \in \mathcal{N}_a} \mathbf{G}_k \bar{\boldsymbol{\Lambda}}_k \mathbf{h}_k^T & \mathbf{G}_1 \bar{\boldsymbol{\Lambda}}_1 & \cdots & \mathbf{G}_{N_a} \bar{\boldsymbol{\Lambda}}_{N_a} \\ \sum_{k \in \mathcal{N}_a} \mathbf{h}_k \bar{\boldsymbol{\Lambda}}_k \mathbf{G}_k^T & \sum_{k \in \mathcal{N}_a} \mathbf{h}_k \bar{\boldsymbol{\Lambda}}_k \mathbf{h}_k^T & \mathbf{h}_1 \bar{\boldsymbol{\Lambda}}_1 & \cdots & \mathbf{h}_{N_a} \bar{\boldsymbol{\Lambda}}_{N_a} \\ \bar{\boldsymbol{\Lambda}}_1 \mathbf{G}_1^T & \bar{\boldsymbol{\Lambda}}_1 \mathbf{h}_1^T & \bar{\boldsymbol{\Lambda}}_1 & & \\ \vdots & \vdots & & \ddots & \\ \bar{\boldsymbol{\Lambda}}_{N_a} \mathbf{G}_{N_a}^T & \bar{\boldsymbol{\Lambda}}_{N_a} \mathbf{h}_{N_a}^T & & & \bar{\boldsymbol{\Lambda}}_{N_a} \end{bmatrix} \quad (68)$$

The overall FIM \mathbf{J}_θ is the sum of (67) and (68). By applying the notion of EFI, we have the 3×3 EFIM for the position and the orientation as follows:

$$\mathbf{J}_e(\mathbf{p}, \varphi) = \sum_{k \in \mathcal{N}_a} \sum_{j \in \mathcal{N}_b} \begin{bmatrix} \lambda_{kj} \mathbf{q}_{kj} \mathbf{q}_{kj}^T & \lambda_{kj} h_{kj} \mathbf{q}_{kj} \\ \lambda_{kj} h_{kj} \mathbf{q}_{kj} & \lambda_{kj} h_{kj}^2 \end{bmatrix} \quad (69)$$

where λ_{kj} is given by (70), shown at the bottom of the page.

Note that in the absence of *a priori* channel knowledge, the above result is still valid, with the RII of (70) degenerating to (71), shown at the bottom of the page, where $\mathbf{D}_{kj} = [\mathbf{0} \quad \mathbf{I}_{2L_{kj}-1}]$.

B. Proof of Proposition 3

Since $\mathbf{q}\mathbf{q}^T$ is always positive semidefinite, we need to simply prove that there exists a unique \mathbf{p}^* such that $\mathbf{q}^* = \mathbf{0}$.

Proof: Let \mathbf{p} be an arbitrary reference point, and

$$\mathbf{p}^* = \mathbf{p} + \mathbf{g}(\varphi)$$

where $\mathbf{g}(\varphi) = [g_x(\varphi)g_y(\varphi)]^T$, and $g_x(\varphi)$ and $g_y(\varphi)$ denote the relative distance in x and y directions, respectively. Then, h_{kj} corresponding to \mathbf{p} can be written as a sum of two parts

$$h_{kj} = h_{kj}^* + \tilde{h}_{kj}$$

where h_{kj}^* corresponds to \mathbf{p}^*

$$h_{kj}^* = \frac{d}{d\varphi} \Delta x_k(\mathbf{p}^*, \varphi) \cos \phi_{kj} + \frac{d}{d\varphi} \Delta y_k(\mathbf{p}^*, \varphi) \sin \phi_{kj}$$

and

$$\begin{aligned} \tilde{h}_{kj} &= \frac{d}{d\varphi} g_x(\varphi) \cos \phi_{kj} + \frac{d}{d\varphi} g_y(\varphi) \sin \phi_{kj} \\ &\triangleq \dot{g}_x \cos \phi_{kj} + \dot{g}_y \sin \phi_{kj} = \dot{\mathbf{g}}^T \mathbf{q}_{kj}. \end{aligned}$$

Hence, \mathbf{q} corresponding to the reference position \mathbf{p} is given by

$$\mathbf{q} = \underbrace{\sum_{k \in \mathcal{N}_a} \sum_{j \in \mathcal{N}_b} \lambda_{kj} h_{kj}^* \mathbf{q}_{kj}}_{\triangleq \mathbf{q}^*} + \underbrace{\sum_{k \in \mathcal{N}_a} \sum_{j \in \mathcal{N}_b} \lambda_{kj} \tilde{h}_{kj} \mathbf{q}_{kj}}_{\triangleq \tilde{\mathbf{q}}} \quad (72)$$

and $\tilde{\mathbf{q}}$ can be written as

$$\begin{aligned} \tilde{\mathbf{q}} &= \sum_{k \in \mathcal{N}_a} \sum_{j \in \mathcal{N}_b} \mathbf{q}_{kj}^T \dot{\mathbf{g}} \lambda_{kj} \mathbf{q}_{kj} \\ &= \sum_{k \in \mathcal{N}_a} \sum_{j \in \mathcal{N}_b} \lambda_{kj} \mathbf{q}_{kj} \mathbf{q}_{kj}^T \dot{\mathbf{g}} = \sum_{k \in \mathcal{N}_a} \mathbf{J}_e(\mathbf{p}_k^{\text{Array}}) \dot{\mathbf{g}}. \end{aligned} \quad (73)$$

Since $\sum_{k \in \mathcal{N}_a} \mathbf{J}_e(\mathbf{p}_k^{\text{Array}}) \succ \mathbf{0}$, we have $\mathbf{q}^* = \mathbf{0}$ if and only if

$$\dot{\mathbf{g}} = \left(\sum_{k \in \mathcal{N}_a} \mathbf{J}_e(\mathbf{p}_k^{\text{Array}}) \right)^{-1} \mathbf{q}$$

implying that there exists only one $\dot{\mathbf{g}}$, and hence only one $\mathbf{g}(\varphi)$, such that $\mathbf{q}^* = \mathbf{0}$. Therefore, the orientation center \mathbf{p}^* is unique. \square

C. Proof of Corollary 5

Proof: We first prove that the SOEB is independent of the reference point \mathbf{p} . It is equivalent to show that the EFI for the orientation given by (27) equals the EFI for the orientation based on \mathbf{p}^* , given by

$$J_e^*(\varphi) = \sum_{k \in \mathcal{N}_a} \sum_{j \in \mathcal{N}_b} \lambda_{kj} h_{kj}^{*2}.$$

Let $\mathbf{J} = \sum_{k \in \mathcal{N}_a} \mathbf{J}_e(\mathbf{p}_k^{\text{Array}})$. From (72) and (73), we have $\mathbf{q} = \tilde{\mathbf{q}} = \mathbf{J} \dot{\mathbf{g}}$, and hence

$$\mathbf{q}^T \mathbf{J}^{-1} \mathbf{q} = \tilde{\mathbf{q}}^T \mathbf{J}^{-1} \tilde{\mathbf{q}} = \tilde{\mathbf{q}}^T \dot{\mathbf{g}} = \sum_{k \in \mathcal{N}_a} \sum_{j \in \mathcal{N}_b} \lambda_{kj} \tilde{h}_{kj}^2.$$

On the other hand, we also have

$$\sum_{k \in \mathcal{N}_a} \sum_{j \in \mathcal{N}_b} \lambda_{kj} h_{kj}^* \tilde{h}_{kj} = \mathbf{q}^* \dot{\mathbf{g}} = 0.$$

Therefore, we can verify that the EFI for the orientation in (27)

$$\begin{aligned} J_e(\varphi) &= \sum_{k \in \mathcal{N}_a} \sum_{j \in \mathcal{N}_b} \lambda_{kj} (h_{kj}^* + \tilde{h}_{kj})^2 - \tilde{\mathbf{q}}^T \mathbf{J}^{-1} \tilde{\mathbf{q}} \\ &= \sum_{k \in \mathcal{N}_a} \sum_{j \in \mathcal{N}_b} \lambda_{kj} h_{kj}^{*2} + 2 \sum_{k \in \mathcal{N}_a} \sum_{j \in \mathcal{N}_b} \lambda_{kj} h_{kj}^* \tilde{h}_{kj} \\ &= J_e^*(\varphi). \end{aligned} \quad (74)$$

$$\lambda_{kj} \triangleq \frac{1}{c^2} \left\{ \mathbf{1}_{kj}^T \tilde{\Psi}_{kj} \mathbf{1}_{kj} + c^2 \Xi_{d,d}^{kj} - \left(\mathbf{1}_{kj}^T \tilde{\Psi}_{kj} + c^2 \Xi_{d,\kappa}^{kj} \right) \left(\tilde{\Psi}_{kj} + c^2 \Xi_{\kappa,\kappa}^{kj} \right)^{-1} \left(\mathbf{1}_{kj}^T \tilde{\Psi}_{kj} + c^2 \Xi_{d,\kappa}^{kj} \right)^T \right\}. \quad (70)$$

$$\lambda_{kj} = \begin{cases} \mathbf{1}_{kj}^T \left\{ \tilde{\Psi}_{kj} - \left(\tilde{\Psi}_{kj} \mathbf{D}_{kj}^T \right) \left(\mathbf{D}_{kj} \tilde{\Psi}_{kj} \mathbf{D}_{kj}^T \right)^{-1} \left(\mathbf{D}_{kj} \tilde{\Psi}_{kj} \right) \right\} \mathbf{1}_{kj} / c^2, & \text{LOS} \\ 0, & \text{NLOS} \end{cases} \quad (71)$$

This shows that the EFI for the orientation is independent of the reference point, and thus is the SOEB.

We next derive the SPEB for any reference point given in (32). The 3×3 EFIM in (69) can be written, using (72) and (74), as

$$\mathbf{J}_e(\mathbf{p}, \varphi) = \begin{bmatrix} \mathbf{J} & \\ \tilde{\mathbf{q}}^T & J_e(\varphi) + \tilde{\mathbf{q}}^T \mathbf{J}^{-1} \tilde{\mathbf{q}} \end{bmatrix}.$$

Using the equation of Shur's complement [66], we have

$$\begin{aligned} \mathbf{J}_e^{-1}(\mathbf{p}) &= \mathbf{J}^{-1} + \frac{1}{J_e(\varphi)} (\mathbf{J}^{-1} \tilde{\mathbf{q}}) (\mathbf{J}^{-1} \tilde{\mathbf{q}})^T \\ &= \mathbf{J}^{-1} + \frac{1}{J_e(\varphi)} \dot{\mathbf{g}} \dot{\mathbf{g}}^T. \end{aligned} \quad (75)$$

Since the translation $\mathbf{g}(\varphi)$ can be represented as

$$\mathbf{g}(\varphi) = \|\mathbf{p} - \mathbf{p}^*\| \begin{bmatrix} \cos(\varphi + \varphi_0) \\ \sin(\varphi + \varphi_0) \end{bmatrix}$$

where φ_0 is a constant angle, we have $\|\dot{\mathbf{g}}\| = \|\mathbf{p} - \mathbf{p}^*\|$. Then, by taking the trace of both sides of (75), we obtain

$$\begin{aligned} \mathcal{P}(\mathbf{p}) &= \mathcal{P}(\mathbf{p}^*) + \frac{\dot{\mathbf{g}}^T \dot{\mathbf{g}}}{J_e(\varphi)} \\ &= \mathcal{P}(\mathbf{p}^*) + \|\mathbf{p} - \mathbf{p}^*\|^2 \cdot \mathcal{P}(\varphi). \end{aligned} \quad \square$$

D. Proof of Proposition 5

Proof: Take the array center \mathbf{p}_0 as the reference point, and we have

$$\begin{aligned} \sum_{k \in \mathcal{N}_a} h_{kj} &= \sum_{k \in \mathcal{N}_a} \frac{d}{d\varphi} \Delta x_k(\mathbf{p}_0, \varphi) \cos \phi_{kj} \\ &\quad + \sum_{k \in \mathcal{N}_a} \frac{d}{d\varphi} \Delta y_k(\mathbf{p}_0, \varphi) \sin \phi_{kj} \\ &= \frac{d}{d\varphi} \left(\sum_{k \in \mathcal{N}_a} \Delta x_k(\mathbf{p}_0, \varphi) \right) \cos \phi_{kj} \end{aligned}$$

$$\begin{aligned} &+ \frac{d}{d\varphi} \left(\sum_{k \in \mathcal{N}_a} \Delta y_k(\mathbf{p}_0, \varphi) \right) \sin \phi_{kj} \\ &= 0. \end{aligned}$$

Consequently

$$\mathbf{q} = \sum_{k \in \mathcal{N}_a} \sum_{j \in \mathcal{N}_b} \lambda_j h_{kj} \mathbf{q}_j = \sum_{j \in \mathcal{N}_b} \left(\sum_{k \in \mathcal{N}_a} h_{kj} \right) \lambda_j \mathbf{q}_j = 0$$

implying $\mathbf{p}_0 = \mathbf{p}^*$, i.e., the array center is the orientation center. \square

APPENDIX V

PROOFS OF THE RESULTS IN SECTION V

A. Proof of Theorem 4

In the presence of a time offset, the FIM can be written as (76), shown at the bottom of the page, where

$$\mathbf{J}_p = \begin{bmatrix} \sum_{j \in \mathcal{N}_b} \Xi_{p,p}^j & \mathbf{0} & \Xi_{p,\kappa}^1 & \cdots & \Xi_{p,\kappa}^{N_b} \\ \mathbf{0}^T & \Xi_B & \mathbf{0}^T & \cdots & \mathbf{0}^T \\ \Xi_{p,\kappa}^{1T} & \mathbf{0} & \Xi_{\kappa,\kappa}^1 & & \\ \vdots & \vdots & & \ddots & \\ \Xi_{p,\kappa}^{N_b T} & \mathbf{0} & & & \Xi_{\kappa,\kappa}^{N_b} \end{bmatrix}.$$

Applying the notion of EFI, we obtain the 3×3 EFIM

$$\mathbf{J}_e(\mathbf{p}, B) = \begin{bmatrix} \sum_{j \in \mathcal{N}_b} \lambda_j \mathbf{q}_j \mathbf{q}_j^T & \sum_{j \in \mathcal{N}_b} \lambda_j \mathbf{q}_j \\ \sum_{j \in \mathcal{N}_b} \lambda_j \mathbf{q}_j^T & \sum_{j \in \mathcal{N}_b} \lambda_j + \Xi_B \end{bmatrix}$$

where λ_j is given by (63b), and another step of EFI leads to (34) and (35).

B. Proof of Theorem 5

We consider orientation-unaware case, whereas orientation-aware case is a special case with a reduced parameter set. The FIM using an antenna array can be written as (77), shown at the bottom of the page, where $\mathbf{l}_n = [\mathbf{l}_{k,1}^T \ \mathbf{l}_{k,2}^T \ \cdots \ \mathbf{l}_{k,N_b}^T]$, and

$$\mathbf{J}_\theta = \frac{1}{c^2} \begin{bmatrix} \sum_{j \in \mathcal{N}_b} \mathbf{G}_j \bar{\Psi}_j \mathbf{G}_j^T & \sum_{j \in \mathcal{N}_b} \mathbf{G}_j \bar{\Psi}_j \mathbf{l}_j & \mathbf{G}_1 \bar{\Psi}_1 & \cdots & \mathbf{G}_{N_b} \bar{\Psi}_{N_b} \\ \sum_{j \in \mathcal{N}_b} \mathbf{l}_j^T \bar{\Psi}_j \mathbf{G}_j & \sum_{j \in \mathcal{N}_b} \mathbf{l}_j^T \bar{\Psi}_j \mathbf{l}_j & \mathbf{l}_1^T \bar{\Psi}_1 & \cdots & \mathbf{l}_{N_b}^T \bar{\Psi}_{N_b} \\ \bar{\Psi}_1 \mathbf{G}_1^T & \bar{\Psi}_1 \mathbf{l}_1 & \bar{\Psi}_1 & & \\ \vdots & \vdots & & \ddots & \\ \bar{\Psi}_{N_b} \mathbf{G}_{N_b}^T & \bar{\Psi}_{N_b} \mathbf{l}_{N_b} & & & \bar{\Psi}_{N_b} \end{bmatrix} + \mathbf{J}_p \quad (76)$$

$$\mathbf{J}_\theta = \frac{1}{c^2} \begin{bmatrix} \sum_{k \in \mathcal{N}_a} \mathbf{G}_k \bar{\Lambda}_k \mathbf{G}_k^T & \sum_{k \in \mathcal{N}_a} \mathbf{G}_k \bar{\Lambda}_k \mathbf{h}_k^T & \sum_{k \in \mathcal{N}_a} \mathbf{g}_k \bar{\Lambda}_k \mathbf{l}_k^T & \mathbf{G}_1 \bar{\Lambda}_1 & \cdots & \mathbf{G}_{N_a} \bar{\Lambda}_{N_a} \\ \sum_{k \in \mathcal{N}_a} \mathbf{h}_k \bar{\Lambda}_k \mathbf{G}_k^T & \sum_{k \in \mathcal{N}_a} \mathbf{h}_k \bar{\Lambda}_k \mathbf{h}_k^T & \sum_{k \in \mathcal{N}_a} \mathbf{h}_k \bar{\Lambda}_k \mathbf{l}_k^T & \mathbf{h}_1 \bar{\Lambda}_1 & \cdots & \mathbf{h}_{N_a} \bar{\Lambda}_{N_a} \\ \sum_{k \in \mathcal{N}_a} \mathbf{l}_k \bar{\Lambda}_k \mathbf{G}_k^T & \sum_{k \in \mathcal{N}_a} \mathbf{l}_k \bar{\Lambda}_k \mathbf{h}_k^T & \sum_{k \in \mathcal{N}_a} \mathbf{l}_k \bar{\Lambda}_k \mathbf{l}_k^T & \mathbf{l}_1 \bar{\Lambda}_1 & \cdots & \mathbf{l}_{N_a} \bar{\Lambda}_{N_a} \\ \bar{\Lambda}_1 \mathbf{G}_1^T & \bar{\Lambda}_1 \mathbf{h}_1^T & \bar{\Lambda}_1 \mathbf{l}_1^T & \bar{\Lambda}_1 & & \\ \vdots & \vdots & \vdots & & \ddots & \\ \bar{\Lambda}_{N_a} \mathbf{G}_{N_a}^T & \bar{\Lambda}_{N_a} \mathbf{h}_{N_a}^T & \bar{\Lambda}_{N_a} \mathbf{l}_{N_a}^T & & & \bar{\Lambda}_{N_a} \end{bmatrix} + \mathbf{J}_p \quad (77)$$

$$\mathbf{J}_p = \begin{bmatrix} \sum_{k \in \mathcal{N}_a} \sum_{j \in \mathcal{N}_b} \Xi_{p,p}^{kj} & \sum_{k \in \mathcal{N}_a} \sum_{j \in \mathcal{N}_b} \Xi_{p,\varphi}^{kj} & \mathbf{0} & \Xi_{p,1} & \cdots & \Xi_{p,N_a} \\ \sum_{k \in \mathcal{N}_a} \sum_{j \in \mathcal{N}_b} \Xi_{p,\varphi}^{kjT} & \sum_{k \in \mathcal{N}_a} \sum_{j \in \mathcal{N}_b} \Xi_{\varphi,\varphi}^{kj} & \mathbf{0} & \Xi_{\varphi,1} & \cdots & \Xi_{\varphi,N_a} \\ \mathbf{0}^T & 0 & \Xi_B & \mathbf{0}^T & \cdots & \mathbf{0}^T \\ \Xi_{p,1}^T & \Xi_{\varphi,1}^T & \mathbf{0} & \Xi_1 & & \\ \vdots & \vdots & \vdots & & \ddots & \\ \Xi_{p,N_a}^T & \Xi_{\varphi,N_a}^T & \mathbf{0} & & & \Xi_{N_a} \end{bmatrix}. \quad (78)$$

$$\mathbf{J}_e^{\text{Array-B}} = \begin{bmatrix} \sum_{k \in \mathcal{N}_a} \sum_{j \in \mathcal{N}_b} \bar{\lambda}_{kj} \mathbf{q}_{kj} \mathbf{q}_{kj}^T + \Xi_p & \sum_{k \in \mathcal{N}_a} \sum_{j \in \mathcal{N}_b} \bar{\lambda}_{kj} h_{kj} \mathbf{q}_{kj} & \sum_{k \in \mathcal{N}_a} \sum_{j \in \mathcal{N}_b} \bar{\lambda}_{kj} \mathbf{q}_{kj} \\ \sum_{k \in \mathcal{N}_a} \sum_{j \in \mathcal{N}_b} \bar{\lambda}_{kj} h_{kj} \mathbf{q}_{kj}^T & \sum_{k \in \mathcal{N}_a} \sum_{j \in \mathcal{N}_b} \bar{\lambda}_{kj} h_{kj}^2 + \Xi_\varphi & \sum_{k \in \mathcal{N}_a} \sum_{j \in \mathcal{N}_b} \bar{\lambda}_{kj} h_{kj} \\ \sum_{k \in \mathcal{N}_a} \sum_{j \in \mathcal{N}_b} \bar{\lambda}_{kj} \mathbf{q}_{kj}^T & \sum_{k \in \mathcal{N}_a} \sum_{j \in \mathcal{N}_b} \bar{\lambda}_{kj} h_{kj} & \sum_{k \in \mathcal{N}_a} \sum_{j \in \mathcal{N}_b} \bar{\lambda}_{kj} + \Xi_B \end{bmatrix}. \quad (79)$$

$$\mathbf{J}_e^{\text{Array-B}} = \begin{bmatrix} N_a \sum_{j \in \mathcal{N}_b} \bar{\lambda}_{kj} \mathbf{J}_r(\bar{\phi}_j) + \Xi_p & \mathbf{0} & N_a \sum_{j \in \mathcal{N}_b} \bar{\lambda}_j \bar{\mathbf{q}}_j \\ \mathbf{0}^T & \sum_{k \in \mathcal{N}_a} \sum_{j \in \mathcal{N}_b} \bar{\lambda}_{kj} \bar{h}_{kj}^2 + \Xi_\varphi & 0 \\ N_a \sum_{j \in \mathcal{N}_b} \bar{\lambda}_j \bar{\mathbf{q}}_j^T & 0 & N_a \sum_{j \in \mathcal{N}_b} \bar{\lambda}_j + \Xi_B \end{bmatrix} \quad (80)$$

\mathbf{J}_p is given by (78), shown at the top of the page. Applying the notion of EFI to \mathbf{J}_θ , we obtain the 4×4 EFIM in (37).

C. Proof of Corollary 8

We incorporate the *a priori* knowledge of the array center and orientation into (37), and obtain the EFIM in far-field scenarios as (79), shown at the top of the page. Recall that in far-field scenarios, $\mathbf{p}_0 = \mathbf{p}^*$, implying that $\sum_{k \in \mathcal{N}_a} \sum_{j \in \mathcal{N}_b} \lambda_{kj} h_{kj} \mathbf{q}_{kj} = \mathbf{0}$ and $\sum_{k \in \mathcal{N}_a} \sum_{j \in \mathcal{N}_b} \lambda_{kj} h_{kj} = 0$. Also, we have $\bar{\lambda}_{kj} = \bar{\lambda}_j$ and $\bar{\phi}_{kj} = \bar{\phi}_j$ for all k , and hence the EFIM can be written as (80), shown at the top of the page, where \bar{h}_{kj} and $\bar{\mathbf{q}}_j$ is a function of $\bar{\mathbf{p}}_0$.

ACKNOWLEDGMENT

The authors would like to thank R. G. Gallager, A. Conti, H. Wymeersch, W. M. Gifford, and W. Suwansantisuk for their valuable suggestion and careful reading of the manuscript. They would also like to thank the anonymous reviewers for their constructive comments.

REFERENCES

- [1] A. Sayed, A. Tarighat, and N. Khajehnouri, "Network-based wireless location: Challenges faced in developing techniques for accurate wireless location information," *IEEE Signal Process. Mag.*, vol. 22, no. 4, pp. 24–40, Jul. 2005.
- [2] K. Pahlavan, X. Li, and J. P. Makela, "Indoor geolocation science and technology," *IEEE Commun. Mag.*, vol. 40, no. 2, pp. 112–118, Feb. 2002.
- [3] J. J. Caffery and G. L. Stuber, "Overview of radiolocation in CDMA cellular systems," *IEEE Commun. Mag.*, vol. 36, no. 4, pp. 38–45, Apr. 1998.
- [4] N. Patwari, J. N. Ash, S. Kyperountas, A. O. Hero, III, R. L. Moses, and N. S. Correal, "Locating the nodes: Cooperative localization in wireless sensor networks," *IEEE Signal Process. Mag.*, vol. 22, no. 4, pp. 54–69, Jul. 2005.
- [5] C.-Y. Chong and S. P. Kumar, "Sensor networks: Evolution, opportunities, and challenges," *Proc. IEEE*, vol. 91, no. 8, pp. 1247–1256, Aug. 2003.
- [6] J. J. Spilker, Jr., "GPS signal structure and performance characteristics," *J. Inst. Navig.*, vol. 25, no. 2, pp. 121–146, 1978.
- [7] L. Kaplan, "Global node selection for localization in a distributed sensor network," *IEEE Trans. Aerosp. Electron. Syst.*, vol. 42, no. 1, pp. 113–135, Jan. 2006.
- [8] D. B. Jourdan, D. Dardari, and M. Z. Win, "Position error bound for UWB localization in dense cluttered environments," *IEEE Trans. Aerosp. Electron. Syst.*, vol. 44, no. 2, pp. 613–628, Apr. 2008.
- [9] S. Gezici, Z. Tian, G. B. Giannakis, H. Kobayashi, A. F. Molisch, H. V. Poor, and Z. Sahinoglu, "Localization via ultra-wideband radios: A look at positioning aspects for future sensor networks," *IEEE Signal Process. Mag.*, vol. 22, no. 4, pp. 70–84, Jul. 2005.
- [10] C. Falsi, D. Dardari, L. Mucchi, and M. Z. Win, "Time of arrival estimation for UWB localizers in realistic environments," *EURASIP J. Appl. Signal Process.*, vol. 2006, pp. 1–13, 2006.
- [11] Y. Shen and M. Z. Win, "Localization accuracy using wideband antenna arrays," *IEEE Trans. Commun.*, vol. 58, no. 1, pp. 270–280, Jan. 2010.
- [12] A. F. Molisch, "Ultra-wide-band propagation channels," *Proc. IEEE*, vol. 97, no. 2, pp. 353–371, Feb. 2009.
- [13] M. Z. Win and R. A. Scholtz, "Impulse radio: How it works," *IEEE Commun. Lett.*, vol. 2, no. 2, pp. 36–38, Feb. 1998.
- [14] M. Z. Win and R. A. Scholtz, "Characterization of ultra-wide bandwidth wireless indoor communications channel: A communication theoretic view," *IEEE J. Sel. Areas Commun.*, vol. 20, no. 9, pp. 1613–1627, Dec. 2002.
- [15] M. Z. Win, "A unified spectral analysis of generalized time-hopping spread-spectrum signals in the presence of timing jitter," *IEEE J. Sel. Areas Commun.*, vol. 20, no. 9, pp. 1664–1676, Dec. 2002.
- [16] Z. N. Low, J. H. Cheong, C. L. Law, W. T. Ng, and Y. J. Lee, "Pulse detection algorithm for line-of-sight (LOS) UWB ranging applications," *IEEE Antennas Wireless Propag. Lett.*, vol. 4, pp. 63–67, 2005.
- [17] Z. Zhang, C. L. Law, and Y. L. Guan, "BA-POC-based ranging method with multipath mitigation," *IEEE Antennas Wireless Propag. Lett.*, vol. 4, pp. 492–495, 2005.
- [18] D. Dardari, C.-C. Chong, and M. Z. Win, "Threshold-based time-of-arrival estimators in UWB dense multipath channels," *IEEE Trans. Commun.*, vol. 56, no. 8, pp. 1366–1378, Aug. 2008.
- [19] D. Dardari, A. Conti, U. J. Ferner, A. Giorgetti, and M. Z. Win, "Ranging with ultrawide bandwidth signals in multipath environments," *Proc. IEEE*, vol. 97, no. 2, pp. 404–426, Feb. 2009.
- [20] J.-Y. Lee and R. A. Scholtz, "Ranging in a dense multipath environment using an UWB radio link," *IEEE J. Sel. Areas Commun.*, vol. 20, no. 9, pp. 1677–1683, Dec. 2002.
- [21] A. F. Molisch, "Ultrawideband propagation channels-theory, measurements, and modeling," *IEEE Trans. Veh. Technol.*, vol. 54, no. 5, pp. 1528–1545, Sep. 2005.
- [22] M. Z. Win, G. Chrisikos, and N. R. Sollenberger, "Performance of rake reception in dense multipath channels: Implications of spreading bandwidth and selection diversity order," *IEEE J. Sel. Areas Commun.*, vol. 18, no. 8, pp. 1516–1525, Aug. 2000.

- [23] L. Yang and G. B. Giannakis, "Ultra-wideband communications: An idea whose time has come," *IEEE Signal Process. Mag.*, vol. 21, no. 6, pp. 26–54, Nov. 2004.
- [24] T. Q. S. Quek and M. Z. Win, "Analysis of UWB transmitted-reference communication systems in dense multipath channels," *IEEE J. Sel. Areas Commun.*, vol. 23, no. 9, pp. 1863–1874, Sep. 2005.
- [25] W. Suwansantisuk, M. Z. Win, and L. A. Shepp, "On the performance of wide-bandwidth signal acquisition in dense multipath channels," *IEEE Trans. Veh. Technol.*, vol. 54, no. 5, pp. 1584–1594, Sep. 2005.
- [26] A. F. Molisch, D. Cassioli, C.-C. Chong, S. Emami, A. Fort, B. Kannan, J. Karedal, J. Kunisch, H. Schantz, K. Siwiak, and M. Z. Win, "A comprehensive standardized model for ultrawideband propagation channels," *IEEE Trans. Antennas Propag.*, vol. 54, no. 11, pp. 3151–3166, Nov. 2006.
- [27] L. Maillaender, "On the geolocation bounds for round-trip time-of-arrival and all non-line-of-sight channels," *EURASIP J. Adv. Signal Process.*, vol. 2008, p. 10, 2008.
- [28] Y. Qi and H. Kobayashi, "Cramér-Rao lower bound for geolocation in non-line-of-sight environment," in *Proc. IEEE Int. Conf. Acoust. Speech Signal Process.*, Orlando, FL, May 2002, pp. 2473–2476.
- [29] Y. Qi, H. Suda, and H. Kobayashi, "On time-of-arrival positioning in a multipath environment," in *Proc. IEEE Semiannu. Veh. Technol. Conf.*, Los Angeles, CA, Sep. 2004, pp. 3540–3544.
- [30] Y. Qi, H. Kobayashi, and H. Suda, "Analysis of wireless geolocation in a non-line-of-sight environment," *IEEE Trans. Wireless Commun.*, vol. 5, no. 3, pp. 672–681, Mar. 2006.
- [31] J. Caffery, Ed., *Wireless Location in CDMA Cellular Radio Systems*. Boston, MA: Kluwer, 2000.
- [32] T. Rappaport, J. Reed, and B. Woerner, "Position location using wireless communications on highways of the future," *IEEE Commun. Mag.*, vol. 34, no. 10, pp. 33–41, Oct. 1996.
- [33] D. Niculescu and B. Nath, "Ad hoc positioning system (APS) using AOA," in *Proc. IEEE Conf. Comput. Commun.*, Mar.–Apr. 2003, vol. 3, pp. 1734–1743.
- [34] N. Patwari and A. O. Hero, III, "Using proximity and quantized RSS for sensor localization in wireless networks," in *Proc. IEEE/ACM 2nd Workshop Wireless Sensor Nets. Appl.*, 2003, pp. 20–29.
- [35] T. Pavani, G. Costa, M. Mazzotti, A. Conti, and D. Dardari, "Experimental results on indoor localization techniques through wireless sensors network," in *Proc. IEEE Semiannu. Veh. Technol. Conf.*, May 2006, vol. 2, pp. 663–667.
- [36] A. F. Molisch, *Wireless Communications*, 1st ed. Piscataway, NJ: IEEE Press/Wiley, 2005.
- [37] B. Van Veen and K. Buckley, "Beamforming: A versatile approach to spatial filtering," *IEEE Signal Process. Mag.*, vol. 5, no. 2, pp. 4–24, Apr. 1988.
- [38] H. Krim and M. Viberg, "Two decades of array signal processing research: The parametric approach," *IEEE Signal Process. Mag.*, vol. 13, no. 4, pp. 67–94, Jul. 1996.
- [39] R. Engelbrecht, "Passive source localization from spatially correlated angle-of-arrival data," *IEEE Trans. Signal Process.*, vol. SP-31, no. 4, pp. 842–846, Apr. 1983.
- [40] C.-C. Chong, C.-M. Tan, D. I. Laurenson, S. McLaughlin, M. A. Beach, and A. R. Nix, "A new statistical wideband spatio-temporal channel model for 5-GHz band WLAN systems," *IEEE J. Sel. Areas Commun.*, vol. 21, no. 2, pp. 139–150, Feb. 2003.
- [41] P. Deng and P. Fan, "An AOA assisted TOA positioning system," in *Proc. Int. Conf. Commun. Technol.*, Beijing, China, 2000, vol. 2, pp. 1501–1504.
- [42] L. Cong and W. Zhuang, "Hybrid TDOA/AOA mobile user location for wideband CDMA cellular systems," *IEEE Trans. Wireless Commun.*, vol. 1, no. 3, pp. 439–447, Jul. 2002.
- [43] C. Chang and A. Sahai, "Estimation bounds for localization," in *Proc. IEEE Conf. Sensor Ad Hoc Commun. Netw.*, Santa Clara, CA, Oct. 2004, pp. 415–424.
- [44] M. Hamilton and P. Schultheiss, "Passive ranging in multipath dominant environments. I. known multipath parameters," *IEEE Trans. Signal Process.*, vol. 40, no. 1, pp. 1–12, Jan. 1992.
- [45] J. Lee and S. Yoo, "Large error performance of UWB ranging," in *Proc. IEEE Int. Conf. Ultra-Wideband*, Zurich, Switzerland, 2005, pp. 308–313.
- [46] Y. Shen and M. Z. Win, "Fundamental limits of wideband localization accuracy via Fisher information," in *Proc. IEEE Wireless Commun. Netw. Conf.*, Kowloon, Hong Kong, Mar. 2007, pp. 3046–3051.
- [47] Y. Shen and M. Z. Win, "Effect of path-overlap on localization accuracy in dense multipath environments," in *Proc. IEEE Int. Conf. Commun.*, Beijing, China, May 2008, pp. 4197–4202.
- [48] M. Silventoinen and T. Rantalainen, "Mobile station emergency locating in GSM," in *Proc. IEEE Int. Conf. Personal Wireless Commun.*, New Delhi, India, 1996, pp. 232–238.
- [49] J. Caffery and G. Stuber, "Radio location in urban CDMA microcells," in *Proc. IEEE Int. Symp. Personal Indoor Mobile Radio Commun.*, Toronto, ON, Canada, 1995, vol. 2, pp. 858–862.
- [50] H. L. Van Trees, *Detection, Estimation and Modulation Theory*. New York: Wiley, 1968, vol. 1.
- [51] H. V. Poor, *An Introduction to Signal Detection and Estimation*, 2nd ed. New York: Springer-Verlag, 1994.
- [52] M. Spirito, "On the accuracy of cellular mobile station location estimation," *IEEE Trans. Veh. Technol.*, vol. 50, no. 3, pp. 674–685, May 2001.
- [53] M. Gavish and E. Fogel, "Effect of bias on bearing-only target location," *IEEE Trans. Aerosp. Electron. Syst.*, vol. 26, no. 1, pp. 22–26, Jan. 1990.
- [54] H. Koorapaty, H. Grubeck, and M. Cedervall, "Effect of biased measurement errors on accuracy of position location methods," in *Proc. IEEE Global Telecomm. Conf.*, Sydney, NSW, Australia, 1998, vol. 3, pp. 1497–1502.
- [55] M. Wylie and J. Holtzman, "The non-line of sight problem in mobile location estimation," in *Record 5th IEEE Int. Conf. Universal Personal Commun.*, Cambridge, MA, 1996, vol. 2, pp. 827–831.
- [56] S.-S. Woo, H.-R. You, and J.-S. Koh, "The NLOS mitigation technique for position location using IS-95CDMA networks," in *Proc. IEEE Semiannu. Veh. Technol. Conf.*, Boston, MA, 2000, vol. 6, pp. 2556–2560.
- [57] S. Al-Jazzar, J. J. Caffery, and H.-R. You, "A scattering model based approach to NLOS mitigation in TOA location systems," in *Proc. IEEE Semiannu. Veh. Technol. Conf.*, 2002, vol. 2, pp. 861–865.
- [58] P.-C. Chen, "A non-line-of-sight error mitigation algorithm in location estimation," in *Proc. IEEE Wireless Commun. Netw. Conf.*, Sep. 1999, vol. 1, pp. 316–320.
- [59] L. Xiong, "A selective model to suppress NLOS signals in angle-of-arrival (AOA) location estimation," in *Proc. 9th IEEE Int. Symp. Personal Indoor Mobile Radio Commun.*, Boston, MA, 1998, vol. 1, pp. 461–465.
- [60] H. Wang, L. Yip, K. Yao, and D. Estrin, "Lower bounds of localization uncertainty in sensor networks," in *Proc. IEEE Int. Conf. Acoust. Speech Signal Process.*, Montreal, QC, Canada, May 2004, pp. 917–920.
- [61] M. Wax and A. Leshem, "Joint estimation of time delays and directions of arrival of multiple reflections of a known signal," *IEEE Trans. Signal Process.*, vol. 45, no. 10, pp. 2477–2484, Oct. 1997.
- [62] C. Botteron, A. Host-Madsen, and M. Fattouche, "Cramer-Rao bounds for the estimation of multipath parameters and mobiles' positions in asynchronous DS-CDMA systems," *IEEE Trans. Signal Process.*, vol. 52, no. 4, pp. 862–875, Apr. 2004.
- [63] Y. Shen, H. Wymeersch, and M. Z. Win, "Fundamental limits of wideband localization—Part II: Cooperative networks," *IEEE Trans. Inf. Theory*, vol. 56, no. 10, Oct. 2010, DOI: 10.1109/TIT.2010.2059720.
- [64] A. A. Saleh and R. A. Valenzuela, "A statistical model for indoor multipath propagation," *IEEE J. Sel. Areas Commun.*, vol. 5, no. 2, pp. 128–137, Feb. 1987.
- [65] I. Reuven and H. Messer, "A Barankin-type lower bound on the estimation error of a hybrid parameter vector," *IEEE Trans. Inf. Theory*, vol. 43, no. 3, pp. 1084–1093, May 1997.
- [66] R. A. Horn and C. R. Johnson, *Matrix Analysis*, 1st ed. Cambridge, U.K.: Cambridge Univ. Press, 1985.
- [67] R. A. Scholtz, "How do you define bandwidth?," in *Proc. Int. Telemeeting Conf.*, Los Angeles, CA, Oct. 1972, pp. 281–288.
- [68] W. M. Lovelace and J. K. Townsend, "The effects of timing jitter and tracking on the performance of impulse radio," *IEEE J. Sel. Areas Commun.*, vol. 20, no. 9, pp. 1646–1651, Dec. 2002.
- [69] S. W. Golomb and R. A. Scholtz, "Generalized Barker sequences," *IEEE Trans. Inf. Theory*, vol. IT-11, no. 4, pp. 533–537, Oct. 1965.
- [70] S. W. Golomb and M. Z. Win, "Recent results on polyphase sequences," *IEEE Trans. Inf. Theory*, vol. 44, no. 2, pp. 817–824, Mar. 1998.
- [71] S. W. Golomb and G. Gong, *Signal Design for Good Correlation: For Wireless Communication, Cryptography, and Radar*. Cambridge, U.K.: Cambridge Univ. Press, 2005.
- [72] D. Cassioli, M. Z. Win, and A. F. Molisch, "The ultra-wide bandwidth indoor channel: From statistical model to simulations," *IEEE J. Sel. Areas Commun.*, vol. 20, no. 6, pp. 1247–1257, Aug. 2002.

Yuan Shen (S'05) received the B.S. degree in electrical engineering (with highest honor) from Tsinghua University, Beijing, China, in 2005 and the S.M. degree in electrical engineering from the Massachusetts Institute of Technology (MIT), Cambridge, in 2008, where he is currently working towards the Ph.D. degree at the Wireless Communications and Network Science Laboratory.

He was with the Hewlett-Packard Labs, in winter 2009, the Corporate R&D of Qualcomm Inc., in summer 2008, and the Intelligent Transportation Information System Laboratory, Tsinghua University, from 2003 to 2005. His research interests include communication theory, information theory, and statistical signal processing. His current research focuses on wideband localization, cooperative networks, and ultrawide bandwidth communications.

Mr. Shen served as a member of the Technical Program Committee (TPC) for the IEEE Global Communications Conference (GLOBECOM) in 2010, the IEEE International Conference on Communications (ICC) in 2010, and the IEEE Wireless Communications & Networking Conference (WCNC) in 2009 and 2010. He received the Marconi Young Scholar Award from the Marconi Society in 2010, Ernst A. Guillemin Thesis Award (first place) for the best S.M. thesis from the Department of Electrical Engineering and Computer Science at MIT in 2008, the Roberto Padovani Scholarship from Qualcomm Inc. in 2008, the Best Paper Award from the IEEE WCNC in 2007, and the Walter A. Rosenblith Presidential Fellowship from MIT in 2005.

Moe Z. Win (S'85–M'87–SM'97–F'04) received both the Ph.D. degree in electrical engineering and the M.S. degree in applied mathematics as a Presidential Fellow at the University of Southern California (USC) in 1998. He received the M.S. degree in electrical engineering from USC in 1989, and the B.S. degree (*magna cum laude*) in electrical engineering from Texas A&M University in 1987.

He is an Associate Professor at the Massachusetts Institute of Technology (MIT). Prior to joining MIT, he was at AT&T Research Laboratories for five years and at the Jet Propulsion Laboratory for seven years. His research encompasses developing fundamental theories, designing algorithms, and conducting experimentation for a broad range of real-world problems. His current research topics include location-aware networks, intrinsically secure wireless networks, aggregate interference in heterogeneous networks, ultrawide bandwidth systems, multiple antenna systems, time-varying channels, optical transmission systems, and space communications systems.

He is an IEEE Distinguished Lecturer and elected Fellow of the IEEE, cited for "contributions to wideband wireless transmission." He was honored with the IEEE Eric E. Sumner Award (2006), an IEEE Technical Field Award for "pioneering contributions to ultra-wide band communications science and technology." Together with students and colleagues, his papers have received several awards including the IEEE Communications Society's Guglielmo Marconi Best Paper Award (2008) and the IEEE Antennas and Propagation Society's Sergei A. Schelkunoff Transactions Prize Paper Award (2003). His other recognitions include the Laurea Honoris Causa from the University of Ferrara, Italy (2008), the Technical Recognition Award of the IEEE ComSoc Radio Communications Committee (2008), Wireless Educator of the Year Award (2007), the Fulbright Foundation Senior Scholar Lecturing and Research Fellowship (2004), the U.S. Presidential Early Career Award for Scientists and Engineers (2004), the AIAA Young Aerospace Engineer of the Year (2004), and the Office of Naval Research Young Investigator Award (2003).

Prof. Win has been actively involved in organizing and chairing a number of international conferences. He served as the Technical Program Chair for the IEEE Wireless Communications and Networking Conference in 2009, the IEEE Conference on Ultra Wideband in 2006, the IEEE Communication Theory Symposia of ICC-2004 and Globecom-2000, and the IEEE Conference on Ultra Wideband Systems and Technologies in 2002; Technical Program Vice-Chair for the IEEE International Conference on Communications in 2002; and the Tutorial Chair for ICC-2009 and the IEEE Semiannual International Vehicular Technology Conference in Fall 2001. He was the chair (2004-2006) and secretary (2002-2004) for the Radio Communications Committee of the IEEE Communications Society. He is currently an Editor for the IEEE TRANSACTIONS ON WIRELESS COMMUNICATIONS. He served as Area Editor for Modulation and Signal Design (2003-2006), Editor for Wideband Wireless and Diversity (2003-2006), and Editor for Equalization and Diversity (1998-2003), all for the IEEE TRANSACTIONS ON COMMUNICATIONS. He was Guest-Editor for the PROCEEDINGS OF THE IEEE (Special Issue on UWB Technology and Emerging Applications) in 2009 and the IEEE JOURNAL ON SELECTED AREAS IN COMMUNICATIONS (Special Issue on Ultra-Wideband Radio in Multiaccess Wireless Communications) in 2002.

Fundamental Limits of Wideband Localization— Part II: Cooperative Networks

Yuan Shen, *Student Member, IEEE*, Henk Wymeersch, *Member, IEEE*, and Moe Z. Win, *Fellow, IEEE*

Abstract—The availability of position information is of great importance in many commercial, governmental, and military applications. Localization is commonly accomplished through the use of radio communication between mobile devices (agents) and fixed infrastructure (anchors). However, precise determination of agent positions is a challenging task, especially in harsh environments due to radio blockage or limited anchor deployment. In these situations, cooperation among agents can significantly improve localization accuracy and reduce localization outage probabilities. A general framework of analyzing the fundamental limits of wideband localization has been developed in Part I of the paper. Here, we build on this framework and establish the fundamental limits of wideband cooperative location-aware networks. Our analysis is based on the waveforms received at the nodes, in conjunction with Fisher information inequality. We provide a geometrical interpretation of equivalent Fisher information (EFI) for cooperative networks. This approach allows us to succinctly derive fundamental performance limits and their scaling behaviors, and to treat anchors and agents in a unified way from the perspective of localization accuracy. Our results yield important insights into how and when cooperation is beneficial.

Index Terms—Cooperative localization, Cramér–Rao bound (CRB), equivalent Fisher information (EFI), information inequality, ranging information (RI), squared position error bound (SPEB).

I. INTRODUCTION

THE availability of absolute or relative positional information is of great importance in many applications, such as localization services in cellular networks, search-and-rescue operations, asset tracking, blue force tracking, vehicle routing, and intruder detection [1]–[8]. Location-aware networks generally consist of two kinds of nodes: anchors and agents (see Fig. 1), where anchors have known positions while agents have

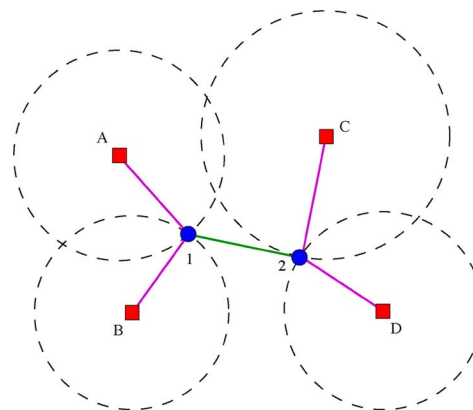


Fig. 1. Cooperative localization: the anchors (A, B, C, and D) communicate with the agents (1 and 2). Agent 1 is not in the communication/ranging range of anchor C and D, while agent 2 is not in the communication/ranging range of anchors A and B. Neither agents can trilaterate its position based solely on the information from its neighboring anchors. However, cooperation between agents 1 and 2 enables both agents to be localized.

unknown positions. Conventionally, each agent localizes itself based on range measurements from at least three distinct anchors (in 2-D localization). Two common examples include the global positioning system (GPS) [9], [10] and beacon localization [11], [12]. In GPS, an agent can determine its location based on the signals received from a constellation of GPS satellites. However, GPS does not operate well in harsh environments, such as indoors or in urban canyons, since the signals cannot propagate through obstacles [7]–[9]. Beacon localization, on the other hand, relies on terrestrial anchors, such as WiFi access points or GSM base stations [11], [12]. However, in areas where network coverage is sparse, e.g., in emergency situations, localization errors can be unacceptably large.

Conventionally, high-accuracy localization can only be achieved using high-power anchors or a high-density anchor deployment, both of which are cost prohibitive and impractical in realistic settings. Hence, there is a need for localization systems that can achieve high accuracy in harsh environments with limited infrastructure requirements [6]–[8]. A practical way to address this need is through a combination of *wideband transmission* and *cooperative localization*. The fine delay resolution and robustness of wide bandwidth or ultrawide bandwidth (UWB) transmission enable accurate and reliable range (distance) measurements in harsh environments [13]–[18].¹ Hence, these transmission techniques are particularly well suited for localization. Cooperative localization is an emerging paradigm that circumvents the needs for high-power, high-density anchor deployment, and offers additional localization

Manuscript received June 21, 2009; revised February 19, 2010. Date of current version September 15, 2010. This work was supported in part by the National Science Foundation under Grant ECCS-0901034, the Office of Naval Research Presidential Early Career Award for Scientists and Engineers (PECASE) N00014-09-1-0435, and the MIT Institute for Soldier Nanotechnologies. The material in this paper was presented in part at the IEEE Wireless Communications and Networking Conference, Hong Kong, March 2007 and the IEEE International Symposium on Spread Spectrum Techniques & Applications, Bologna, Italy, August 2008.

Y. Shen and M. Z. Win are with the Laboratory for Information and Decision Systems (LIDS), Massachusetts Institute of Technology, Cambridge, MA 02139 USA (e-mail: shenyuan@mit.edu; moewin@mit.edu).

H. Wymeersch was with the Laboratory for Information and Decision Systems (LIDS), Massachusetts Institute of Technology, Cambridge, MA 02139 USA. He is now with the Department of Signals and Systems, Chalmers University of Technology, Gothenburg, Sweden (e-mail: henkw@chalmers.se).

Communicated by M. Franceschetti, Associate Editor for Communication Networks.

Color versions of one or more of the figures in this paper are available online at <http://ieeexplore.ieee.org>.

Digital Object Identifier 10.1109/TIT.2010.2059720

¹Other aspects of UWB technology can be found in [19]–[25].

accuracy by enabling the agents to help each other in estimating their positions [5], [6], [26]–[28]. In Fig. 1, for example, since each agent is in the communication/ranging range of only two anchors, neither agents can trilaterate its position based solely on the information from its neighboring anchors. However, cooperation enables both agents to be localized.

Understanding the fundamental limits of localization is crucial not only for providing a performance benchmark but also for guiding the deployment and operation of location-aware networks. Localization accuracy is fundamentally limited due to random phenomena such as noise, fading, shadowing, and multipath propagation. The impact of these phenomena has been investigated for noncooperative localization [7], [8], [29]–[31]. However, little is known regarding the bounds for cooperative localization. In particular, bounds on the cooperative localization performance were previously derived in [27] and [28] using only specific ranging models. In other words, these works start from signal metrics, extracted from the received waveforms.² Such a process may discard information relevant for localization. Furthermore, the statistical models for those signal metrics depend heavily on the measurement processes. For instance, the ranging error of the time-of-arrival (TOA) metric is commonly modeled as additive Gaussian [27], [28], [31]. However, other studies (both theoretical [15], [38], [39] and experimental [8], [18]) indicate that the ranging error is not Gaussian. Hence, when deriving the fundamental limits of localization accuracy, it is important to start from the received waveforms rather than from signal metrics extracted from those waveforms.

In Part I [29], we have developed a general framework to characterize the localization accuracy of a given agent. In this paper, we build on the framework and determine fundamental properties of *cooperative* location-aware networks employing wideband transmission. The main contributions of this paper are as follows.

- We derive the fundamental limits of localization accuracy for wideband wireless cooperative networks in terms of a performance measure called the squared position error bound (SPEB).
- We employ the notion of equivalent Fisher information (EFI) to derive the network localization information, and show that this information can be decomposed into basic building blocks associated with every pair of the nodes, called the ranging information (RI).
- We quantify the contribution of the *a priori* knowledge of the channel parameters and the agents' positions to the network localization information, and show that agents and anchors can be treated in a unified way: anchors are special agents with infinite *a priori* position knowledge.
- We put forth a geometric interpretation of the EFI matrix (EFIM) using eigendecomposition, providing insights into the network localization problem.
- We derive scaling laws for the SPEB for both dense and extended location-aware networks, characterizing the behavior of cooperative location-aware networks in an asymptotic regime.

²Commonly used signal metrics include time-of-arrival (TOA) [7], [8], [15], [17], [32], time-difference-of-arrival (TDOA) [33], [34], angle-of-arrival (AOA) [7], [35], and received signal strength (RSS) [7], [36], [37].

The proposed framework generalizes the existing work on non-cooperative localization [29] to cooperative networks, provides insights into the network localization problem, and can guide the design and deployment of location-aware networks.

The rest of the paper is organized as follows. Section II presents the system model and the concept of SPEB. In Section III, we apply the notion of EFI to derive the SPEB. Then, in Section IV, we provide a geometric interpretation of EFIM for localization and derive scaling laws for the SPEB. Finally, numerical results are given in Section V, and conclusions are drawn in the last section.

Notation: The notation $\mathbb{E}_{\mathbf{x}}\{\cdot\}$ is the expectation operator with respect to the random vectors \mathbf{x} ; $\mathbf{A} \succ \mathbf{B}$ and $\mathbf{A} \succeq \mathbf{B}$ denote that the matrix $\mathbf{A} - \mathbf{B}$ is positive definite and positive semidefinite, respectively; $\text{tr}\{\cdot\}$ denotes the trace of a square matrix; $[\cdot]^T$ denotes the transpose of its argument; $[\cdot]_{n \times n, k}$ denotes the k th $n \times n$ submatrix that starts from element $n(k-1) + 1$ on the diagonal of its argument; $[\cdot]_{r_1:r_2, c_1:c_2}$ denotes a submatrix composed of the rows r_1 to r_2 and the columns c_1 to c_2 of its argument; and $\|\cdot\|$ denotes the Euclidean norm of its argument. We also denote by $f(\mathbf{x})$ the probability density function (pdf) $f_{\mathbf{X}}(\mathbf{x})$ of the random vector \mathbf{X} unless specified otherwise.

II. SYSTEM MODEL

In this section, we describe the wideband channel model and formulate the localization problem. We briefly review the information inequality and the performance measure called SPEB.

A. Signal Model

Consider a synchronous network consisting of N_b anchors (or beacons) and N_a agents with fixed topology.³ Anchors have perfect knowledge of their positions, while each agent attempts to estimate its position based on the waveforms received from neighboring nodes (see Fig. 1). Unlike conventional localization techniques, we consider a cooperative setting, where agents utilize waveforms received from neighboring agents in addition to those from anchors. The set of agents is denoted by $\mathcal{N}_a = \{1, 2, \dots, N_a\}$, while the set of anchors is $\mathcal{N}_b = \{N_a + 1, N_a + 2, \dots, N_a + N_b\}$. The position of node k is denoted by $\mathbf{p}_k \triangleq [x_k \ y_k]^T$.⁴ Let ϕ_{kj} denote the angle from node k to node j , i.e.,

$$\phi_{kj} = \tan^{-1} \frac{y_k - y_j}{x_k - x_j}$$

and $\mathbf{q}_{kj} \triangleq [\cos \phi_{kj} \ \sin \phi_{kj}]^T$ denote the corresponding unit vector.

The received waveform at the k th agent ($k \in \mathcal{N}_a$) from the j th node ($j \in \mathcal{N}_b \cup \mathcal{N}_a \setminus \{k\}$) can be written as [24], [41]

$$r_{kj}(t) = \sum_{l=1}^{L_{kj}} \alpha_{kj}^{(l)} s(t - \tau_{kj}^{(l)}) + z_{kj}(t), \quad t \in [0, T_{ob}] \quad (1)$$

³We consider synchronous networks for notional convenience. Our approach is also valid for asynchronous networks, where devices employ round-trip time-of-flight measurements [25], [40].

⁴For convenience, we focus on 2-D localization where $\mathbf{p}_k \in \mathbb{R}^2$, and we will later mention extensions to 3-D localization.

where $s(t)$ is a known wideband waveform with Fourier transform $S(f)$, $\alpha_{kj}^{(l)}$ and $\tau_{kj}^{(l)}$ are the amplitude and delay, respectively, of the l th path,⁵ L_{kj} is the number of multipath components, $z_{kj}(t)$ represents the observation noise, modeled as additive white Gaussian processes with two-sided power spectral density $N_0/2$, and $[0, T_{\text{ob}})$ is the observation interval. The relationship between the positions of nodes and the delays of the propagation paths is

$$\tau_{kj}^{(l)} = \frac{1}{c} \left[\|\mathbf{p}_k - \mathbf{p}_j\| + b_{kj}^{(l)} \right], \quad j \in \mathcal{N}_b \cup \mathcal{N}_a \setminus \{k\} \quad (2)$$

where c is the propagation speed of the signal, and $b_{kj}^{(l)} \geq 0$ is a range bias induced by nonline-of-sight (NLOS) propagation. Line-of-sight (LOS) signals occur when the direct path between nodes k and j is unobstructed, such that $b_{kj}^{(1)} = 0$.

B. Error Bounds on Position Estimation

We first introduce $\boldsymbol{\theta}$ as the vector of unknown parameters

$$\boldsymbol{\theta} = \left[\mathbf{P}^T \quad \tilde{\boldsymbol{\theta}}_1^T \quad \tilde{\boldsymbol{\theta}}_2^T \quad \cdots \quad \tilde{\boldsymbol{\theta}}_{N_a}^T \right]^T$$

where \mathbf{P} consists of all the agents' positions

$$\mathbf{P} = \left[\mathbf{p}_1^T \quad \mathbf{p}_2^T \quad \cdots \quad \mathbf{p}_{N_a}^T \right]^T$$

and $\tilde{\boldsymbol{\theta}}_k$ is the vector of the multipath parameters associated with the waveforms received at the k th agent⁶

$$\tilde{\boldsymbol{\theta}}_k = \left[\boldsymbol{\kappa}_{k,1}^T \quad \cdots \quad \boldsymbol{\kappa}_{k,k-1}^T \quad \boldsymbol{\kappa}_{k,k+1}^T \quad \cdots \quad \boldsymbol{\kappa}_{k,N_a+N_b}^T \right]^T$$

in which $\boldsymbol{\kappa}_{kj}$ is the vector of the multipath parameters associated with $r_{kj}(t)$ ⁷

$$\boldsymbol{\kappa}_{kj} = \left[b_{kj}^{(1)} \quad \alpha_{kj}^{(1)} \quad \cdots \quad b_{kj}^{(L_{kj})} \quad \alpha_{kj}^{(L_{kj})} \right]^T.$$

Second, we introduce \mathbf{r} as the vector representation of all the received waveforms, given by $\mathbf{r} = [\mathbf{r}_1^T \quad \mathbf{r}_2^T \quad \cdots \quad \mathbf{r}_{N_a}^T]^T$, where

$$\mathbf{r}_k = \left[\mathbf{r}_{k,1}^T \quad \cdots \quad \mathbf{r}_{k,k-1}^T \quad \mathbf{r}_{k,k+1}^T \quad \cdots \quad \mathbf{r}_{k,N_a+N_b}^T \right]^T$$

in which \mathbf{r}_{kj} is obtained from the Karhunen–Loève (KL) expansion of $r_{kj}(t)$ [42], [43]. We tacitly assume that when nodes j and k cannot communicate directly, the corresponding entry \mathbf{r}_{kj} is omitted in \mathbf{r} .

We can now introduce an estimator $\hat{\boldsymbol{\theta}}$ of the unknown parameter $\boldsymbol{\theta}$ based on the observation \mathbf{r} . The mean squared error (MSE) matrix of $\hat{\boldsymbol{\theta}}$ satisfies the information inequality [42]–[44]

$$\mathbb{E}_{\mathbf{r}, \boldsymbol{\theta}} \{ (\hat{\boldsymbol{\theta}} - \boldsymbol{\theta})(\hat{\boldsymbol{\theta}} - \boldsymbol{\theta})^T \} \succeq \mathbf{J}_{\boldsymbol{\theta}}^{-1} \quad (3)$$

⁵We consider the general case where the wideband channel is not necessarily reciprocal. Our results can be easily specialized to the reciprocal case, where we have $L_{kj} = L_{jk}$, $\alpha_{kj}^{(l)} = \alpha_{jk}^{(l)}$, and $\tau_{kj}^{(l)} = \tau_{jk}^{(l)}$ hence $b_{kj}^{(l)} = b_{jk}^{(l)}$, for $l = 1, 2, \dots, L_{kj}$.

⁶In cases where the channel is reciprocal, only half of the multipath parameters are needed. Without loss of generality, we only use $\{\alpha_{kj}^{(l)}, b_{kj}^{(l)} : k, j \in \mathcal{N}_a, k > j\}$.

⁷The bias $b_{kj}^{(1)} = 0$ for LOS signals. From the perspective of Bayesian estimation, it can be thought of as a random parameter with infinite *a priori* Fisher information [29].

where $\mathbf{J}_{\boldsymbol{\theta}}$ is the Fisher information matrix (FIM) for $\boldsymbol{\theta}$,⁸ given by

$$\mathbf{J}_{\boldsymbol{\theta}} = \mathbb{E}_{\mathbf{r}, \boldsymbol{\theta}} \left\{ -\frac{\partial^2}{\partial \boldsymbol{\theta} \partial \boldsymbol{\theta}^T} \ln f(\mathbf{r}, \boldsymbol{\theta}) \right\} \quad (4)$$

in which $f(\mathbf{r}, \boldsymbol{\theta})$ is the joint pdf of the observation \mathbf{r} and the parameter vector $\boldsymbol{\theta}$. For an estimate $\hat{\mathbf{p}}_k$ of the k th agent's position, (3) implies that

$$\mathbb{E}_{\mathbf{r}, \boldsymbol{\theta}} \{ (\hat{\mathbf{p}}_k - \mathbf{p}_k)(\hat{\mathbf{p}}_k - \mathbf{p}_k)^T \} \succeq [\mathbf{J}_{\boldsymbol{\theta}}^{-1}]_{2 \times 2, k}.$$

One natural measure for position accuracy is the average squared position error $\mathbb{E}_{\mathbf{r}, \boldsymbol{\theta}} \{ \|\hat{\mathbf{p}}_k - \mathbf{p}_k\|^2 \}$, which can be bounded below by $\mathcal{P}(\mathbf{p}_k)$ defined in the following.

Definition 1 (SPEB [29]): The SPEB of the k th agent is defined to be

$$\mathcal{P}(\mathbf{p}_k) \triangleq \text{tr} \left\{ [\mathbf{J}_{\boldsymbol{\theta}}^{-1}]_{2 \times 2, k} \right\}.$$

Since the error of the position estimate $\hat{\mathbf{p}}_k - \mathbf{p}_k$ is a vector, it may also be of interest to know the position error in a particular direction. The directional position error along a given unit vector \mathbf{u} is the position error projected on it, i.e., $\mathbf{u}^T(\hat{\mathbf{p}}_k - \mathbf{p}_k)$, and its average squared error $\mathbb{E}_{\mathbf{r}, \boldsymbol{\theta}} \{ \|\mathbf{u}^T(\hat{\mathbf{p}}_k - \mathbf{p}_k)\|^2 \}$ can be bounded below by $\mathcal{P}(\mathbf{p}_k; \mathbf{u})$ defined in the following.⁹

Definition 2 (Directional Position Error Bound): The directional position error bound (DPEB) of the k th agent with constraint $\mathbf{u}_{\perp}^T(\hat{\mathbf{p}}_k - \mathbf{p}_k) = 0$ is defined to be

$$\mathcal{P}(\mathbf{p}_k; \mathbf{u}) \triangleq \mathbf{u}^T [\mathbf{J}_{\boldsymbol{\theta}}^{-1}]_{2 \times 2, k} \mathbf{u}$$

where $\mathbf{u}, \mathbf{u}_{\perp} \in \mathbb{R}^2$ are unit vectors such that $\langle \mathbf{u}, \mathbf{u}_{\perp} \rangle = 0$.

Proposition 1: The SPEB of the k th agent is the sum of the DPEBs in any two orthogonal directions, i.e.,

$$\mathcal{P}(\mathbf{p}_k) = \mathcal{P}(\mathbf{p}_k; \mathbf{u}) + \mathcal{P}(\mathbf{p}_k; \mathbf{u}_{\perp}). \quad (5)$$

Proof: See Appendix I. \square

C. Joint PDF of Observations and Parameters

Evaluation of (4) requires knowledge of the joint distribution $f(\mathbf{r}, \boldsymbol{\theta})$. We can write $f(\mathbf{r}, \boldsymbol{\theta}) = f(\mathbf{r} | \boldsymbol{\theta}) f(\boldsymbol{\theta})$, where $f(\mathbf{r} | \boldsymbol{\theta})$ is the likelihood function, and $f(\boldsymbol{\theta})$ is the *a priori* distribution of the parameter $\boldsymbol{\theta}$.¹⁰ In this section, we describe the structure of both functions in detail.

Since the received waveforms $r_{kj}(t)$ are independent conditioned on the parameter $\boldsymbol{\theta}$, $f(\mathbf{r} | \boldsymbol{\theta})$ can be expressed as [42], [43]

$$f(\mathbf{r} | \boldsymbol{\theta}) = \prod_{k \in \mathcal{N}_a} \prod_{j \in \mathcal{N}_b \cup \mathcal{N}_a \setminus \{k\}} f(\mathbf{r}_{kj} | \boldsymbol{\theta}) \quad (6)$$

⁸With a slight abuse of notation, $\mathbb{E}_{\mathbf{r}, \boldsymbol{\theta}} \{ \cdot \}$ in (3) and (4) will be used for deterministic, random, and hybrid cases, with the understanding that the expectation operation is not performed over the deterministic components of $\boldsymbol{\theta}$ [43], [44]. Note also that for the deterministic components, the lower bound is valid for their unbiased estimates.

⁹In higher dimensions, this notion can be extended to the position error in any subspaces, such as a hyperplane.

¹⁰When a subset of the parameters are deterministic, they are eliminated from $f(\boldsymbol{\theta})$.

where

$$f(\mathbf{r}_{kj} | \boldsymbol{\theta}) \propto \exp \left\{ \frac{2}{N_0} \int_0^{T_{\text{ob}}} r_{kj}(t) \sum_{l=1}^{L_{kj}} \alpha_{kj}^{(l)} s(t - \tau_{kj}^{(l)}) dt - \frac{1}{N_0} \int_0^{T_{\text{ob}}} \left[\sum_{l=1}^{L_{kj}} \alpha_{kj}^{(l)} s(t - \tau_{kj}^{(l)}) \right]^2 dt \right\}. \quad (7)$$

When the multipath parameters $\boldsymbol{\kappa}_{kj}$ are independent conditioned on the nodes' positions,¹¹ $f(\boldsymbol{\theta})$ can be expressed as

$$\begin{aligned} f(\boldsymbol{\theta}) &= f(\mathbf{P}) \prod_{k \in \mathcal{N}_a} f(\tilde{\boldsymbol{\theta}}_k | \mathbf{P}) \\ &= f(\mathbf{P}) \prod_{k \in \mathcal{N}_a} \prod_{j \in \mathcal{N}_b \cup \mathcal{N}_a \setminus \{k\}} f(\boldsymbol{\kappa}_{kj} | \mathbf{P}) \end{aligned} \quad (8)$$

where $f(\mathbf{P})$ is the joint pdf of all the agents' positions, and $f(\boldsymbol{\kappa}_{kj} | \mathbf{P})$ is the joint pdf of the multipath parameters $\boldsymbol{\kappa}_{kj}$ conditioned on the agents' positions. Based on existing propagation models for wideband and UWB channels [14], [25], the joint pdf of the channel parameters can be further written as [29]

$$f(\boldsymbol{\kappa}_{kj} | \mathbf{P}) = f(\boldsymbol{\kappa}_{kj} | d_{kj}) \quad (9)$$

where $d_{kj} = \|\mathbf{p}_k - \mathbf{p}_j\|$ for $k \in \mathcal{N}_a$ and $j \in \mathcal{N}_b \cup \mathcal{N}_a \setminus \{k\}$.

Combining (8) and (6) leads to

$$\begin{aligned} \ln f(\mathbf{r}, \boldsymbol{\theta}) &= \sum_{k \in \mathcal{N}_a} \sum_{j \in \mathcal{N}_b} [\ln f(\mathbf{r}_{kj} | \boldsymbol{\theta}) + \ln f(\boldsymbol{\kappa}_{kj} | \mathbf{P})] \\ &+ \sum_{k \in \mathcal{N}_a} \sum_{j \in \mathcal{N}_a \setminus \{k\}} [\ln f(\mathbf{r}_{kj} | \boldsymbol{\theta}) + \ln f(\boldsymbol{\kappa}_{kj} | \mathbf{P})] \\ &+ \ln f(\mathbf{P}) \end{aligned} \quad (10)$$

where the first and second groups of summation account for the information from anchors and that from agents' cooperation, respectively, and the last term accounts for the information from the *a priori* knowledge of the agents' positions. This implies that the FIM for $\boldsymbol{\theta}$ in (4) can be written as $\mathbf{J}_{\boldsymbol{\theta}} = \mathbf{J}_{\boldsymbol{\theta}}^A + \mathbf{J}_{\boldsymbol{\theta}}^C + \mathbf{J}_{\boldsymbol{\theta}}^P$, where $\mathbf{J}_{\boldsymbol{\theta}}^A$, $\mathbf{J}_{\boldsymbol{\theta}}^C$, and $\mathbf{J}_{\boldsymbol{\theta}}^P$ correspond to the localization information from anchors, agents' cooperation, and *a priori* knowledge of the agents' positions, respectively.

III. EVALUATION OF FIM

In this section, we briefly review the notion of EFI [29] and apply it to derive the SPEB for each agent. We consider both the cases with and without *a priori* knowledge of the agents' positions. We also introduce the concept of RI, which turns out to be the basic building block for the EFIM.

A. EFIM and RI

We saw in the previous section that the SPEB can be obtained by inverting the FIM $\mathbf{J}_{\boldsymbol{\theta}}$ in (4). However, $\mathbf{J}_{\boldsymbol{\theta}}$ is a matrix of very high dimensions, while only a much smaller submatrix $[\mathbf{J}_{\boldsymbol{\theta}}^{-1}]_{2N_a \times 2N_a}$ is of interest. To gain insights into localization

¹¹This is a common model for analyzing wideband communication, unless two nodes are close to each other so that the channels from a third node to them are correlated. Our analysis can also account for the correlated channels, in which case the SPEB will be higher than that corresponding to the independent channels.

problem, we will employ the notions of EFIM and RI [29]. For the completeness of the paper, we briefly review the notions in the following.

Definition 3 (EFIM): Given a parameter vector $\boldsymbol{\theta} = [\boldsymbol{\theta}_1^T \ \boldsymbol{\theta}_2^T]^T$ and the FIM $\mathbf{J}_{\boldsymbol{\theta}}$ of the form

$$\mathbf{J}_{\boldsymbol{\theta}} = \begin{bmatrix} \mathbf{A} & \mathbf{B} \\ \mathbf{B}^T & \mathbf{C} \end{bmatrix}$$

where $\boldsymbol{\theta} \in \mathbb{R}^N$, $\boldsymbol{\theta}_1 \in \mathbb{R}^n$, $\mathbf{A} \in \mathbb{R}^{n \times n}$, $\mathbf{B} \in \mathbb{R}^{n \times (N-n)}$, and $\mathbf{C} \in \mathbb{R}^{(N-n) \times (N-n)}$ with $n < N$, the EFIM for $\boldsymbol{\theta}_1$ is given by

$$\mathbf{J}_e(\boldsymbol{\theta}_1) \triangleq \mathbf{A} - \mathbf{B}\mathbf{C}^{-1}\mathbf{B}^T. \quad (11)$$

Note that the EFIM retains all the necessary information to derive the information inequality for the parameter $\boldsymbol{\theta}_1$, in a sense that $[\mathbf{J}_{\boldsymbol{\theta}}^{-1}]_{n \times n} = [\mathbf{J}_e(\boldsymbol{\theta}_1)]^{-1}$, so that the MSE matrix of the estimates of $\boldsymbol{\theta}_1$ is "bounded" below by $[\mathbf{J}_e(\boldsymbol{\theta}_1)]^{-1}$. The right-hand side of (11) is known as the Schur's complement of matrix \mathbf{A} [45], and it has been used for simplifying the Cramér–Rao bounds (CRBs) [31], [32], [46].

Definition 4 (RI): The RI is a 2×2 matrix of the form $\lambda \mathbf{J}_r(\phi)$, where λ is a nonnegative number called the ranging information intensity (RII) and the matrix $\mathbf{J}_r(\phi)$ is called the ranging direction matrix (RDM) with the following structure:

$$\mathbf{J}_r(\phi) \triangleq \begin{bmatrix} \cos^2 \phi & \cos \phi \sin \phi \\ \cos \phi \sin \phi & \sin^2 \phi \end{bmatrix}.$$

The RDM $\mathbf{J}_r(\phi)$ has exactly one nonzero eigenvalue equal to 1 with corresponding eigenvector $\mathbf{q} = [\cos \phi \ \sin \phi]^T$, i.e., $\mathbf{J}_r(\phi) = \mathbf{q}\mathbf{q}^T$. Thus, the corresponding RI is "1-D" along the direction ϕ .

B. EFIM Without a Priori Position Knowledge

In this section, we consider the case in which *a priori* knowledge of the agents' positions is unavailable, i.e., $f(\mathbf{P})$ is eliminated from (8). We first prove a general theorem, describing the structure of the EFIM, followed by a special case, where there is no *a priori* knowledge regarding the channel parameters.

Theorem 1: When *a priori* knowledge of the agents' positions is unavailable, and the channel parameters corresponding to different waveforms are mutually independent, the EFIM for the agents' positions is a $2N_a \times 2N_a$ matrix, structured as (12), shown at the bottom of the next page, where $\mathbf{J}_e^A(\mathbf{p}_k)$ and \mathbf{C}_{kj} can be expressed in terms of the RI

$$\mathbf{J}_e^A(\mathbf{p}_k) = \sum_{j \in \mathcal{N}_b} \lambda_{kj} \mathbf{J}_r(\phi_{kj})$$

and

$$\mathbf{C}_{kj} = \mathbf{C}_{jk} = (\lambda_{kj} + \lambda_{jk}) \mathbf{J}_r(\phi_{kj})$$

with λ_{kj} given by (35) in Appendix II.

Proof: See Appendix II. \square

Remark 1: We make the following remarks.

- To obtain the SPEB of a specific agent, we can apply EFI analysis again and further reduce $\mathbf{J}_e(\mathbf{P})$ into a 2×2 EFIM.

- The RI is the basic building block of the EFIM for localization, and each RI corresponds to an individual received waveform. The RII λ_{kj} is determined by the power and bandwidth of the received waveform, the multipath propagation, as well as the *a priori* channel knowledge. Note that each received waveform provides only 1-D information for localization along the angle ϕ_{kj} .
- The EFIM $\mathbf{J}_e(\mathbf{P})$ can be decomposed into localization information from anchors and that from agents' cooperation. The former part is represented as a block-diagonal matrix whose nonzero elements are $\mathbf{J}_e^A(\mathbf{p}_k)$, for the k th agent, and each $\mathbf{J}_e^A(\mathbf{p}_k)$ is a weighted sum of RDMs over anchors. Hence, the localization information from anchors is not interrelated among agents. The latter part is a highly structured matrix consisting of RIs \mathbf{C}_{kj} . Hence, the localization information from agents' cooperation is highly interrelated. This is intuitive since the effectiveness of the localization information provided by a particular agent depends on its position error.

Theorem 2: When *a priori* knowledge of the agents' positions and the channel parameters is unavailable, the EFIM for the agents' positions is a $2N_a \times 2N_a$ matrix, structured as in (12) with the RII λ_{kj} given by

$$\lambda_{kj} = \begin{cases} 8\pi^2\beta^2/c^2 \cdot (1 - \chi_{kj}) \text{SNR}_{kj}^{(1)}, & \text{LOS signal} \\ 0, & \text{NLOS signal} \end{cases}$$

where β is the effective bandwidth of transmitted waveform $s(t)$

$$\beta = \left(\frac{\int_{-\infty}^{+\infty} f^2 |S(f)|^2 df}{\int_{-\infty}^{+\infty} |S(f)|^2 df} \right)^{1/2}$$

$\text{SNR}_{kj}^{(1)}$ is the SNR of the *first* path in $r_{kj}(t)$

$$\text{SNR}_{kj}^{(1)} = \frac{|\alpha_{kj}^{(1)}|^2 \int_{-\infty}^{+\infty} |S(f)|^2 df}{N_0} \quad (13)$$

and $0 \leq \chi_{kj} \leq 1$ is called the *path-overlap coefficient*, which depends on the first contiguous cluster¹² in LOS signals.

Proof: See Appendix III. \square

Remark 2: We make the following remarks.

- The theorem shows that when *a priori* knowledge of channel parameters is unavailable, the NLOS signals do not contribute to localization accuracy, and hence these signals can be discarded. This agrees with the previous

¹²The first contiguous cluster is the first group of non-disjoint paths. Two paths that arrive at time τ_i and τ_j are called non-disjoint if $|\tau_i - \tau_j|$ is less than the duration of $s(t)$ [29].

observations in [8], [31], and [32] although the authors considered different models.

- For LOS signals, the RII is determined by the first contiguous cluster [29], implying that it is not necessary to process the latter multipath components. In particular, the RII is determined by the effective bandwidth β , the first path's SNR, and the propagation effect characterized by χ_{kj} .
- Since $\chi_{kj} \geq 0$, path overlap always deteriorates the accuracy unless $\chi_{kj} = 0$, in which the first signal component $s(t - \tau_{kj}^{(1)})$ does not overlap with later components $s(t - \tau_{kj}^{(l)})$ for $l > 1$.

C. EFIM With a Priori Position Knowledge

We now consider the case in which the *a priori* knowledge of the agents' positions, characterized by $f(\mathbf{P})$, is available. We first derive the EFIM, based on which we prove that agents and anchors can be treated in a unified way under this framework. We then present a special scenario in which the *a priori* knowledge of the agents' positions satisfies certain conditions so that we can gain insights into the EFIM.

Theorem 3: When *a priori* knowledge of the agents' positions is available, and the channel parameters corresponding to different waveforms are mutually independent, the EFIM for the agents' positions is a $2N_a \times 2N_a$ matrix, given by¹³

$$\mathbf{J}_e(\mathbf{P}) = \mathbf{J}_e^A(\mathbf{P}) + \mathbf{J}_e^C(\mathbf{P}) + \mathbf{\Xi}_P \quad (14)$$

where

$$\begin{aligned} [\mathbf{J}_e^A(\mathbf{P})]_{2k-1:2k, 2m-1:2m} &= \begin{cases} \sum_{j \in \mathcal{N}_b} \mathbf{R}_k(\mathbf{r}_{kj}), & k = m \\ \mathbf{0}, & k \neq m \end{cases} \\ [\mathbf{J}_e^C(\mathbf{P})]_{2k-1:2k, 2m-1:2m} &= \begin{cases} \sum_{j \in \mathcal{N}_a \setminus \{k\}} [\mathbf{R}_k(\mathbf{r}_{kj}) + \mathbf{R}_k(\mathbf{r}_{jk})], & k = m \\ -[\mathbf{R}_k(\mathbf{r}_{km}) + \mathbf{R}_k(\mathbf{r}_{mk})], & k \neq m \end{cases} \end{aligned}$$

and

$$\mathbf{\Xi}_P = \mathbb{E}_P \left\{ -\frac{\partial^2}{\partial \mathbf{P} \partial \mathbf{P}^T} \ln f(\mathbf{P}) \right\}$$

with $\mathbf{R}_k(\mathbf{r}_{kj}) \in \mathbb{R}^{2 \times 2}$ given by (15), shown at the bottom of the next page. Block matrix $\mathbf{\Phi}_{kj}(\mathbf{x}, \mathbf{y})$ in (15) is defined as (27) in Appendix II.

Proof: See Appendix IV. \square

¹³Note that $\mathbf{J}_e(\mathbf{P})$ in (14) does not depend on any particular value of the random vector \mathbf{P} , whereas $\mathbf{J}_e(\mathbf{P})$ in (12) is a function of the deterministic vector \mathbf{P} .

$$\mathbf{J}_e(\mathbf{P}) = \begin{bmatrix} \mathbf{J}_e^A(\mathbf{p}_1) + \sum_{j \in \mathcal{N}_a \setminus \{1\}} \mathbf{C}_{1,j} & -\mathbf{C}_{1,2} & \cdots & -\mathbf{C}_{1,N_a} \\ -\mathbf{C}_{1,2} & \mathbf{J}_e^A(\mathbf{p}_2) + \sum_{j \in \mathcal{N}_a \setminus \{2\}} \mathbf{C}_{2,j} & & -\mathbf{C}_{2,N_a} \\ \vdots & & \ddots & \\ -\mathbf{C}_{1,N_a} & -\mathbf{C}_{2,N_a} & & \mathbf{J}_e^A(\mathbf{p}_{N_a}) + \sum_{j \in \mathcal{N}_a \setminus \{N_a\}} \mathbf{C}_{N_a,j} \end{bmatrix} \quad (12)$$

Remark 3: The EFIM for agents' positions is derived in (14) for the case when *a priori* knowledge of the agents' positions is available. Compared to (12) in the Theorem 1, the EFIM in (14) retains the same structure of the localization information from both anchors and cooperation, except that all RIs in Theorem 3 are obtained by averaging the 2×2 matrices over the possible agents' positions. In addition, the localization information from the position knowledge is characterized in terms of an additive component $\Xi_{\mathbf{P}}$. This knowledge improves localization because $\Xi_{\mathbf{P}}$ is positive semidefinite.

Based on the result of Theorem 3, we can now treat anchors and agents in a unified way, as will be shown in the following theorem.

Theorem 4: Anchors are equivalent to agents with infinite *a priori* position knowledge in the following sense: when the k th agent has infinite *a priori* position knowledge, i.e., $\Xi_{\mathbf{p}_k} = \lim_{t^2 \rightarrow \infty} \text{diag}\{t^2, t^2\}$, then

$$\mathbf{J}_e(\mathbf{P}_{\bar{k}}) = [\mathbf{J}_e(\mathbf{P})]_{\bar{k}}$$

where $\mathbf{P}_{\bar{k}}$ is the vector \mathbf{P} without rows $2k - 1$ to $2k$, and $[\mathbf{J}_e(\mathbf{P})]_{\bar{k}}$ is the matrix $\mathbf{J}_e(\mathbf{P})$ without rows $2k - 1$ to $2k$ and columns $2k - 1$ to $2k$.

Proof: See Appendix V. \square

Remark 4: The theorem shows mathematically that agents are equivalent to anchors if they have infinite *a priori* position knowledge, which agrees with our intuition. As such, it is not necessary to distinguish between agents and anchors. This view will facilitate the analysis of location-aware networks and the design of localization algorithms: every agent can treat the information coming from anchors and other cooperating agents in a unified way.

The general expression of the EFIM for the case with *a priori* position knowledge is given in (14), which is much more involved than that for the case without position knowledge in (12). However, in the special case when

$$\mathbb{E}_{\mathbf{P}}\{g(\mathbf{P})\} = g(\mathbb{E}_{\mathbf{P}}\{\mathbf{P}\}) \quad (16)$$

for the functions $g(\cdot)$ involved in the derivation of the EFIM (see Appendix IV),¹⁴ we can gain insight into the structure of the EFIM as shown by the following corollary.

¹⁴This occurs when every agent's *a priori* position distribution is concentrated in a small area relative to the distance between the agent and the other nodes, so that $g(\mathbf{P})$ is flat in that area.

Corollary 1: When the *a priori* distribution of the agents' positions satisfies (16), and the channel parameters corresponding to different waveforms are mutually independent, the EFIM for the agents' positions is a $2N_a \times 2N_a$ matrix, structured as (17), shown at the bottom of the page, where $\bar{\mathbf{J}}_e^A(\mathbf{p}_k)$ and $\bar{\mathbf{C}}_{kj}$ can be expressed in terms of the RI

$$\bar{\mathbf{J}}_e^A(\mathbf{p}_k) = \sum_{j \in \mathcal{N}_b} \bar{\lambda}_{kj} \mathbf{J}_r(\bar{\phi}_{kj})$$

and

$$\bar{\mathbf{C}}_{kj} = \bar{\mathbf{C}}_{jk} = (\bar{\lambda}_{kj} + \bar{\lambda}_{jk}) \mathbf{J}_r(\bar{\phi}_{kj})$$

where $\bar{\mathbf{P}} = \mathbb{E}_{\mathbf{P}}\{\mathbf{P}\}$, $\bar{\lambda}_{kj}$ is the RII given in (35) evaluated at $\bar{\mathbf{P}}$, and $\bar{\phi}_{kj}$ is the angle from $\bar{\mathbf{p}}_k$ to $\bar{\mathbf{p}}_j$.

Proof: See Appendix IV. \square

D. Discussions

We will now discuss the results derived in the previous sections. Our discussion includes 1) the EFIM for the agents in noncooperative localization, 2) an application of the cooperative localization to tracking, 3) a recursive method to construct an EFIM for large networks, and 4) the extension to 3-D scenarios.

1) *Noncooperative Localization:* When the agents do not cooperate, the matrices corresponding to the agents' cooperation in (12) in Theorem 1 and (17) in Corollary 1 are discarded. In particular, the EFIM $\mathbf{J}_e(\mathbf{P})$ in Theorem 1 reverts to

$$\mathbf{J}_e(\mathbf{P}) = \text{diag}\{\mathbf{J}_e^A(\mathbf{p}_1), \mathbf{J}_e^A(\mathbf{p}_2), \dots, \mathbf{J}_e^A(\mathbf{p}_{N_a})\}$$

and hence the 2×2 EFIM for the k th agent is equal to $\mathbf{J}_e(\mathbf{p}_k) = \mathbf{J}_e^A(\mathbf{p}_k)$. Similarly, the EFIM $\mathbf{J}_e(\mathbf{P})$ in Corollary 1 reverts to

$$\mathbf{J}_e(\mathbf{P}) = \text{diag}\{\bar{\mathbf{J}}_e^A(\mathbf{p}_1), \bar{\mathbf{J}}_e^A(\mathbf{p}_2), \dots, \bar{\mathbf{J}}_e^A(\mathbf{p}_{N_a})\} + \Xi_{\mathbf{P}}.$$

Furthermore, when the agents' positions are independent *a priori*, $\Xi_{\mathbf{P}} = \text{diag}\{\Xi_{\mathbf{p}_1}, \Xi_{\mathbf{p}_2}, \dots, \Xi_{\mathbf{p}_{N_a}}\}$ and the 2×2 EFIM for the k th agent can be written as $\mathbf{J}_e(\mathbf{p}_k) = \bar{\mathbf{J}}_e^A(\mathbf{p}_k) + \Xi_{\mathbf{p}_k}$.

2) *Spatial Versus Temporal Cooperation for Localization:* Rather than multiple agents in cooperation, a single agent can "cooperate" with itself over time. Such temporal cooperative localization can easily be analyzed within our framework, as follows.

Consider a single agent moving in sequence to N different positions according to piecewise linear walk and receiving waveforms from neighboring anchors at each position. The N positions can be written as $\mathbf{P} = [\mathbf{p}_1^T \ \mathbf{p}_2^T \ \dots \ \mathbf{p}_N^T]^T$, and

$$\mathbf{R}_k(\mathbf{r}_{kj}) = \mathbb{E}_{\mathbf{P}}\{\Phi_{kj}(d_{kj}, d_{kj}) \mathbf{q}_{kj} \mathbf{q}_{kj}^T\} - \mathbb{E}_{\mathbf{P}}\{\mathbf{q}_{kj} \Phi_{kj}(d_{kj}, \mathbf{p}_k)\} \mathbb{E}_{\mathbf{P}}\{\Phi_{kj}(\kappa_{kj}, \kappa_{kj})\}^{-1} \mathbb{E}_{\mathbf{P}}\{\Phi_{kj}(\mathbf{p}_k, d_{kj}) \mathbf{q}_{kj}^T\}. \quad (15)$$

$$\mathbf{J}_e(\mathbf{P}) = \begin{bmatrix} \bar{\mathbf{J}}_e^A(\mathbf{p}_1) + \sum_{j \in \mathcal{N}_a \setminus \{1\}} \bar{\mathbf{C}}_{1,j} & -\bar{\mathbf{C}}_{1,2} & \dots & -\bar{\mathbf{C}}_{1,N_a} \\ -\bar{\mathbf{C}}_{1,2} & \bar{\mathbf{J}}_e^A(\mathbf{p}_2) + \sum_{j \in \mathcal{N}_a \setminus \{2\}} \bar{\mathbf{C}}_{2,j} & & -\bar{\mathbf{C}}_{2,N_a} \\ \vdots & & \ddots & \\ -\bar{\mathbf{C}}_{1,N_a} & -\bar{\mathbf{C}}_{2,N_a} & & \bar{\mathbf{J}}_e^A(\mathbf{p}_{N_a}) + \sum_{j \in \mathcal{N}_a \setminus \{N_a\}} \bar{\mathbf{C}}_{N_a,j} \end{bmatrix} + \Xi_{\mathbf{P}} \quad (17)$$

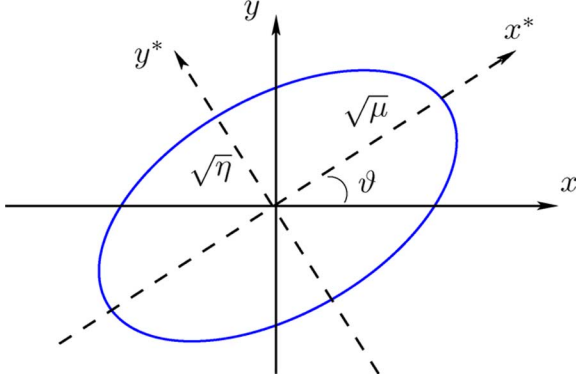


Fig. 2. Geometric interpretation of the EFIM as an information ellipse. In the rotated coordinate system (rotated over an angle ϑ), the major and minor axes of the ellipse are given by $\sqrt{\mu}$ and $\sqrt{\eta}$, respectively.

The first and second columns of \mathbf{U}_ϑ are the eigenvectors corresponding to eigenvalues μ and η , respectively. By the properties of eigenvalues, we have

$$\mu + \eta = \text{tr}\{\mathbf{J}_e(\mathbf{p})\} = \sum_{j \in \mathcal{N}_b} \lambda_j.$$

Note in (20) that $\mathbf{J}_e(\mathbf{p})$ depends only on μ , η , and ϑ , and we will denote $\mathbf{J}_e(\mathbf{p})$ by $\mathbf{F}(\mu, \eta, \vartheta)$ when needed.

Proposition 2: The SPEB is independent of the coordinate system.

Proof: See Appendix VI. \square

Remark 5: The proposition implies that if we rotate the original coordinate system by an angle ϑ prescribed by (20) and denote the agent's position in the new coordinate by \mathbf{p}^* , then the SPEB is

$$\mathcal{P}(\mathbf{p}) = \mathcal{P}(\mathbf{p}^*) = \text{tr} \left\{ \begin{bmatrix} \mu & 0 \\ 0 & \eta \end{bmatrix}^{-1} \right\} = \frac{1}{\mu} + \frac{1}{\eta}.$$

The EFIM in the new coordinate system is diagonal, and thus the localization information in these new axes is decoupled. Consequently, the SPEB is also decoupled in these two orthogonal directions.

Definition 5 (Information Ellipse): Let \mathbf{J} be a 2×2 positive-definite matrix. The information ellipse of \mathbf{J} is defined as the sets of points $\mathbf{x} \in \mathbb{R}^2$ such that

$$\mathbf{x}\mathbf{J}^{-1}\mathbf{x}^T = 1.$$

Geometrically, the EFIM in (20) corresponds to an information ellipse with major and minor axes equal to $\sqrt{\mu}$ and $\sqrt{\eta}$, respectively, and a rotation ϑ from the reference coordinate, as depicted in Fig. 2. Hence, the information ellipse is completely characterized by μ , η , and ϑ . Note that the RI is expressed as $\lambda \mathbf{J}_r(\phi) = \mathbf{F}(\lambda, 0, \phi)$, and it corresponds to a degenerate ellipse. In the following proposition, we will show how an anchor contributes to the information ellipse of an agent.

Proposition 3: Let $\mathbf{J}_e(\mathbf{p}) = \mathbf{F}(\mu, \eta, \vartheta)$ and $\mathcal{P}(\mathbf{p})$ denote the EFIM and the SPEB of an agent, respectively. When that agent

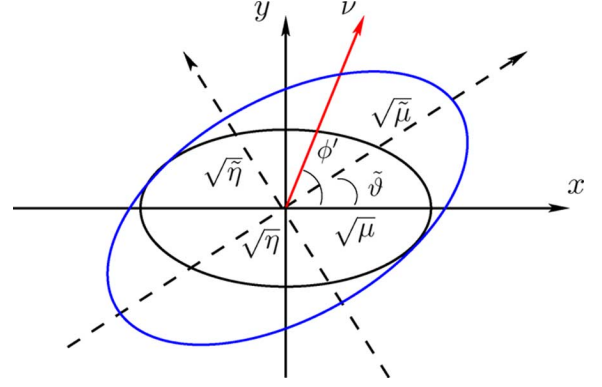


Fig. 3. Updating of the information ellipse for noncooperative localization. The original information ellipse of the agent is characterized by $\mathbf{F}(\mu, \eta, 0)$. The RI from an additional anchor is given by $\mathbf{F}(\nu, 0, \phi)$. The new information ellipse of the agent then grows along the direction ϕ' , but not along the orthogonal direction. The new information ellipse corresponds to $\mathbf{F}(\tilde{\mu}, \tilde{\eta}, \tilde{\vartheta})$.

obtains RI $\mathbf{F}(\nu, 0, \phi)$ from a new anchor, the new EFIM for the agent will be

$$\begin{aligned} \tilde{\mathbf{J}}_e(\mathbf{p}) &= \mathbf{F}(\tilde{\mu}, \tilde{\eta}, \tilde{\vartheta}) \\ &= \mathbf{F}(\mu, \eta, \vartheta) + \mathbf{F}(\nu, 0, \phi) \end{aligned}$$

where the parameters for the new information ellipse are

$$\begin{aligned} \tilde{\mu} &= \frac{\mu + \eta + \nu}{2} + \frac{1}{2} \sqrt{[\mu - \eta + \nu \cos 2\phi']^2 + \nu^2 \sin^2 2\phi'} \\ \tilde{\eta} &= \frac{\mu + \eta + \nu}{2} - \frac{1}{2} \sqrt{[\mu - \eta + \nu \cos 2\phi']^2 + \nu^2 \sin^2 2\phi'} \end{aligned}$$

and

$$\tilde{\vartheta} = \vartheta + \frac{1}{2} \arctan \frac{\nu \sin 2\phi'}{\mu - \eta + \nu \cos 2\phi'}$$

with $\phi' \triangleq \phi - \vartheta$. Correspondingly, the new SPEB becomes

$$\tilde{\mathcal{P}}(\mathbf{p}) = \frac{1}{\tilde{\mu}} + \frac{1}{\tilde{\eta}} = \frac{\mu + \eta + \nu}{\mu\eta + \nu[\eta + (\mu - \eta) \sin^2 \phi']}. \quad (21)$$

Remark 6: The geometric interpretation for the proposition is depicted in Fig. 3. For a fixed RII ν , we see from (21) that $\tilde{\mathcal{P}}(\mathbf{p})$ can be minimized through ϕ' (equivalently, through ϕ) in the denominator, leading to

$$\min_{\phi} \tilde{\mathcal{P}}(\mathbf{p}) = \frac{\mu + \eta + \nu}{\mu(\eta + \nu)}$$

and the minimum is achieved when $\phi = \vartheta \pm \pi/2$. In such a case, the anchor is along the direction of the eigenvector corresponding to the smallest eigenvalue η . Observe also that the denominator in (21) is equal to $\tilde{\mu} \cdot \tilde{\eta}$, which is proportional to the squared area of the new information ellipse corresponding to $\tilde{\mathbf{J}}_e(\mathbf{p})$. Hence, for a fixed ν , the minimum SPEB is achieved when the new anchor is along the minor axis of the information ellipse corresponding to $\mathbf{J}_e(\mathbf{p})$. Equivalently, this choice of anchor position maximizes the area of the new information ellipse.

On the other hand, the maximum SPEB occurs when the anchor is along the direction of the eigenvector corresponding to

the largest eigenvalue μ , i.e., the major axis of the information ellipse corresponding to $\mathbf{J}_e(\mathbf{p})$. Equivalently, this minimizes the area of the new information ellipse, and thus

$$\max_{\phi} \tilde{\mathcal{P}}(\mathbf{p}) = \frac{\mu + \eta + \nu}{\eta(\mu + \nu)}$$

and the maximum is achieved when $\phi = \vartheta \pm \pi$. Note also that

$$\frac{1}{\mu} < \tilde{\mathcal{P}}(\mathbf{p}) \leq \mathcal{P}(\mathbf{p})$$

where the left-hand side $1/\mu = \lim_{\nu \rightarrow \infty} \min_{\phi} \tilde{\mathcal{P}}(\mathbf{p})$, and the right-hand side $\mathcal{P}(\mathbf{p}) = \lim_{\nu \rightarrow 0} \tilde{\mathcal{P}}(\mathbf{p})$.

B. Interpretation for Cooperative Localization

The EFIM for all the agents in cooperative location-aware network is given, respectively, by (17) and (12) for the cases with and without *a priori* position knowledge. Further applying the notion of EFI, one can obtain the EFIM for individual agents. In general, the exact EFIM expression for the individual agents is complicated. However, we can find lower and upper bounds on the individual EFIM to gain some insights into the localization problem.

Proposition 4: Let $\mathbf{J}_e^A(\mathbf{p}_k) = \mathbf{F}(\mu_k, \eta_k, \vartheta_k)$ denote the EFIM for agent k that corresponds to the localization information from anchors, and let $\mathbf{C}_{kj} = \mathbf{F}(\nu_{kj}, 0, \phi_{kj})$ denote the RI for that agent obtained from cooperation with agent j . The EFIM $\mathbf{J}_e(\mathbf{p}_k)$ for agent k can be bounded as follows:

$$\mathbf{J}_e^L(\mathbf{p}_k) \preceq \mathbf{J}_e(\mathbf{p}_k) \preceq \mathbf{J}_e^U(\mathbf{p}_k)$$

where

$$\mathbf{J}_e^L(\mathbf{p}_k) = \mathbf{J}_e^A(\mathbf{p}_k) + \sum_{j \in \mathcal{N}_a \setminus \{k\}} \xi_{kj}^L \mathbf{C}_{kj} \quad (22)$$

$$\mathbf{J}_e^U(\mathbf{p}_k) = \mathbf{J}_e^A(\mathbf{p}_k) + \sum_{j \in \mathcal{N}_a \setminus \{k\}} \xi_{kj}^U \mathbf{C}_{kj} \quad (23)$$

with coefficients $0 \leq \xi_{kj}^L \leq \xi_{kj}^U \leq 1$ given by (44) and (46).

Proof: See Appendix VI. \square

Remark 7: The bounds for the EFIM can be written as weighted sums of RIs from the neighboring nodes, and such linear forms can facilitate analysis and design of location-aware networks. Moreover, it turns out that $\xi_{kj}^L = \xi_{kj}^U$ when there are only two agents in cooperation, leading to the following corollary.

Corollary 2: Let $\mathbf{J}_e^A(\mathbf{p}_1) = \mathbf{F}(\mu_1, \eta_1, \vartheta_1)$ and $\mathbf{J}_e^A(\mathbf{p}_2) = \mathbf{F}(\mu_2, \eta_2, \vartheta_2)$ denote the EFIMs for agents 1 and 2 from anchors, respectively, and let $\mathbf{C}_{1,2} = \mathbf{F}(\nu_{1,2}, 0, \phi_{1,2})$ denote the RI from their cooperation. The EFIMs for the two agents are given, respectively, by (see also Fig. 4)

$$\mathbf{J}_e(\mathbf{p}_1) = \mathbf{J}_e^A(\mathbf{p}_1) + \xi_{1,2} \nu_{1,2} \mathbf{J}_r(\phi_{1,2})$$

and

$$\mathbf{J}_e(\mathbf{p}_2) = \mathbf{J}_e^A(\mathbf{p}_2) + \xi_{2,1} \nu_{1,2} \mathbf{J}_r(\phi_{1,2})$$

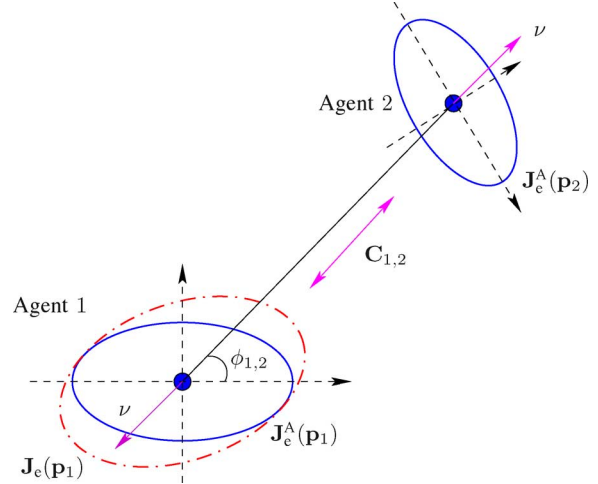


Fig. 4. Updating of the information ellipse for cooperative localization. Based on the anchors, the k th agent has information $\mathbf{J}_e^A(\mathbf{p}_k)$. The cooperative information between the two agents is given by $\mathbf{C}_{1,2} = \mathbf{F}(\nu, 0, \phi_{1,2})$. The total EFIM for agent 1 is then $\mathbf{J}_e(\mathbf{p}_1) = \mathbf{J}_e^A(\mathbf{p}_1) + \xi_{1,2} \mathbf{C}_{1,2}$. The new information ellipse grows along the line connecting the two agents.

where

$$\xi_{1,2} = \frac{1}{1 + \nu_{1,2} \Delta_2(\phi_{1,2})}$$

and

$$\xi_{2,1} = \frac{1}{1 + \nu_{1,2} \Delta_1(\phi_{1,2})}$$

with

$$\Delta_k(\phi_{1,2}) = \mathbf{q}_{12}^T [\mathbf{J}_e^A(\mathbf{p}_k)]^{-1} \mathbf{q}_{12}$$

for $k = 1, 2$.

Remark 8: The results follow directly from Proposition 4. We make the following remarks.

- Cooperation provides agent 1 with RI $\xi_{1,2} \nu_{1,2} \mathbf{J}_r(\phi_{1,2})$ with $0 \leq \xi_{1,2} \leq 1$. Hence, agent 1 obtains an RII $\xi_{1,2} \nu_{1,2}$ from cooperation instead of the full RII $\nu_{1,2}$. This degradation in RII is due to the inherent uncertainty of the second agent's position. We introduce the *effective* RII $\tilde{\nu}_{1,2} = \xi_{1,2} \nu_{1,2}$.
- The effective RII has the following geometric interpretation. The value $\Delta_2(\phi_{1,2})$ is the DPEB of agent 2 (based solely on the anchors) along the angle $\phi_{1,2}$ between the two agents. This implies that the larger the uncertainty of agent 2 along the angle $\phi_{1,2}$, the less effective cooperation is. For a given $\Delta_2(\phi_{1,2})$, the effective RII $\tilde{\nu}_{1,2}$ increases monotonically with $\nu_{1,2}$, and has the following asymptotic limits:

$$\lim_{\nu_{1,2} \rightarrow 0} \tilde{\nu}_{1,2} = 0$$

$$\lim_{\nu_{1,2} \rightarrow \infty} \tilde{\nu}_{1,2} = 1/\Delta_2(\phi_{1,2}).$$

Hence, the maximum effective RII that agent 2 can provide to agent 1 equals the inverse of the DPEB of agent 2 (based solely on the anchors) along the angle $\phi_{1,2}$ between the two agents.

- When i) the two agents happen to be oriented such that $\phi_{1,2} = \vartheta_2$, and ii) agent 2 is certain about its position along that angle ($\mu_2 = +\infty$), then $\Delta_2(\phi_{1,2}) = 0$ and $\mathbf{J}_e(\mathbf{p}_1) = \mathbf{J}_e^A(\mathbf{p}_1) + \mathbf{C}_{1,2}$, i.e., agent 2 can be thought of as an anchor from the standpoint of providing RI to agent 1. From this perspective, anchors and agents are equivalent for localization, where anchors are special agents with zero SPEB, or equivalently, infinite $\mathbf{J}_e^A(\mathbf{p}_k)$ in all directions.

C. Scaling Laws for Location-Aware Networks

In this section, we derive scaling laws of the SPEB for both noncooperative and cooperative location-aware networks. Scaling laws give us insight into the benefit of cooperation for localization in large networks. As we will see, agents and anchors contribute equally to the scaling laws for cooperative location-aware networks.

We focus on two types of random networks: *dense* networks and *extended* networks [47], [48]. In both types of networks, we consider the N_b anchors and N_a agents randomly located (uniformly distributed) in the plane. In dense networks, adding nodes increases the node density, while the area remains constant. In extended networks, the area increases proportional to the number of nodes, while both the anchor and the agent densities remain constant. Without loss of generality, we consider one round of transmission from each node to another. All transmission powers are the same, while large- and small-scale fading can be arbitrary. Medium access control is assumed so that these signals do not interfere with one another.

Definition 6 (Scaling of SPEB): Consider a network with n nodes randomly located in a given area. We say that the SPEB of individual agents scales as $\Theta(f(n))$ for some function $f(n)$, denoted by $\mathcal{P}(\mathbf{p}) \in \Theta(f(n))$, if there are deterministic constants $0 < c_1 < c_2 < +\infty$ such that

$$\mathbb{P}\{c_1 f(n) \leq \mathcal{P}(\mathbf{p}) \leq c_2 f(n)\} = 1 - \epsilon(n) \quad (24)$$

where $\lim_{n \rightarrow \infty} \epsilon(n) = 0$.

Theorem 5: In dense networks, the SPEB of each agent scales as $\Theta(1/N_b)$ for noncooperative localization, and as $\Theta(1/(N_b + N_a))$ for cooperative localization.

Proof: See Appendix VII. \square

Theorem 6: In extended networks with an amplitude loss exponent b ,¹⁷ the SPEB of each agent scales as

$$\mathcal{P}(\mathbf{p}) \in \begin{cases} \Theta(1/\log N_b), & b = 1 \\ \Theta(1), & b > 1 \\ \Theta(1/N_b^{b-1}), & 0 < b < 1 \end{cases}$$

¹⁷Note that the amplitude loss exponent is b , while the corresponding power loss exponent is $2b$. The amplitude loss exponent b is environment dependent and can range from approximately 0.8 (e.g., hallways inside buildings) to 4 (e.g., dense urban environments) [49].

for noncooperative localization, and

$$\mathcal{P}(\mathbf{p}) \in \begin{cases} \Theta(1/\log(N_b + N_a)), & b = 1 \\ \Theta(1), & b > 1 \\ \Theta(1/(N_b + N_a)^{b-1}), & 0 < b < 1 \end{cases}$$

for cooperative localization.

Proof: See Appendix VII. \square

Remark 9: We make the following remarks.

- In dense networks, the SPEB scales inversely proportional to the number of anchors for noncooperative localization, and inversely proportional to the number of nodes for cooperative localization. The gain from cooperation is given by $\Theta(1 + N_a/N_b)$, and hence the benefit is most pronounced when the number of anchors is limited. Moreover, it is proven in Appendix VII that $\epsilon(n)$ decreases exponentially with the number of nodes.
- In extended networks with an amplitude loss exponent equal to 1, the SPEB scales inversely proportional to the logarithm of the number of anchors for noncooperative localization, and inversely proportional to the logarithm of the number of nodes for cooperative localization. This implies that the SPEB in extended networks decreases much more slowly than that in dense networks, and the gain from cooperation is now reduced to $\Theta(\log(N_b + N_a)/\log N_b)$. Moreover, it is shown in Appendix VII that $\epsilon(n)$ decreases as $\exp(-(\log n)^2/8)/\log n$.
- In extended networks with an amplitude loss exponent greater than 1, the SPEB converges to a strict positive value as the network grows. This agrees with our intuition that as more nodes are added, the benefit of the additional nodes diminishes due to the rapidly decaying RII provided by those nodes. It can be shown that the SPEB converges to a smaller value in the cooperative case than that in the noncooperative case, i.e., a constant gain can be obtained by cooperation.

V. NUMERICAL RESULTS

In this section, we examine several numerical examples pertaining to cooperative localization and illustrate practical applications of our analytical results.

A. Effective RI

We first investigate the behavior of the effective RII $\tilde{\nu}_{1,2}$ from Corollary 2 when two agents cooperate. The effective RII $\tilde{\nu}_{1,2}$ is plotted in Fig. 5 as a function of the RII $\nu_{1,2}$ for $\mathbf{J}_e^A(\mathbf{p}_2) = \mathbf{F}(\mu_2 = 2, \eta_2 = 1, \vartheta_2 = 0)$ and various values of $\phi_{1,2}$. The corresponding asymptotic limits are also plotted for large values of $\nu_{1,2}$. We observe that effective RII increases from 0 to $1/\Delta_2(\phi_{1,2})$ as the RII $\nu_{1,2}$ increases. For a fixed RII, the second agent will provide the maximum effective RII at $\phi_{1,2} = \vartheta_2$, along which angle the second agent has the minimum DPEB (i.e., $1/\mu_2 = 0.5$). On the other hand, the second agent will provide the minimum effective RII at $\phi_{1,2} = \vartheta_2 \pm \pi/2$, along which angle the second agent has the maximum DPEB (i.e., $1/\eta_2 = 1$).

B. Benefit of Cooperation

We now consider the SPEB performance as a function of the number of agents for cooperative localization. The network

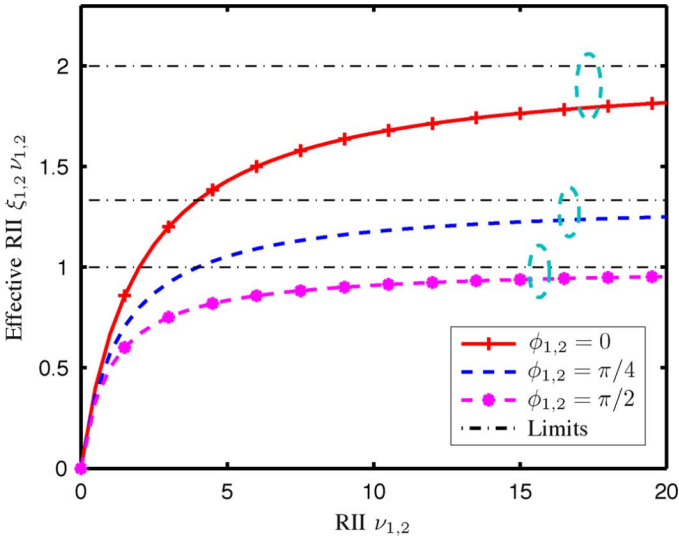


Fig. 5. Effective RII $\xi_{1,2} \nu_{1,2}$ as a function of the RII $\nu_{1,2}$, for $\mathbf{J}_{A,2} = \mathbf{F}(\mu_2 = 2, \eta_2 = 1, \vartheta_2 = 0)$, and different angle of arrival $\phi_{1,2}$.

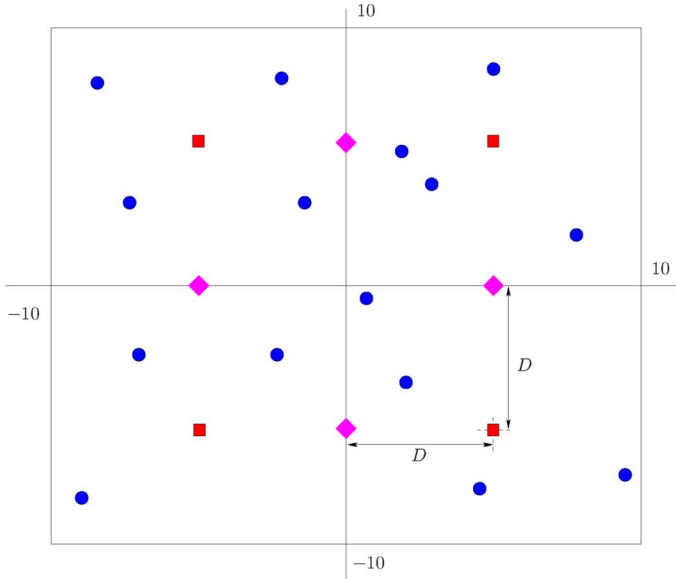


Fig. 6. Typical network deployment of two sets of anchors (set I: squares, set II: diamonds) and $N_a = 15$ agents. The agents are distributed uniformly over the $[-10, 10] \times [-10, 10]$ map, while the locations of the anchors are controlled by D .

configuration is shown in Fig. 6. The agents randomly (uniformly distributed) reside in a 20 m by 20 m area. There are two sets of anchors [shown as squares (set I) and diamonds (set II) in Fig. 6], with a configuration determined by the parameter D . Since fading does not affect the scaling behavior as shown Section IV-C, we consider a network with signals that obey the free-space path-loss model for simplicity, so that the RII $\lambda_{kj} \propto 1/d_{kj}^2$.

Fig. 7 shows the average SPEB over all the agents as a function of the number of agents, obtained by Monte Carlo simulation, for $D = 10$. We see that as the number of agents increases, the average SPEB decreases significantly, roughly proportional to the number of agents. Note that the anchor configuration set II yields a lower SPEB. Intuitively, this is due to the fact that

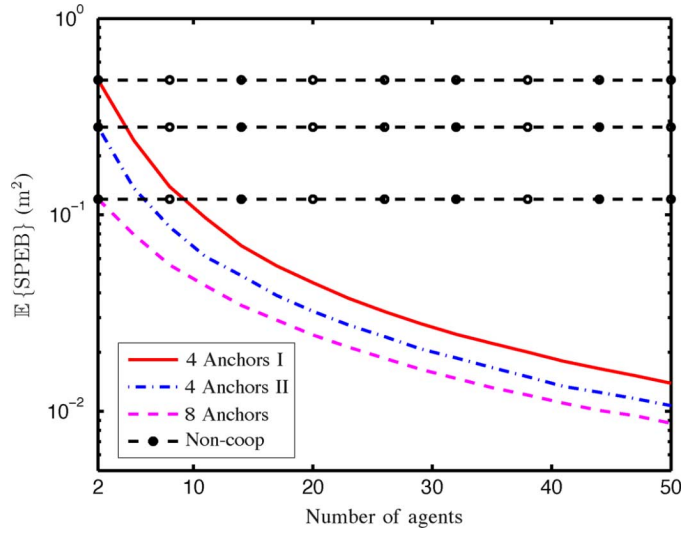


Fig. 7. The average SPEB as a function of the number of agents in the network for various anchor configurations ($D = 10$).

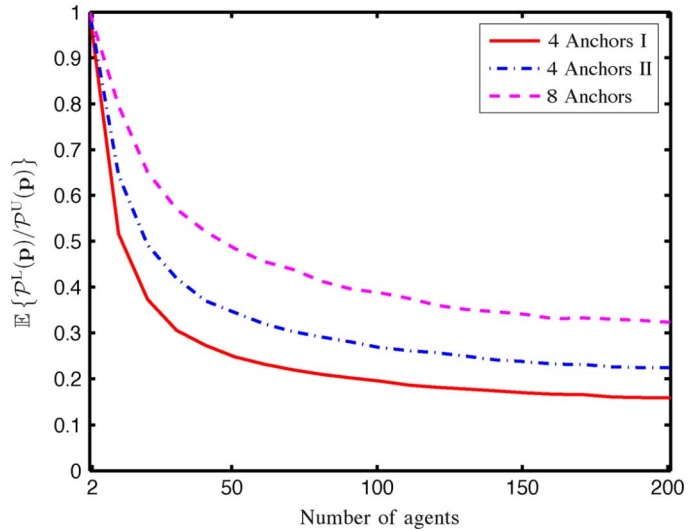


Fig. 8. Ratio of upper and lower approximations of the SPEB, $\mathcal{P}^L(\mathbf{p})$ and $\mathcal{P}^U(\mathbf{p})$, as a function of the number of agents for anchor set I, set II, and both.

the anchors in set II (distance D from the center) cover the area better than the anchors in set I (distance $\sqrt{2}D$ from the center).

Define the upper and lower approximations of agent k 's SPEB as

$$\mathcal{P}^U(\mathbf{p}_k) \triangleq \text{tr} \left\{ [\mathbf{J}_e^L(\mathbf{p}_k)]^{-1} \right\}$$

and

$$\mathcal{P}^L(\mathbf{p}_k) \triangleq \text{tr} \left\{ [\mathbf{J}_e^U(\mathbf{p}_k)]^{-1} \right\}$$

where $\mathbf{J}_e^L(\mathbf{p}_k)$ and $\mathbf{J}_e^U(\mathbf{p}_k)$ are given by (22) and (23), respectively, in Theorem 4. Fig. 8 shows the average ratio of the lower and upper approximations of the SPEB, obtained by Monte Carlo simulation, for anchor set I, set II, and both sets. When there are only two agents in cooperation, the bounds coincide, as we expect from Corollary 2. As the number of

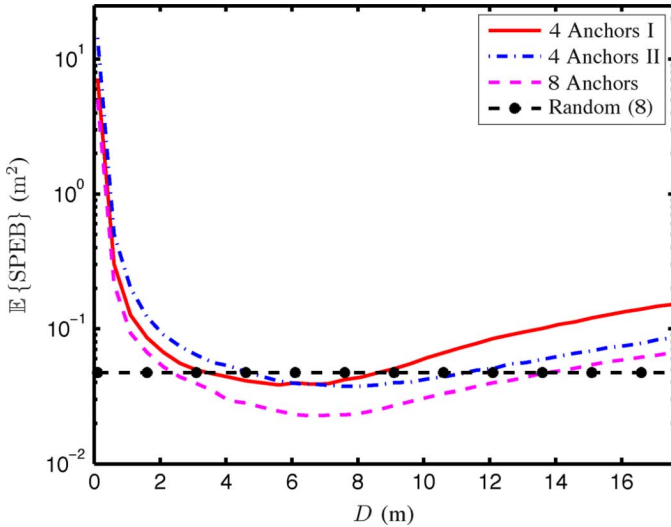


Fig. 9. The mean SPEB with respect to anchor deployment. There are $N_a = 15$ agents.

agents increases, the ratio deviates from 1, or equivalently, the approximations become looser, due to the fact that upper approximation ignores more cooperative information, and the lower approximation considers more agents to be equivalent to anchors. Nevertheless, the ratio converges to a positive constant, implying that the upper and lower approximations decrease at the same rate in an asymptotical regime, as shown in the proof of Theorem 5.

C. Anchor Deployment

Finally, we investigate the effect of anchor deployment in more detail. We consider a scenario with $N_a = 15$ agents. The anchor placement is controlled through D (see Fig. 6). Fig. 9 shows the average SPEB as a function of D for different anchor configurations (set I, set II, and both sets). We see that the SPEB first decreases, and then increases, as a function of D . When D is close to 0, all the anchors are located closely in the middle of the area, and hence the RIs from those anchors to a particular agent are nearly in the same direction. This will greatly increase the error of each agent's position since every $\mathbf{J}_e^A(\mathbf{p}_k)$ is close to singular, resulting in poor overall SPEB performance. As the anchors begin to move away from the center, they provide RIs along different directions to each agent, which lowers the average SPEB. Then, as the distances of the anchors to the center increase further, the anchors become far away from more and more agents. Hence, the RII decreases due to the path-loss phenomena, and this leads to the increase in the average SPEB. Observe also that anchor set I is better than anchor set II for $D < 7$ m. This is because, for a fixed $D < 7$ m, anchor set I can cover a larger area. For $D > 7$ m, anchor set I suffers more from path loss than anchor set II.

For the sake of comparison, we have also included the average SPEB when eight anchors are deployed 1) according to set I and II simultaneously, and 2) randomly in a $[-10 \text{ m}, 10 \text{ m}] \times [-10 \text{ m}, 10 \text{ m}]$ area. The figure shows that intelligent anchor deployment can be beneficial compared to random deployment, indicating the need for anchor deployment strategies.

VI. CONCLUSION

In this paper, we have investigated the fundamental limits on the localization accuracy for wideband cooperative location-aware networks. We have derived the SPEB by applying the notion of EFI to characterize the localization accuracy. Since our analysis exploits the received waveforms rather than specific signal metrics, the SPEB incorporates *all* the localization information inherent in the received waveforms. Our methodology unifies the localization information from anchors and that from cooperation among agents in a canonical form, viz. RI, and the total localization information is a sum of these individual RIs. We have put forth a geometrical interpretation of the EFIM based on eigendecomposition, and this interpretation has facilitated the theoretical analysis of the localization information for cooperative networks. We have also derived scaling laws for the SPEB in both dense and extended networks, showing the benefit of cooperation in an asymptotic regime. Our results provide fundamental new insights into the essence of the localization problem, and can be used as guidelines for localization system design as well as benchmarks for cooperative location-aware networks.

APPENDIX I

PROOF OF PROPOSITION 1

Proof: The right-hand side of (5) can be written as

$$\begin{aligned} & \mathcal{P}(\mathbf{p}_k; \mathbf{u}) + \mathcal{P}(\mathbf{p}_k; \mathbf{u}_\perp) \\ &= \text{tr} \left\{ \mathbf{u}^T [\mathbf{J}_\theta^{-1}]_{2 \times 2, k} \mathbf{u} \right\} + \text{tr} \left\{ \mathbf{u}_\perp^T [\mathbf{J}_\theta^{-1}]_{2 \times 2, k} \mathbf{u}_\perp \right\} \\ &= \text{tr} \left\{ [\mathbf{J}_\theta^{-1}]_{2 \times 2, k} \mathbf{u} \mathbf{u}^T \right\} + \text{tr} \left\{ [\mathbf{J}_\theta^{-1}]_{2 \times 2, k} \mathbf{u}_\perp \mathbf{u}_\perp^T \right\} \\ &= \text{tr} \left\{ [\mathbf{J}_\theta^{-1}]_{2 \times 2, k} \right\} = \mathcal{P}(\mathbf{p}_k) \end{aligned}$$

where we have used the fact $\mathbf{u} \mathbf{u}^T + \mathbf{u}_\perp \mathbf{u}_\perp^T = \mathbf{I}$. \square

APPENDIX II

PROOF OF THEOREM 1

We proceed in two steps: we first show that the EFIM is structured as in (12), and then derive the details of the RI.

A. Derivation of the EFIM Structure

When *a priori* knowledge of the agents' positions is unavailable, the log-likelihood function in (10) becomes

$$\begin{aligned} \ln f(\mathbf{r}, \boldsymbol{\kappa} | \mathbf{P}) &= \sum_{k \in \mathcal{N}_a} \sum_{j \in \mathcal{N}_b \cup \mathcal{N}_a \setminus \{k\}} \left[\ln f(\mathbf{r}_{kj} | \mathbf{p}_k, \mathbf{p}_j, \boldsymbol{\kappa}_{kj}) \right. \\ & \quad \left. + \ln f(\boldsymbol{\kappa}_{kj} | \mathbf{p}_k, \mathbf{p}_j) \right] \quad (25) \end{aligned}$$

where $\boldsymbol{\kappa}$ denotes the vector of the channel parameters containing all $\boldsymbol{\kappa}_{kj}$ with $k \in \mathcal{N}_a$ and $j \in \mathcal{N}_b \cup \mathcal{N}_a \setminus \{k\}$. For notational convenience, we now introduce

$$\Phi(\mathbf{x}, \mathbf{y}) \triangleq \mathbb{E}_{\mathbf{r}, \boldsymbol{\kappa}} \left\{ -\frac{\partial^2 \ln f(\mathbf{r}, \boldsymbol{\kappa} | \mathbf{P})}{\partial \mathbf{x} \partial \mathbf{y}^T} \right\} \quad (26)$$

$$\begin{aligned} \Phi_{kj}(\mathbf{x}, \mathbf{y}) &\triangleq \mathbb{E}_{\mathbf{r}, \boldsymbol{\kappa}} \left\{ -\frac{\partial^2}{\partial \mathbf{x} \partial \mathbf{y}^T} \left[\ln f(\mathbf{r}_{kj} | \mathbf{p}_k, \mathbf{p}_j, \boldsymbol{\kappa}_{kj}) \right. \right. \\ & \quad \left. \left. + \ln f(\boldsymbol{\kappa}_{kj} | \mathbf{p}_k, \mathbf{p}_j) \right] \right\} \quad (27) \end{aligned}$$

as well as

$$\begin{aligned}\Upsilon(\mathbf{x}, \mathbf{y}, \mathbf{z}) &\triangleq \Phi(\mathbf{x}, \mathbf{y}) [\Phi(\mathbf{y}, \mathbf{y})]^{-1} \Phi(\mathbf{y}, \mathbf{z}) \\ \Upsilon_{kj}(\mathbf{x}, \mathbf{y}, \mathbf{z}) &\triangleq \Phi_{kj}(\mathbf{x}, \mathbf{y}) [\Phi_{kj}(\mathbf{y}, \mathbf{y})]^{-1} \Phi_{kj}(\mathbf{y}, \mathbf{z}).\end{aligned}$$

Since $\Phi(\tilde{\boldsymbol{\theta}}_k, \tilde{\boldsymbol{\theta}}_j) = \mathbf{0}$ for $k \neq j$, the EFIM for \mathbf{P} can be derived as

$$\mathbf{J}_e(\mathbf{P}) = \Phi(\mathbf{P}, \mathbf{P}) - \sum_{k \in \mathcal{N}_a} \Upsilon(\mathbf{P}, \tilde{\boldsymbol{\theta}}_k, \mathbf{P}). \quad (28)$$

Structure of $\Phi(\mathbf{P}, \mathbf{P})$: Due to the structure in (25), we can express $\Phi(\mathbf{P}, \mathbf{P})$ as

$$\begin{aligned}\Phi(\mathbf{P}, \mathbf{P}) &= \sum_{k \in \mathcal{N}_a} \sum_{j \in \mathcal{N}_b} \Phi_{kj}(\mathbf{P}, \mathbf{P}) + \sum_{k \in \mathcal{N}_a} \sum_{j \in \mathcal{N}_a \setminus \{k\}} \Phi_{kj}(\mathbf{P}, \mathbf{P}) \\ &\triangleq \mathbf{K}_A + \mathbf{K}_C\end{aligned}$$

where $\mathbf{K}_A \in \mathbb{R}^{2N_a \times 2N_a}$ is a block-diagonal matrix, consisting of 2×2 block matrices, given by

$$[\mathbf{K}_A]_{2k-1:2k, 2m-1:2m} = \begin{cases} \sum_{j \in \mathcal{N}_b} \Phi_{kj}(\mathbf{p}_k, \mathbf{p}_k), & k = m \\ \mathbf{0}, & k \neq m. \end{cases}$$

On the other hand, $\mathbf{K}_C \in \mathbb{R}^{2N_a \times 2N_a}$ is also a block matrix, consisting of 2×2 block matrices, given by (29), shown at the bottom of the page.

Structure of $\Upsilon(\mathbf{P}, \tilde{\boldsymbol{\theta}}_k, \mathbf{P})$: Since $\Phi(\boldsymbol{\kappa}_{ki}, \boldsymbol{\kappa}_{kj}) = \mathbf{0}$ for $i \neq j$, we find that

$$\begin{aligned}\sum_{k \in \mathcal{N}_a} \Upsilon(\mathbf{P}, \tilde{\boldsymbol{\theta}}_k, \mathbf{P}) &= \sum_{k \in \mathcal{N}_a} \sum_{j \in \mathcal{N}_b} \Upsilon_{kj}(\mathbf{P}, \boldsymbol{\kappa}_{kj}, \mathbf{P}) \\ &\quad + \sum_{k \in \mathcal{N}_a} \sum_{j \in \mathcal{N}_a \setminus \{k\}} \Upsilon_{kj}(\mathbf{P}, \boldsymbol{\kappa}_{kj}, \mathbf{P}) \\ &\triangleq \mathbf{M}_A + \mathbf{M}_C\end{aligned}$$

where $\mathbf{M}_A \in \mathbb{R}^{2N_a \times 2N_a}$ is a block-diagonal matrix, consisting of 2×2 block matrices, given by

$$[\mathbf{M}_A]_{2k-1:2k, 2m-1:2m} = \begin{cases} \sum_{j \in \mathcal{N}_b} \Upsilon_{kj}(\mathbf{p}_k, \boldsymbol{\kappa}_{kj}, \mathbf{p}_k), & k = m \\ \mathbf{0}, & k \neq m. \end{cases}$$

On the other hand, $\mathbf{M}_C \in \mathbb{R}^{2N_a \times 2N_a}$ is also a block matrix, consisting of 2×2 block matrices, given by (30), shown at the bottom of the page.

Structure of $\mathbf{J}_e(\mathbf{P})$: Combining these results, we find that the EFIM in (28) can be written as

$$\mathbf{J}_e(\mathbf{P}) = \underbrace{\{\mathbf{K}_A - \mathbf{M}_A\}}_{\text{from anchors}} + \underbrace{\{\mathbf{K}_C - \mathbf{M}_C\}}_{\text{from cooperation}} \quad (31)$$

from which we obtain (12). In (12), $\mathbf{J}_e^A(\mathbf{p}_k) = \sum_{j \in \mathcal{N}_b} \mathbf{R}_k(\mathbf{r}_{kj})$ and $\mathbf{C}_{kj} = \mathbf{C}_{jk} = \mathbf{R}_k(\mathbf{r}_{kj}) + \mathbf{R}_k(\mathbf{r}_{jk})$ in which we have introduced the RI

$$\mathbf{R}_k(\mathbf{r}_{kj}) = \Phi_{kj}(\mathbf{p}_k, \mathbf{p}_k) - \Upsilon_{kj}(\mathbf{p}_k, \boldsymbol{\kappa}_{kj}, \mathbf{p}_k). \quad (32)$$

Note that in the derivation, we used

$$\Phi_{km}(\mathbf{p}_k, \mathbf{p}_m) = -\Phi_{km}(\mathbf{p}_k, \mathbf{p}_k)$$

and

$$\Upsilon_{km}(\mathbf{p}_k, \boldsymbol{\kappa}_{km}, \mathbf{p}_m) = -\Upsilon_{km}(\mathbf{p}_k, \boldsymbol{\kappa}_{km}, \mathbf{p}_k).$$

Since $\mathbf{J}_e(\mathbf{P})$ in (12) can be expressed in terms of the RIs $\mathbf{R}_k(\mathbf{r}_{kj})$, for $k \in \mathcal{N}_a$ and $j \in \mathcal{N}_b \cup \mathcal{N}_a \setminus \{k\}$, we will examine next the details of the RIs.

B. Details of the RI

We now consider the detailed expression of the RI $\mathbf{R}_k(\mathbf{r}_{kj})$ in (32). We first introduce

$$\Xi_{kj}(\mathbf{x}, \mathbf{y}) \triangleq \mathbb{E}_{\boldsymbol{\kappa}} \left\{ -\frac{\partial^2 \ln f(\boldsymbol{\kappa}_{kj} | \mathbf{p}_k, \mathbf{p}_j)}{\partial \mathbf{x} \partial \mathbf{y}^T} \right\}$$

and

$$\Psi_{kj} \triangleq \mathbb{E}_{\mathbf{r}, \boldsymbol{\kappa}} \left\{ -\frac{\partial^2 \ln f(\mathbf{r}_{kj} | \mathbf{p}_k, \mathbf{p}_j, \boldsymbol{\kappa}_{kj})}{\partial \tilde{\boldsymbol{\kappa}}_{kj} \partial \tilde{\boldsymbol{\kappa}}_{kj}^T} \right\} \quad (33)$$

where $\tilde{\boldsymbol{\kappa}}_{kj} = [\tau_{kj}^{(1)} \ \tilde{\alpha}_{kj}^{(1)} \ \tau_{kj}^{(2)} \ \tilde{\alpha}_{kj}^{(2)} \ \dots \ \tau_{kj}^{(L_{kj})} \ \tilde{\alpha}_{kj}^{(L_{kj})}]^T$ with $\tilde{\alpha}_{kj}^{(l)} \triangleq \alpha_{kj}^{(l)}/c$.

From (2) and (9), we note that $d_{kj} = \|\mathbf{p}_k - \mathbf{p}_j\|$ and that $f(\mathbf{r}_{kj} | \mathbf{p}_k, \mathbf{p}_j, \boldsymbol{\kappa}_{kj})$ and $f(\boldsymbol{\kappa}_{kj} | \mathbf{p}_k, \mathbf{p}_j)$ only depend on $\mathbf{p}_k, \mathbf{p}_j$ through d_{kj} . Using the chain rule, we have

$$\Phi_{kj}(\mathbf{p}_k, \mathbf{p}_k) = \frac{\partial d_{kj}}{\partial \mathbf{p}_k} \Phi_{kj}(d_{kj}, d_{kj}) \frac{\partial d_{kj}}{\partial \mathbf{p}_k^T}$$

and

$$\Upsilon_{kj}(\mathbf{p}_k, \boldsymbol{\kappa}_{kj}, \mathbf{p}_k) = \frac{\partial d_{kj}}{\partial \mathbf{p}_k} \Upsilon_{kj}(d_{kj}, \boldsymbol{\kappa}_{kj}, d_{kj}) \frac{\partial d_{kj}}{\partial \mathbf{p}_k^T}$$

and hence $\mathbf{R}_k(\mathbf{r}_{kj})$ can be expressed as

$$\begin{aligned}\mathbf{R}_k(\mathbf{r}_{kj}) &= \Phi_{kj}(d_{kj}, d_{kj}) \mathbf{q}_{kj} \mathbf{q}_{kj}^T \\ &\quad - \Upsilon_{kj}(d_{kj}, \boldsymbol{\kappa}_{kj}, d_{kj}) \mathbf{q}_{kj} \mathbf{q}_{kj}^T \\ &= \lambda_{kj} \mathbf{q}_{kj} \mathbf{q}_{kj}^T\end{aligned} \quad (34)$$

$$[\mathbf{K}_C]_{2k-1:2k, 2m-1:2m} = \begin{cases} \sum_{j \in \mathcal{N}_a \setminus \{k\}} [\Phi_{kj}(\mathbf{p}_k, \mathbf{p}_k) + \Phi_{jk}(\mathbf{p}_k, \mathbf{p}_k)], & k = m \\ \Phi_{km}(\mathbf{p}_k, \mathbf{p}_m) + \Phi_{mk}(\mathbf{p}_k, \mathbf{p}_m), & k \neq m. \end{cases} \quad (29)$$

$$[\mathbf{M}_C]_{2k-1:2k, 2m-1:2m} = \begin{cases} \sum_{j \in \mathcal{N}_a \setminus \{k\}} [\Upsilon_{kj}(\mathbf{p}_k, \boldsymbol{\kappa}_{kj}, \mathbf{p}_k) + \Upsilon_{jk}(\mathbf{p}_k, \boldsymbol{\kappa}_{jk}, \mathbf{p}_k)], & k = m \\ \Upsilon_{km}(\mathbf{p}_k, \boldsymbol{\kappa}_{km}, \mathbf{p}_m) + \Upsilon_{mk}(\mathbf{p}_k, \boldsymbol{\kappa}_{mk}, \mathbf{p}_m), & k \neq m. \end{cases} \quad (30)$$

where $\mathbf{q}_{kj} \triangleq \partial d_{kj} / \partial \mathbf{p}_k = -\partial d_{kj} / \partial \mathbf{p}_j = [\cos \phi_{kj} \quad \sin \phi_{kj}]^T$, and λ_{kj} is given by (35), shown at the bottom of the page, where $\mathbf{l}_{kj} \triangleq \underbrace{[1 \ 0 \ \cdots \ 1 \ 0]^T}_{2L_{kj}}$.

APPENDIX III

PROOF OF THEOREM 2

Proof: When *a priori* channel knowledge is unavailable, we have $\Xi_{kj}(d_{kj}, d_{kj}) = 0$, and $\Xi_{kj}(d_{kj}, \boldsymbol{\kappa}_{kj}) = \mathbf{0}$. For NLOS signals, the RII in (35) becomes $\lambda_{kj} = 0$ since $\Xi_{kj}(\boldsymbol{\kappa}_{kj}, \boldsymbol{\kappa}_{kj}) = \mathbf{0}$. For LOS signals, however, after some algebra, the RII becomes

$$\lambda_{kj} = \frac{1}{c^2} \mathbf{l}_{kj}^T \boldsymbol{\Psi}_{kj} (\boldsymbol{\Psi}_{kj} + \Xi_{kj}(\boldsymbol{\kappa}_{kj}, \boldsymbol{\kappa}_{kj}))^{-1} \Xi_{kj}(\boldsymbol{\kappa}_{kj}, \boldsymbol{\kappa}_{kj}) \mathbf{l}_{kj} \quad (36)$$

where $\Xi_{kj}(\boldsymbol{\kappa}_{kj}, \boldsymbol{\kappa}_{kj}) = \lim_{t^2 \rightarrow \infty} \text{diag}\{t^2, \mathbf{0}\}$ since the Fisher information for known $b_{kj}^{(1)} = 0$ is infinity. To simplify (36), we partition $\boldsymbol{\Psi}_{kj}$ as

$$\boldsymbol{\Psi}_{kj} = \begin{bmatrix} u_{kj}^2 & \mathbf{k}_{kj}^T \\ \mathbf{k}_{kj} & \check{\boldsymbol{\Psi}}_{kj} \end{bmatrix}$$

where $u_{kj}^2 = 8\pi^2 \beta^2 \text{SNR}_{kj}^{(1)}$ obtained from (33) through some algebra. As $t^2 \rightarrow \infty$ in (36), we have

$$\lambda_{kj} = \frac{8\pi^2 \beta^2}{c^2} (1 - \chi_{kj}) \text{SNR}_{kj}^{(1)}$$

where

$$\chi_{kj} \triangleq \frac{\mathbf{k}_{kj}^T \check{\boldsymbol{\Psi}}_{kj}^{-1} \mathbf{k}_{kj}}{8\pi^2 \beta^2 \text{SNR}_{kj}^{(1)}} \quad (37)$$

is called path-overlap coefficient [29].

We next show that only the first contiguous cluster contains information for localization. Let us focus on χ_{kj} . If the length of the first contiguous cluster in the received waveform is \tilde{L}_{kj} , where $1 \leq \tilde{L}_{kj} \leq L_{kj}$, we have [29]

$$\mathbf{k}_{kj} \triangleq \begin{bmatrix} \tilde{\mathbf{k}}_{kj}^T & \mathbf{0}^T \end{bmatrix}^T \quad \text{and} \quad \check{\boldsymbol{\Psi}}_{kj} \triangleq \begin{bmatrix} \check{\boldsymbol{\Psi}}_{kj} & \mathbf{0} \\ \mathbf{0} & \boxtimes \end{bmatrix}$$

where $\tilde{\mathbf{k}}_{kj} \in \mathbb{R}^{2\tilde{L}_{kj}-1}$, $\check{\boldsymbol{\Psi}}_{kj} \in \mathbb{R}^{(2\tilde{L}_{kj}-1) \times (2\tilde{L}_{kj}-1)}$, and \boxtimes is a block matrix that is irrelevant to the rest of the derivation. Hence, (37) becomes

$$\lambda_{kj} = \frac{\tilde{\mathbf{k}}_{kj}^T \check{\boldsymbol{\Psi}}_{kj}^{-1} \tilde{\mathbf{k}}_{kj}}{8\pi^2 \beta^2 \text{SNR}_{kj}^{(1)}}$$

which depends only on the first \tilde{L}_{kj} paths, implying that only the first contiguous cluster of LOS signals contains information for localization. \square

APPENDIX IV

PROOF OF THEOREM 3 AND COROLLARY 1

Proof: When the *a priori* knowledge of the agents' position is available, the derivation of EFIM (25) becomes

$$\ln f(\mathbf{r}, \boldsymbol{\theta}) = \sum_{k \in \mathcal{N}_a} \sum_{j \in \mathcal{N}_b \cup \mathcal{N}_a \setminus \{k\}} [\ln f(\mathbf{r}_{kj} | \mathbf{p}_k, \mathbf{p}_j, \boldsymbol{\kappa}_{kj}) + \ln f(\boldsymbol{\kappa}_{kj} | \mathbf{p}_k, \mathbf{p}_j)] + \ln f(\mathbf{P}).$$

Following the notations and derivations in Appendix II-A, we obtain the EFIM given by (14). This completes the proof of Theorem 3. Note that the structure of (14) is similar to that of (31) except the additional term $\Xi_{\mathbf{P}}$.

The EFIM in (14) is applicable to general case. Note that $\mathbf{R}_k(\mathbf{r}_{kj})$ in this case cannot be further simplified as that in (34) since we need to take expectation over the random parameter \mathbf{P} in (32). However, when condition (16) holds for functions $\Phi_{kj}(d_{kj}, d_{kj}) \mathbf{q}_{kj} \mathbf{q}_{kj}^T$, $\mathbf{q}_{kj} \Phi_{kj}(d_{kj}, \mathbf{p}_k)$, and $\Phi_{kj}(\boldsymbol{\kappa}_{kj}, \boldsymbol{\kappa}_{kj})$, the expectations of those functions with respect to \mathbf{P} can be replaced by the values of the functions at $\bar{\mathbf{P}}$. In such a case, the RI in (15) can be written as

$$\mathbf{R}_k(\mathbf{r}_{kj}) = \bar{\lambda}_{kj} \mathbf{J}_r(\bar{\phi}_{kj})$$

where $\bar{\lambda}_{kj}$ is the RII given in (35) evaluated at $\bar{\mathbf{P}}$, and $\bar{\phi}_{kj}$ is the angle from $\bar{\mathbf{p}}_k$ to $\bar{\mathbf{p}}_j$. \square

APPENDIX V

PROOF OF THEOREM 4

Proof: Consider a cooperative network with N_a agents, whose overall EFIM is given by (14). If agent N_a has infinite *a priori* position knowledge, i.e., $\Xi_{\mathbf{p}_{N_a}} = \lim_{t^2 \rightarrow \infty} \text{diag}\{t^2, t^2\}$, then we apply the notion of EFI to eliminate the parameter vector \mathbf{p}_{N_a} in (14) and have

$$\mathbf{J}_e(\mathbf{p}_1, \dots, \mathbf{p}_{N_a-1}) = [\mathbf{J}_e(\mathbf{P})]_{2(N_a-1) \times 2(N_a-1)} \quad (38)$$

where we have used

$$\lim_{t^2 \rightarrow \infty} \left(\sum_{j \in \mathcal{N}_b} \mathbf{R}_{N_a}(\mathbf{r}_{N_a,j}) + \sum_{j \in \mathcal{N}_a \setminus \{N_a\}} [\mathbf{R}_{N_a}(\mathbf{r}_{N_a,j}) + \mathbf{R}_{N_a}(\mathbf{r}_{j,N_a})] + \begin{bmatrix} t^2 & \\ & t^2 \end{bmatrix} \right)^{-1} = \mathbf{0}. \quad (39)$$

Note that if we let $\mathcal{N}'_b \triangleq \mathcal{N}_b \cup \{N_a\}$, $\mathcal{N}'_a \triangleq \mathcal{N}_a \setminus \{N_a\}$, and $\mathbf{R}'_k(\mathbf{r}_{k,N_a}) = \mathbf{R}_k(\mathbf{r}_{N_a,k}) + \mathbf{R}_k(\mathbf{r}_{k,N_a})$ for $k \in \mathcal{N}'_a$ in (38), the

$$\lambda_{kj} \triangleq \frac{1}{c^2} \left[\mathbf{l}_{kj}^T \boldsymbol{\Psi}_{kj} \mathbf{l}_{kj} + c^2 \Xi_{kj}(d_{kj}, d_{kj}) - (\mathbf{l}_{kj}^T \boldsymbol{\Psi}_{kj} + c^2 \Xi_{kj}(d_{kj}, \boldsymbol{\kappa}_{kj})) (\boldsymbol{\Psi}_{kj} + c^2 \Xi_{kj}(\boldsymbol{\kappa}_{kj}, \boldsymbol{\kappa}_{kj}))^{-1} (\mathbf{l}_{kj}^T \boldsymbol{\Psi}_{kj} + c^2 \Xi_{kj}(d_{kj}, \boldsymbol{\kappa}_{kj}))^T \right] \quad (35)$$

structure of (38) becomes the same as that of (14), with a dimension decrease by 2. Therefore, the new RI $\mathbf{R}'_k(\mathbf{r}_{k,N_a})$ is fully utilizable, i.e., agent N_a with infinite *a priori* position knowledge is effectively an anchor. \square

APPENDIX VI PROOFS FOR SECTION IV

A. Proof of Proposition 2

Proof: If the current coordinate system is rotated by angle ϕ and translated by $\mathbf{p}_0 = [x_0 \ y_0]^T$, then the position of the agent in the new coordinate system is $\tilde{\mathbf{p}} = \mathbf{U}_\phi \mathbf{p} + \mathbf{p}_0$. Consequently, the EFIM for $\tilde{\mathbf{p}}$ is

$$\begin{aligned} \mathbf{J}_e(\tilde{\mathbf{p}}) &= \left[\frac{\partial \mathbf{p}}{\partial \tilde{\mathbf{p}}} \right]^T \mathbf{J}_e(\mathbf{p}) \left[\frac{\partial \mathbf{p}}{\partial \tilde{\mathbf{p}}} \right] \\ &= \mathbf{U}_\phi^T \mathbf{J}_e(\mathbf{p}) \mathbf{U}_\phi. \end{aligned} \quad (40)$$

Due to the cyclic property of the trace operator [45], we immediately find that

$$\mathcal{P}(\tilde{\mathbf{p}}) = \text{tr}\{[\mathbf{J}_e(\tilde{\mathbf{p}})]^{-1}\} = \text{tr}\{[\mathbf{J}_e(\mathbf{p})]^{-1}\} = \mathcal{P}(\mathbf{p}). \quad (41)$$

\square

B. Proof of Proposition 4

Proof: Without loss of generality, we focus on the first agent.

Lower Bound: Consider the EFIM $\mathbf{J}_e^L(\mathbf{P})$ shown in (42), shown at the bottom of the page. It can be obtained from $\mathbf{J}_e(\mathbf{P})$ by setting all $\mathbf{C}_{kj} = \mathbf{0}$ for $1 < k, j \leq N_a$. This EFIM corresponds to the situation where cooperation among agents 2 to N_a is completely ignored. One can show using elementary algebra that $\mathbf{J}_e^L(\mathbf{P}) \preceq \mathbf{J}_e(\mathbf{P})$, which agrees with intuition since the cooperation information among agents 2 to N_a is not exploited. Applying the notion of EFI, we have the EFIM for the first agent as

$$\begin{aligned} \mathbf{J}_e^L(\mathbf{p}_1) &= \mathbf{J}_e^A(\mathbf{p}_1) \\ &+ \sum_{j \in \mathcal{N}_a \setminus \{1\}} \left[\mathbf{C}_{1,j} - \mathbf{C}_{1,j} (\mathbf{J}_e^A(\mathbf{p}_j) + \mathbf{C}_{1,j})^{-1} \mathbf{C}_{1,j} \right]. \end{aligned}$$

Since $\mathbf{C}_{1,j} = \nu_{1,j} \mathbf{q}_{\phi_{1,j}} \mathbf{q}_{\phi_{1,j}}^T$ where $\mathbf{q}_{\phi_{1,j}} \triangleq [\cos \phi_{1,j} \ \sin \phi_{1,j}]^T$, we can express $\mathbf{J}_e^L(\mathbf{p}_1)$ as

$$\mathbf{J}_e^L(\mathbf{p}_1) = \mathbf{J}_e^A(\mathbf{p}_1) + \sum_{j \in \mathcal{N}_a \setminus \{1\}} \xi_{1,j}^L \mathbf{C}_{1,j} \quad (43)$$

where $\xi_{1,j}^L \triangleq 1 - \nu_{1,j} \mathbf{q}_{\phi_{1,j}}^T (\mathbf{J}_e^A(\mathbf{p}_j) + \mathbf{C}_{1,j})^{-1} \mathbf{q}_{\phi_{1,j}}$. The coefficient $\xi_{1,j}^L$ can be simplified as

$$\begin{aligned} \xi_{1,j}^L &= 1 - \nu_{1,j} \mathbf{q}_{\vartheta_j - \phi_{1,j}}^T \\ &\cdot \left(\begin{bmatrix} \mu_j & \\ & \eta_j \end{bmatrix} + \nu_{1,j} \mathbf{q}_{\vartheta_j - \phi_{1,j}} \mathbf{q}_{\vartheta_j - \phi_{1,j}}^T \right)^{-1} \mathbf{q}_{\vartheta_j - \phi_{1,j}} \\ &= \frac{1}{1 + \nu_{1,j} \Delta_j(\phi_{1,j})} \end{aligned} \quad (44)$$

where

$$\Delta_j(\phi_{1,j}) = \frac{1}{\mu_j} \cos^2(\vartheta_j - \phi_{1,j}) + \frac{1}{\eta_j} \sin^2(\vartheta_j - \phi_{1,j}).$$

Upper Bound: Consider the EFIM $\mathbf{J}_e^U(\mathbf{P})$ shown in (45), at the bottom of the page. It can be obtained from $\mathbf{J}_e(\mathbf{P})$ by doubling the diagonal elements \mathbf{C}_{kj} and setting the off-diagonal elements $-\mathbf{C}_{kj} = \mathbf{0}$ for $1 < k, j \leq N_a$. One can show using elementary algebra that $\mathbf{J}_e^U(\mathbf{P}) \succeq \mathbf{J}_e(\mathbf{P})$, which agrees with intuition since more cooperation information among agents 2 to N_a is assumed in (45). Applying the notion of EFI and following the similar analysis leading to (43) and (44), we obtain the EFIM for agent 1 as

$$\mathbf{J}_e^U(\mathbf{p}_1) = \mathbf{J}_e^A(\mathbf{p}_1) + \sum_{j \in \mathcal{N}_a \setminus \{1\}} \xi_{1,j}^U \mathbf{C}_{1,j}$$

where

$$\xi_{1,j}^U = \frac{1}{1 + \nu_{1,j} \tilde{\Delta}_j(\phi_{1,j})} \quad (46)$$

in which

$$\tilde{\Delta}_j(\phi_{1,j}) = \frac{1}{\tilde{\mu}_j} \cos^2(\tilde{\vartheta}_j - \phi_{1,j}) + \frac{1}{\tilde{\eta}_j} \sin^2(\tilde{\vartheta}_j - \phi_{1,j})$$

with $\tilde{\mu}_j$, $\tilde{\eta}_j$, and $\tilde{\vartheta}_j$ satisfying

$$\mathbf{F}(\tilde{\mu}_j, \tilde{\eta}_j, \tilde{\vartheta}_j) = \mathbf{J}_e^A(\mathbf{p}_j) + \sum_{k \in \mathcal{N}_a \setminus \{1,j\}} 2\mathbf{C}_{jk}. \quad \square$$

$$\mathbf{J}_e^L(\mathbf{P}) = \begin{bmatrix} \mathbf{J}_e^A(\mathbf{p}_1) + \sum_{j \in \mathcal{N}_a \setminus \{1\}} \mathbf{C}_{1,j} & -\mathbf{C}_{1,2} & \cdots & -\mathbf{C}_{1,N_a} \\ -\mathbf{C}_{1,2} & \mathbf{J}_e^A(\mathbf{p}_2) + \mathbf{C}_{1,2} & & 0 \\ \vdots & & \ddots & \\ -\mathbf{C}_{1,N_a} & 0 & & \mathbf{J}_e^A(\mathbf{p}_{N_a}) + \mathbf{C}_{1,N_a} \end{bmatrix}. \quad (42)$$

$$\begin{aligned} &\mathbf{J}_e^U(\mathbf{P}) \\ &= \begin{bmatrix} \mathbf{J}_e^A(\mathbf{p}_1) + \sum_{j \in \mathcal{N}_a \setminus \{1\}} \mathbf{C}_{1,j} & -\mathbf{C}_{1,2} & \cdots & -\mathbf{C}_{1,N_a} \\ -\mathbf{C}_{1,2} & \mathbf{J}_e^A(\mathbf{p}_2) + \mathbf{C}_{1,2} + \sum_{j \in \mathcal{N}_a \setminus \{1,2\}} 2\mathbf{C}_{2,j} & & 0 \\ \vdots & & \ddots & \\ -\mathbf{C}_{1,N_a} & 0 & & \mathbf{J}_e^A(\mathbf{p}_{N_a}) + \mathbf{C}_{1,N_a} + \sum_{j \in \mathcal{N}_a \setminus \{1,N_a\}} 2\mathbf{C}_{N_a,j} \end{bmatrix}. \end{aligned} \quad (45)$$

APPENDIX VII
PROOF OF THE SCALING LAWS

Lemma 1: Let ϕ_i 's be N independent identically distributed (i.i.d.) random variables with uniform distribution over $[0, 2\pi)$. Then, for any $0 < \epsilon \leq 1$, there exist an $N_0 \in \mathbb{N}$, such that $\forall N > N_0$

$$\mathbb{P} \left\{ \sum_{k=1}^N \sum_{j=1}^N \sin^2(\phi_k - \phi_j) < \frac{N^2}{32} \right\} < \epsilon. \quad (47)$$

Proof: First, we note that replacing ϕ_i with $\phi_i \bmod \pi$ preserves the value of $\sin^2(\phi_k - \phi_j)$. Hence, we can consider ϕ_i 's to be i.i.d. and uniformly distributed in $[0, \pi)$.

We order the N ϕ_i 's, such that $0 \leq \phi_{(1)} \leq \phi_{(2)} \leq \dots \leq \phi_{(N)} < \pi$. Using order statistics [50], we find that the joint pdf of the $\phi_{(i)}$'s is

$$f(\phi_{(1)}, \phi_{(2)}, \dots, \phi_{(N)}) = \frac{N!}{\pi^N} \mathbf{1}_{\{0 \leq \phi_{(1)} \leq \phi_{(2)} \leq \dots \leq \phi_{(N)} < \pi\}} \quad (48)$$

where $\mathbf{1}$ is the indicator function. From (48), the marginal pdf of $\phi_{(k)}$ can be derived as [50]

$$f_{\phi_{(k)}}(x) = \frac{1}{\pi^N} \frac{N!}{(k-1)!(N-k)!} x^{k-1} (\pi-x)^{N-k} \mathbf{1}_{\{0 \leq x < \pi\}}.$$

Now consider a large $N = 8K$ for some integer K , and let $\delta \triangleq \pi/6$. The function $f_{\phi_{(K)}}(x)$ has a maximum at $x = \pi/8$, and is monotonically decreasing in $[\pi/8, \pi) \supset [\delta, \pi)$. Therefore, we have

$$\mathbb{P}\{\phi_{(K)} > \delta\} \leq (\pi - \delta) f_{\phi_{(K)}}(\delta). \quad (49)$$

Since $\lim_{K \rightarrow \infty} f_{\phi_{(K)}}(\delta) = 0$, there exists $K_1 \in \mathbb{N}$ such that $\mathbb{P}\{\phi_{(K)} > \delta\} < \epsilon/4, \forall K > K_1$. Note also that

$$\mathbb{P}\{\phi_{(7K+1)} < \pi - \delta\} \leq (\pi - \delta) f_{\phi_{(7K+1)}}(\pi - \delta)$$

and hence, for the same K_1 , $\mathbb{P}\{\phi_{(7K+1)} < \pi - \delta\} < \epsilon/4, \forall K > K_1$. Similar arguments show that there exists $K_2 \in \mathbb{N}$ such that $\mathbb{P}\{\phi_{(3K+1)} < \pi/2 - \delta\} < \epsilon/4$ and $\mathbb{P}\{\phi_{(5K)} > \pi/2 + \delta\} < \epsilon/4, \forall K > K_2$.

Combining the above results, we have with a probability $1 - \epsilon$

$$\phi_{(j)} \in \begin{cases} [0, \delta], & j = 1, \dots, K \\ [\pi/2 - \delta, \pi/2 + \delta], & j = 3K + 1, \dots, 5K \\ [\pi - \delta, \pi), & j = 7K + 1, \dots, N \end{cases}$$

when $K > \max\{K_1, K_2\}$. Therefore

$$\begin{aligned} & \sum_{k=1}^N \sum_{j=k+1}^N \sin^2(\phi_{(k)} - \phi_{(j)}) \\ & \geq \sum_{k=1}^K \sum_{j=3K+1}^{5K} \sin^2(\phi_{(k)} - \phi_{(j)}) \\ & \quad + \sum_{k=3K+1}^{5K} \sum_{j=7K+1}^{8K} \sin^2(\phi_{(k)} - \phi_{(j)}) \\ & \stackrel{p}{\geq} \left(\sum_{k=1}^K \sum_{j=3K+1}^{5K} 1 + \sum_{k=3K+1}^{5K} \sum_{j=7K+1}^{8K} 1 \right) \sin^2\left(\frac{\pi}{2} - 2\delta\right) \\ & = K^2 \end{aligned} \quad (50)$$

where $\stackrel{p}{\geq}$ denotes an inequality with probability approaching one as $K \rightarrow \infty$. Substituting $N = 8K$, and noting that the summation in (50) considers only half the terms (with $j > k$), we arrive at (47).

Moreover, the probability in (49) decreases exponentially with K , because if letting $a_K \triangleq f_{\phi_{(K)}}(\delta)$

$$\begin{aligned} & \lim_{K \rightarrow \infty} \frac{a_{K+1}}{a_K} \\ & = \frac{(8K+8)(8K+7) \cdots (8K+1)}{(7K+7)(7K+6) \cdots (7K+1)K} \frac{1}{6} \left(\frac{5}{6}\right)^7 \\ & < 1 \end{aligned} \quad (51)$$

and hence one can see that ϵ in (47) decreases exponentially with N . \square

Lemma 2: Let λ_i 's be N i.i.d. random variables with arbitrary distribution on the support $[0, \lambda_{\max}]$. If $\mathbb{P}\{\lambda_i \leq \lambda_0\} \leq \epsilon < 1/2$ for some $\lambda_0 \in [0, \lambda_{\max}]$, then

$$\mathbb{P}\{\lambda_{(N/2+1)} \leq \lambda_0\} < \tilde{\epsilon}^N \quad (52)$$

where $\lambda_{(i)}$ is the order statistics of λ_i such that $0 \leq \lambda_{(1)} \leq \lambda_{(2)} \leq \dots \leq \lambda_{(N)}$, and $\tilde{\epsilon} = \sqrt{4\epsilon(1-\epsilon)}$.

Proof: Denote the probability density and distribution of λ_i by f_λ and F_λ , respectively. Consider $N = 2K$ for some integer K and $x \in [0, \lambda_{\max}]$ such that $F_\lambda(x) < 1/2$. Using the order statistics, we have

$$\begin{aligned} F_{\lambda_{(K+1)}}(x) &= \sum_{j=K+1}^N \binom{N}{j} F_\lambda(x)^j (1 - F_\lambda(x))^{N-j} \\ &\leq \sum_{j=K+1}^N 2^N F_\lambda(x)^j (1 - F_\lambda(x))^{N-j} \\ &< 2^N (1 - F_\lambda(x))^N \sum_{j=K+1}^{\infty} \left(\frac{F_\lambda(x)}{1 - F_\lambda(x)} \right)^j \\ &= \frac{F_\lambda(x)}{1 - F_\lambda(x)} [4F_\lambda(x)(1 - F_\lambda(x))]^K \\ &< (\sqrt{4F_\lambda(x)(1 - F_\lambda(x))})^N \end{aligned}$$

where the first inequality follows from $\binom{N}{j} \leq 2^N$, the second inequality is due to the extension of finite summation, and the last inequality follows from $F_\lambda(x) < 1/2$. Replacing x with λ_0 gives (52). \square

A. Proof of Theorem 5

Proof: We consider first the noncooperative case, followed by the cooperative case. In either case, without loss of generality, we focus on the first agent at position \mathbf{p}_1 .

Noncooperative Case: We will show that $\mathcal{P}(\mathbf{p}_1) \in \Omega(1/N_b)$ and $\mathcal{P}(\mathbf{p}_1) \in O(1/N_b)$,¹⁸ which implies that $\mathcal{P}(\mathbf{p}_1) \in \Theta(1/N_b)$.

¹⁸Similar to the definition of notation $\Theta(f(n))$, the notation $g(n) \in \Omega(f(n))$ and $g(n) \in O(f(n))$ denote, respectively, that $g(n)$ is bounded below by $c_1 f(n)$ and above by $c_2 f(n)$ with probability approaching one as $n \rightarrow \infty$, for some constant c_1 and c_2 .

For an amplitude loss exponent b , signal powers decay with the distance following $\text{SNR}(r) \propto 1/r^{2b}$. We can express the RII from a node at distance r as

$$\lambda(r) = \frac{Z}{r^{2b}} \mathbb{1}_{\{r_0 \leq r \leq r_{\max}\}}$$

where r_0 is the minimum distance between nodes determined by the node's physical size, r_{\max} is the maximum distance between nodes determined by the fixed area associated with dense network setting, and random variable Z accounts for the large- and small-scale fading. Since $0 \leq Z \leq z_1$ for some $z_1 \in \mathbb{R}^+$, there exists $z_0 \in (0, z_1)$ such that $\mathbb{P}\{Z \leq z_0\} \leq \epsilon_z$ for a given $\epsilon_z \in (0, 1)$. Thus, the RII from the j th anchor is bounded as $0 < \lambda_{\min} \leq \lambda_{1,j} \leq \lambda_{\max}$ with probability

$$\mathbb{P}\{\lambda_{\min} \leq \lambda_{1,j} \leq \lambda_{\max}\} \leq 1 - \epsilon_z$$

where $\lambda_{\min} = z_0/r_{\max}^{2b}$ and $\lambda_{\max} = z_1/r_0^{2b}$.

On the one hand, we have

$$\mathbf{J}_e(\mathbf{p}_1) \preceq \lambda_{\max} \sum_{j \in \mathcal{N}_b} \mathbf{J}_r(\phi_{1,j}). \quad (53)$$

By the Cauchy–Schwarz inequality, we have

$$\text{tr}\{[\mathbf{J}_e(\mathbf{p}_1)]^{-1}\} \cdot \text{tr}\{\mathbf{J}_e(\mathbf{p}_1)\} \geq 4.$$

Since the inequality (53) together with the fact that $\text{tr}\{\mathbf{J}_r(\phi_{1,j})\} = 1$ imply that $\text{tr}\{\mathbf{J}_e(\mathbf{p}_1)\} \leq \lambda_{\max} N_b$, we have that

$$\mathcal{P}(\mathbf{p}_1) = \text{tr}\{[\mathbf{J}_e(\mathbf{p}_1)]\}^{-1} \geq 4/(\lambda_{\max} N_b).$$

Therefore, $\mathcal{P}(\mathbf{p}_1) \in \Omega(1/N_b)$.

On the other hand, for the lower bound, we first order the N_b RII $\lambda_{1,j}$'s, and then the probability of $\lambda_{(N_b/2+1)} \leq \lambda_{\min}$ is exponentially small by Lemma 2, i.e.,

$$\mathbb{P}\{\lambda_{(N_b/2+1)} \leq \lambda_{\min}\} \leq \tilde{\epsilon}^{N_b} \quad (54)$$

for some constant $\tilde{\epsilon} \in (0, 1)$. Let \mathcal{N}'_b denote the set of anchors with RII $\lambda_{(j)}$ such that $j \geq N_b/2 + 1$, and we have that

$$\mathbb{P}\left\{\lambda_{\min} \sum_{j \in \mathcal{N}'_b} \mathbf{J}_r(\phi_{1,j}) \preceq \mathbf{J}_e(\mathbf{p}_1)\right\} \geq 1 - \epsilon_1 \quad (55)$$

where the outage probability ϵ_1 decreases exponentially with N_b . Moreover, since

$$\text{tr}\left\{\left[\sum_{j \in \mathcal{N}'_b} \mathbf{J}_r(\phi_{1,j})\right]^{-1}\right\} = \frac{2N_b/2}{\sum_{k \in \mathcal{N}'_b} \sum_{j \in \mathcal{N}'_b} \sin^2(\phi_{1,k} - \phi_{1,j})} \quad (56)$$

applying Lemma 1 gives

$$\mathbb{P}\left(\frac{1}{\lambda_{\min}} \text{tr}\left\{\left[\sum_{j \in \mathcal{N}'_b} \mathbf{J}_r(\phi_{1,j})\right]^{-1}\right\} \leq \frac{128}{\lambda_{\min} N_b}\right) \geq 1 - \epsilon_2 \quad (57)$$

for sufficiently large N_b . The inequality in (55) implies that

$$\mathcal{P}(\mathbf{p}_1) \leq \frac{1}{\lambda_{\min}} \text{tr}\left\{\left[\sum_{j \in \mathcal{N}'_b} \mathbf{J}_r(\phi_{1,j})\right]^{-1}\right\}$$

and hence $\mathcal{P}(\mathbf{p}_1) \leq 128/(\lambda_{\min} N_b)$ with probability approaching one as $N_b \rightarrow \infty$. Therefore, $\mathcal{P}(\mathbf{p}_1) \in O(1/N_b)$ with probability 1.

Note that since both the outage probability ϵ_1 in (55) and ϵ_2 in (57) decrease exponentially with N_b , the outage probability $\epsilon(N_b)$ of the scaling law in (24) decreases exponentially with N_b .

Cooperative Case: For the cooperative case, we will use the lower and upper approximations of the EFIM from (22) and (23). The upper approximation gives

$$\begin{aligned} \mathbf{J}_e^U(\mathbf{p}_1) &= \mathbf{J}_e^A(\mathbf{p}_1) + \sum_{j \in \mathcal{N}_a \setminus \{1\}} \xi_{1,j}^U \mathbf{C}_{1,j} \\ &\leq \sum_{j \in \mathcal{N}_b \cup \mathcal{N}_a \setminus \{1\}} \lambda_{1,j} \mathbf{J}_r(\phi_{1,j}) \end{aligned}$$

where the inequality is obtained by treating all other agents to be anchors, i.e., $\xi_{1,j}^U = 1 (j \in \mathcal{N}_a)$. In this case, there are equivalently $N_b + N_a - 1$ anchors, and similar analysis as in the noncooperative case shows that $\mathcal{P}(\mathbf{p}_1) \in \Omega(1/(N_b + N_a))$.

On the other hand, from the lower approximation, we have, with probability approaching one, that

$$\begin{aligned} \mathbf{J}_e^L(\mathbf{p}_1) &= \mathbf{J}_e^A(\mathbf{p}_1) + \sum_{j \in \mathcal{N}_a \setminus \{1\}} \xi_{1,j}^L \mathbf{C}_{1,j} \\ &\succeq \tilde{\nu} \sum_{j \in \mathcal{N}_b \cup \mathcal{N}_a \setminus \{1\}} \mathbf{J}_r(\phi_{1,j}) \end{aligned} \quad (58)$$

where $\tilde{\nu} > 0$ is a given lower bound on both the RII $\lambda_{1,j} (j \in \mathcal{N}_b)$ and the effective RII $\xi_{1,j}^L \nu_{1,j} (j \in \mathcal{N}_a)$. From Lemma 2, we can find such $\tilde{\nu}$ for the dense network setting, because there exist constants $0 < c_1, c_2 < +\infty$ such that $\lambda_{1,j} > c_1, \nu_{1,j} > c_1$, and $\Delta_j(\phi_{1,j}) < c_2$ with probability approaching one; defining $\tilde{\nu} \triangleq c_1/(1 + c_1 \cdot c_2)$ implies $\lambda_{1,j} \geq \tilde{\nu}$ and $\xi_{1,j}^L \nu_{1,j} \geq \tilde{\nu}$ since $\xi_{1,j}^L = [1 + \Delta_j(\phi_{1,j}) \nu_{1,j}]^{-1}$. Applying Lemmas 1 and 2, and following a similar line of reasoning as in the noncooperative case, we find $\mathcal{P}(\mathbf{p}_1) \in O(1/(N_b + N_a))$ with probability approaching one as $N_b, N_a \rightarrow +\infty$. Thus, we conclude that the SPEB in cooperative networks scales as $\Theta(1/(N_b + N_a))$. \square

B. Proof of Theorem 6

Proof: Let ρ_b denote the density of anchor nodes uniformly distributed in an extended network. Consider an area within distance R to agent 1, then the expected number of anchors within that area is $N_b = \rho_b \pi R^2$. Following a similar analysis leading to (54), we can show that the effect of large- and small-scale fading together with path loss on the RII can be bounded as $c_1/r^{2b} \leq \lambda(r) \leq c_2/r^{2b}$ for some constants $0 < c_1 < c_2 < +\infty$, with an outage probability exponentially decreasing with N_b and N_a . This implies that, with probability approaching one,

the large- and small-scale fading will not affect the scaling law,¹⁹ and hence we can consider the RII from a node at distance r as

$$\lambda(r) = \frac{1}{r^{2b}} \mathbf{1}_{\{r \geq r_0\}}$$

for the analysis of the scaling laws. Since each anchor is uniformly distributed in the given area, the pdf of the RII can be written as

$$f(\lambda) = \frac{1}{b(R^2 - r_0^2)} \lambda^{-\frac{b+1}{b}} \mathbf{1}_{\{1/R^{2b} \leq \lambda \leq 1/r_0^{2b}\}}$$

with mean

$$\mathbb{E}\{\lambda\} = \begin{cases} \frac{1}{b-1} \frac{r_0^{2-2b} - R^{2-2b}}{R^2 - r_0^2}, & b > 1 \\ \frac{\ln R^2 - \ln r_0^2}{R^2 - r_0^2}, & b = 1 \\ \frac{1}{1-b} \frac{R^{2-2b} - r_0^{2-2b}}{R^2 - r_0^2}, & 0 < b < 1 \end{cases} \quad (59)$$

and second moment

$$\mathbb{E}\{\lambda^2\} = \begin{cases} \frac{1}{2b-1} \frac{r_0^{2-4b} - R^{2-4b}}{R^2 - r_0^2}, & b > 1 \\ \frac{1}{r_0^2 R^2}, & b = 1 \\ \frac{1}{2b-1} \frac{r_0^{2-4b} - R^{2-4b}}{R^2 - r_0^2}, & 0 < b < 1. \end{cases} \quad (60)$$

Note that $N_b \propto R^2$, we can show that the mean scales as

$$\mathbb{E}\{\lambda\} \in \begin{cases} \Theta(1/N_b), & b > 1 \\ \Theta(\log N_b/N_b), & b = 1 \\ \Theta(1/N_b^b), & 0 < b < 1 \end{cases} \quad (61)$$

and the variance always scales as

$$\text{Var}\{\lambda\} \in \Theta(1/N_b). \quad (62)$$

When $b > 1$, it follows that, for fixed densities of anchors and agents, $\text{tr}\{\mathbf{J}_e(\mathbf{p}_1)\} \in \Theta(1)$ with probability approaching one as $N_b \rightarrow +\infty$, which implies that $\mathcal{P}(\mathbf{p}_1) \in \Theta(1)$.

We will show that when $b = 1$, the $\mathcal{P}(\mathbf{p}_1)$ scales as $\Theta(1/\log N_b)$ and $\Theta(1/\log(N_b + N_a))$ for the noncooperative case and cooperative case, respectively. Using a similar argument, we can easily show that for $0 < b < 1$ the SPEB scales as $\Theta(1/N_b^{b-1})$ and $\Theta(1/(N_b + N_a)^{b-1})$ for the noncooperative case and cooperative case, respectively.

Noncooperative Case ($b = 1$): We introduce a random variable $Y_{N_b} = \sum_{j \in \mathcal{N}_b} \lambda_{1,j}/\log(N_b)$. From (61) and (62), we have

$$\lim_{N_b \rightarrow \infty} \mathbb{E}\{Y_{N_b}\} = C$$

¹⁹It will be shown that the overall outage is dominated by the spatial topology for a large number of nodes, and thus we can ignore the outage due to fading.

for some constant C , and

$$\begin{aligned} & \lim_{N_b \rightarrow \infty} \mathbb{E}\{|Y_{N_b} - C|^2\} \\ &= \lim_{N_b \rightarrow \infty} \text{Var}\{Y_{N_b}\} + \lim_{N_b \rightarrow \infty} |\mathbb{E}\{Y_{N_b}\} - C|^2 \\ &+ \lim_{N_b \rightarrow \infty} 2(\mathbb{E}\{Y_{N_b}\} - C) \cdot \mathbb{E}\{Y_{N_b} - \mathbb{E}\{Y_{N_b}\}\} \\ &= 0. \end{aligned}$$

This implies that $\sum_{j \in \mathcal{N}_b} \lambda_{1,j}$ scales as $\Theta(\log N_b)$ with probability approaching one, and hence $\text{tr}\{\mathbf{J}_e(\mathbf{p}_1)\} \in \Theta(\log N_b)$. Using a similar analysis as in Appendix VII-A, we can show that $\mathcal{P}(\mathbf{p}_1) \in \Omega(1/\log N_b)$.

For the upper bound, using the same argument as in Lemma 1, we can show that with probability approaching one, there are $N_b/8$ anchors with angle $\phi_k \in [0, \pi/6]$ and $N_b/8$ anchors with angle $\phi_k \in [\pi/3, \pi/2]$ to the agent. We denote these two disjoint sets of anchors by \mathcal{N}_1 and \mathcal{N}_2 , and define

$$\tilde{\mathbf{J}}_e(\mathbf{p}_1) \triangleq \sum_{j \in \mathcal{N}_1 \cup \mathcal{N}_2} \lambda_{1,j} \mathbf{J}_r(\phi_{1,j})$$

and

$$\tilde{\mathbf{J}}_e^*(\mathbf{p}_1) \triangleq \left(\sum_{j \in \mathcal{N}_1} \lambda_{1,j} \right) \mathbf{J}_r(\pi/6) + \left(\sum_{j \in \mathcal{N}_2} \lambda_{1,j} \right) \mathbf{J}_r(\pi/3).$$

Then, we have

$$\begin{aligned} \text{tr}\{[\mathbf{J}_e(\mathbf{p}_1)]^{-1}\} &\leq \text{tr}\{[\tilde{\mathbf{J}}_e(\mathbf{p}_1)]^{-1}\} \\ &\leq \text{tr}\{[\tilde{\mathbf{J}}_e^*(\mathbf{p}_1)]^{-1}\} \end{aligned} \quad (63)$$

where the first inequality comes from $\mathcal{N}_1 \cup \mathcal{N}_2 \subseteq \mathcal{N}_b$, and the second inequality is due to the fact that the SPEB increases if we set $\phi_{1,j} = \pi/6$ for $j \in \mathcal{N}_1$ and $\phi_{1,j} = \pi/3$ for $j \in \mathcal{N}_2$.²⁰ Since both $\sum_{j \in \mathcal{N}_1} \lambda_{1,j}$ and $\sum_{j \in \mathcal{N}_2} \lambda_{1,j}$ scale as $\Theta(\log N_b)$, $\mathcal{P}(\mathbf{p}_1) \in O(1/\log N_b)$ with probability approaching one. Therefore, the SPEB in noncooperative extended networks scales as $\Theta(1/\log N_b)$.

We finally check the probability of outage, i.e., $\sum_{j \in \mathcal{N}_b} \lambda_{1,j}$ is not in $\Theta(\log N_b)$. For a fixed large N_b , the distribution of $\sum_{j \in \mathcal{N}_b} \lambda_{1,j}/\sqrt{N_b}$ can be approximated as the normal distribution $N(\log N_b/\sqrt{N_b}, 1/N_b)$, and hence²¹

$$\begin{aligned} & \mathbb{P}\left(\left|\sum_{j \in \mathcal{N}_b} \lambda_{1,j} - \log N_b\right| > \frac{1}{2} \log N_b\right) \\ &= 2Q\left(\frac{1}{2} \log N_b\right) \\ &\cong \frac{1}{\log N_b} \exp\left\{-\frac{1}{8} \log^2 N_b\right\} \end{aligned} \quad (64)$$

where $Q(\cdot)$ is the tail probability function of standard normal distribution. Approximations and bounds for the tail probability

²⁰This can be seen from (56) that every element in the sum of the denominator decreases if letting $\phi_{1,j} = \pi/6$ for $j \in \mathcal{N}_1$ and $\phi_{1,j} = \pi/3$ for $j \in \mathcal{N}_2$.

²¹The notation \cong denotes ‘‘on the order of.’’

function can be found in [51]–[53]. Moreover, when $0 < b < 1$, a similar argument leads to

$$\begin{aligned} \mathbb{P} \left(\left| \sum_{k \in \mathcal{N}_b} \lambda_k - N_b^{1-b} \right| > \frac{1}{2} N_b^{1-b} \right) \\ = 2Q \left(\frac{1}{2} N_b^{1-b} \right) \\ \cong \frac{1}{N_b^{1-b}} \exp \left\{ -\frac{1}{8} N_b^{2-2b} \right\}. \end{aligned} \quad (65)$$

Cooperative Case ($b = 1$): The cooperative case can be proved similar to the above noncooperative case in conjunction with the cooperative case of Theorem 5. It turns out that the SPEB can be shown to scale as $\Omega(1/\log(N_b + N_a))$ when all other agents are considered to be anchors. We can also show that, with probability approaching one, the SPEB scales as $O(1/\log(N_b + N_a))$, using the lower approximation of the EFIM, and an argument similar to (63). \square

REFERENCES

- [1] A. Sayed, A. Tarighat, and N. Khajehnouri, "Network-based wireless location: Challenges faced in developing techniques for accurate wireless location information," *IEEE Signal Process. Mag.*, vol. 22, no. 4, pp. 24–40, Jul. 2005.
- [2] K. Pahlavan, X. Li, and J. P. Makela, "Indoor geolocation science and technology," *IEEE Commun. Mag.*, vol. 40, no. 2, pp. 112–118, Feb. 2002.
- [3] J. J. Caffery and G. L. Stuber, "Overview of radiolocation in CDMA cellular systems," *IEEE Commun. Mag.*, vol. 36, no. 4, pp. 38–45, Apr. 1998.
- [4] C.-Y. Chong and S. P. Kumar, "Sensor networks: Evolution, opportunities, and challenges," *Proc. IEEE*, vol. 91, no. 8, pp. 1247–1256, Aug. 2003.
- [5] N. Patwari, J. N. Ash, S. Kyperountas, A. O. Hero, III, R. L. Moses, and N. S. Correal, "Locating the nodes: Cooperative localization in wireless sensor networks," *IEEE Signal Process. Mag.*, vol. 22, no. 4, pp. 54–69, Jul. 2005.
- [6] H. Wymeersch, J. Lien, and M. Z. Win, "Cooperative localization in wireless networks," *Proc. IEEE*, vol. 97, no. 2, pp. 427–450, Feb. 2009.
- [7] S. Gezici, Z. Tian, G. B. Giannakis, H. Kobayashi, A. F. Molisch, H. V. Poor, and Z. Sahinoglu, "Localization via ultra-wideband radios: A look at positioning aspects for future sensor networks," *IEEE Signal Process. Mag.*, vol. 22, no. 4, pp. 70–84, Jul. 2005.
- [8] D. B. Jourdan, D. Dardari, and M. Z. Win, "Position error bound for UWB localization in dense cluttered environments," *IEEE Trans. Aerosp. Electron. Syst.*, vol. 44, no. 2, pp. 613–628, Apr. 2008.
- [9] E. Kaplan, Ed., *Understanding GPS: Principles and Applications*. Reading, MA: Artech House, 1996.
- [10] J. J. Spilker, Jr., "GPS signal structure and performance characteristics," *J. Inst. Navigat.*, vol. 25, no. 2, pp. 121–146, Summer 1978.
- [11] J. Zagami, S. Parl, J. Bussgang, and K. Melillo, "Providing universal location services using a wireless E911 location network," *IEEE Commun. Mag.*, vol. 36, no. 4, pp. 66–71, Apr. 1998.
- [12] J. Hightower, A. LaMarca, and I. Smith, "Practical lessons from place lab," *IEEE Pervasive Comput.*, vol. 5, no. 3, pp. 32–39, Jul.–Sep. 2006.
- [13] M. Z. Win and R. A. Scholtz, "Ultra-wide bandwidth time-hopping spread-spectrum impulse radio for wireless multiple-access communications," *IEEE Trans. Commun.*, vol. 48, no. 4, pp. 679–691, Apr. 2000.
- [14] D. Cassioli, M. Z. Win, and A. F. Molisch, "The ultra-wide bandwidth indoor channel: From statistical model to simulations," *IEEE J. Sel. Areas Commun.*, vol. 20, no. 6, pp. 1247–1257, Aug. 2002.
- [15] J.-Y. Lee and R. A. Scholtz, "Ranging in a dense multipath environment using an UWB radio link," *IEEE J. Sel. Areas Commun.*, vol. 20, no. 9, pp. 1677–1683, Dec. 2002.
- [16] D. Dardari, A. Conti, U. J. Ferner, A. Giorgetti, and M. Z. Win, "Ranging with ultrawide bandwidth signals in multipath environments," *Proc. IEEE*, vol. 97, no. 2, pp. 404–426, Feb. 2009.
- [17] Z. Zhang, C. L. Law, and Y. L. Guan, "BA-POC-based ranging method with multipath mitigation," *IEEE Antennas Wireless Propag. Lett.*, vol. 4, pp. 492–495, 2005.
- [18] Z. N. Low, J. H. Cheong, C. L. Law, W. T. Ng, and Y. J. Lee, "Pulse detection algorithm for line-of-sight (LOS) UWB ranging applications," *IEEE Antennas Wireless Propag. Lett.*, vol. 4, pp. 63–67, 2005.
- [19] D. Cassioli, M. Z. Win, F. Vatalaro, and A. F. Molisch, "Low-complexity rake receivers in ultra-wideband channels," *IEEE Trans. Wireless Commun.*, vol. 6, no. 4, pp. 1265–1275, Apr. 2007.
- [20] T. Q. S. Quek, M. Z. Win, and D. Dardari, "Unified analysis of UWB transmitted-reference schemes in the presence of narrowband interference," *IEEE Trans. Wireless Commun.*, vol. 6, no. 6, pp. 2126–2139, Jun. 2007.
- [21] L. Yang and G. B. Giannakis, "Ultra-wideband communications: An idea whose time has come," *IEEE Signal Process. Mag.*, vol. 21, no. 6, pp. 26–54, Nov. 2004.
- [22] A. Ridolfi and M. Z. Win, "Ultrawide bandwidth signals as shot-noise: A unifying approach," *IEEE J. Sel. Areas Commun.*, vol. 24, no. 4, pp. 899–905, Apr. 2006.
- [23] W. Suwansantisuk and M. Z. Win, "Multipath aided rapid acquisition: Optimal search strategies," *IEEE Trans. Inf. Theory*, vol. 53, no. 1, pp. 174–193, Jan. 2007.
- [24] A. F. Molisch, "Ultrawideband propagation channels—theory, measurements, and modeling," *IEEE Trans. Veh. Technol.*, vol. 54, no. 5, pp. 1528–1545, Sep. 2005.
- [25] A. F. Molisch, "Ultra-wide-band propagation channels," *Proc. IEEE*, vol. 97, no. 2, pp. 353–371, Feb. 2009.
- [26] C. Savarese, J. M. Rabaey, and J. Beutel, "Locating in distributed ad-hoc wireless sensor networks," in *Proc. IEEE Int. Conf. Acoust. Speech Signal Process.*, May 2001, vol. 4, no. 7–11, pp. 2037–2040.
- [27] C. Chang and A. Sahai, "Estimation bounds for localization," in *Proc. IEEE Conf. Sensor Ad Hoc Commun. Netw.*, Santa Clara, CA, Oct. 2004, pp. 415–424.
- [28] E. G. Larsson, "Cramér-Rao bound analysis of distributed positioning in sensor networks," *IEEE Signal Process. Lett.*, vol. 11, no. 3, pp. 334–337, Mar. 2004.
- [29] Y. Shen and M. Z. Win, "Fundamental limits of wideband localization—Part I: A general framework," *IEEE Trans. Inf. Theory*, vol. 56, no. 10, Oct. 2010, DOI: 10.1109/TIT.2010.2060110.
- [30] Y. Shen and M. Z. Win, "Localization accuracy using wideband antenna arrays," *IEEE Trans. Commun.*, vol. 58, no. 1, pp. 270–280, Jan. 2010.
- [31] Y. Qi, H. Kobayashi, and H. Suda, "Analysis of wireless geolocation in a non-line-of-sight environment," *IEEE Trans. Wireless Commun.*, vol. 5, no. 3, pp. 672–681, Mar. 2006.
- [32] L. Mailaender, "On the geolocation bounds for round-trip time-of-arrival and all non-line-of-sight channels," *EURASIP J. Adv. Signal Process.*, vol. 2008, p. 10, 2008.
- [33] J. Caffery, Ed., *Wireless Location in CDMA Cellular Radio Systems*. Boston, MA: Kluwer, 2000.
- [34] T. Rappaport, J. Reed, and B. Woerner, "Position location using wireless communications on highways of the future," *IEEE Commun. Mag.*, vol. 34, no. 10, pp. 33–41, Oct. 1996.
- [35] D. Niculescu and B. Nath, "Ad hoc positioning system (APS) using AOA," in *Proc. IEEE Conf. Comput. Commun.*, Mar./Apr. 2003, vol. 3, pp. 1734–1743.
- [36] N. Patwari and A. O. Hero, III, "Using proximity and quantized RSS for sensor localization in wireless networks," in *Proc. IEEE/ACM 2nd Workshop Wireless Sensor Nets. Appl.*, 2003, pp. 20–29.
- [37] T. Pavani, G. Costa, M. Mazzotti, A. Conti, and D. Dardari, "Experimental results on indoor localization techniques through wireless sensors network," in *Proc. IEEE Semiannu. Veh. Technol. Conf.*, May 2006, vol. 2, pp. 663–667.
- [38] M. Hamilton and P. Schultheiss, "Passive ranging in multipath dominant environments. I. Known multipath parameters," *IEEE Trans. Signal Process.*, vol. 40, no. 1, pp. 1–12, Jan. 1992.
- [39] J. Lee and S. Yoo, "Large error performance of UWB ranging," in *Proc. IEEE Int. Conf. Ultra-Wideband*, Zurich, Switzerland, 2005, pp. 308–313.
- [40] A. F. Molisch, *Wireless Communications*, 1st ed. Piscataway, NJ: IEEE Press/Wiley, 2005.
- [41] A. A. Saleh and R. A. Valenzuela, "A statistical model for indoor multipath propagation," *IEEE J. Sel. Areas Commun.*, vol. 5, no. 2, pp. 128–137, Feb. 1987.
- [42] H. L. Van Trees, *Detection, Estimation and Modulation Theory*. New York: Wiley, 1968, vol. 1.
- [43] H. V. Poor, *An Introduction to Signal Detection and Estimation*, 2nd ed. New York: Springer-Verlag, 1994.
- [44] I. Reuven and H. Messer, "A Barankin-type lower bound on the estimation error of a hybrid parameter vector," *IEEE Trans. Inf. Theory*, vol. 43, no. 3, pp. 1084–1093, May 1997.
- [45] R. A. Horn and C. R. Johnson, *Matrix Analysis*, 1st ed. Cambridge, U.K.: Cambridge Univ. Press, 1985.

- [46] C. Botteron, A. Host-Madsen, and M. Fattouche, "Cramer-Rao bounds for the estimation of multipath parameters and mobiles' positions in asynchronous DS-CDMA systems," *IEEE Trans. Signal Process.*, vol. 52, no. 4, pp. 862–875, Apr. 2004.
- [47] P. Gupta and P. R. Kumar, "The capacity of wireless networks," *IEEE Trans. Inf. Theory*, vol. 46, no. 2, pp. 388–404, Mar. 2000.
- [48] A. Ozgur, O. Leveque, and D. N. C. Tse, "Hierarchical cooperation achieves optimal capacity scaling in ad hoc networks," *IEEE Trans. Inf. Theory*, vol. 53, no. 10, pp. 3549–3572, Oct. 2007.
- [49] A. Goldsmith, *Wireless Communications*. Cambridge, U.K.: Cambridge Univ. Press, 2005.
- [50] B. C. Arnold, N. Balakrishnan, and H. N. Nagaraja, *A First Course in Order Statistics*. New York: Wiley-Interscience, 1992.
- [51] A. Conti, M. Z. Win, and M. Chiani, "On the inverse symbol error probability for diversity reception," *IEEE Trans. Commun.*, vol. 51, no. 5, pp. 753–756, May 2003.
- [52] G. Grimmett and D. Stirzaker, *Probability and Random Processes*, 3rd ed. Oxford, U.K.: Oxford Univ. Press, 2001.
- [53] M. Chiani, D. Dardari, and M. K. Simon, "New exponential bounds and approximations for the computation of error probability in fading channels," *IEEE Trans. Wireless Commun.*, vol. 2, no. 4, pp. 840–845, Jul. 2003.

Yuan Shen (S'05) received the B.S. degree in electrical engineering (with highest honor) from Tsinghua University, Beijing, China, in 2005 and the S.M. degree in electrical engineering from the Massachusetts Institute of Technology (MIT), Cambridge, in 2008, where he is currently working towards the Ph.D. degree at the Wireless Communications and Network Science Laboratory.

He was with the Hewlett-Packard Labs, in winter 2009, the Corporate R&D of Qualcomm Inc., in summer 2008, and the Intelligent Transportation Information System Laboratory, Tsinghua University, from 2003 to 2005. His research interests include communication theory, information theory, and statistical signal processing. His current research focuses on wideband localization, cooperative networks, and ultrawide bandwidth communications.

Mr. Shen served as a member of the Technical Program Committee (TPC) for the IEEE Global Communications Conference (GLOBECOM) in 2010, the IEEE International Conference on Communications (ICC) in 2010, and the IEEE Wireless Communications & Networking Conference (WCNC) in 2009 and 2010. He received the Marconi Young Scholar Award from the Marconi Society in 2010, the Ernst A. Guillemin Thesis Award (first place) for the best S.M. thesis from the Department of Electrical Engineering and Computer Science at MIT in 2008, the Roberto Padovani Scholarship from Qualcomm Inc. in 2008, the Best Paper Award from the IEEE WCNC in 2007, and the Walter A. Rosenblith Presidential Fellowship from MIT in 2005.

Henk Wymeersch (S'98–M'05) received the Ph.D. degree in electrical engineering/applied sciences from Ghent University, Ghent, Belgium, in 2005.

Currently, he is an Assistant Professor with the Department of Signals and Systems, Chalmers University, Gothenburg, Sweden. Prior to joining Chalmers, he was a Postdoctoral Associate with the Laboratory for Information and Decision Systems (LIDS), Massachusetts Institute of Technology (MIT), Cambridge. He is the author of the book *Iterative Receiver Design* (Cambridge, U.K.: Cambridge Univ. Press, 2007). His research interests include algorithm design for wireless transmission, statistical inference, and iterative processing.

Moe Z. Win (S'85–M'87–SM'97–F'04) received both the Ph.D. degree in electrical engineering and the M.S. degree in applied mathematics as a Presidential Fellow at the University of Southern California (USC) in 1998. He received the M.S. degree in electrical engineering from USC in 1989, and the B.S. degree (*magna cum laude*) in electrical engineering from Texas A&M University in 1987.

He is an Associate Professor at the Massachusetts Institute of Technology (MIT). Prior to joining MIT, he was at AT&T Research Laboratories for five years and at the Jet Propulsion Laboratory for seven years. His research encompasses developing fundamental theories, designing algorithms, and conducting experimentation for a broad range of real-world problems. His current research topics include location-aware networks, intrinsically secure wireless networks, aggregate interference in heterogeneous networks, ultrawide bandwidth systems, multiple antenna systems, time-varying channels, optical transmission systems, and space communications systems.

He is an IEEE Distinguished Lecturer and elected Fellow of the IEEE, cited for "contributions to wideband wireless transmission." He was honored with the IEEE Eric E. Sumner Award (2006), an IEEE Technical Field Award for "pioneering contributions to ultra-wide band communications science and technology." Together with students and colleagues, his papers have received several awards including the IEEE Communications Society's Guglielmo Marconi Best Paper Award (2008) and the IEEE Antennas and Propagation Society's Sergei A. Schelkunoff Transactions Prize Paper Award (2003). His other recognitions include the Laurea Honoris Causa from the University of Ferrara, Italy (2008), the Technical Recognition Award of the IEEE ComSoc Radio Communications Committee (2008), Wireless Educator of the Year Award (2007), the Fulbright Foundation Senior Scholar Lecturing and Research Fellowship (2004), the U.S. Presidential Early Career Award for Scientists and Engineers (2004), the AIAA Young Aerospace Engineer of the Year (2004), and the Office of Naval Research Young Investigator Award (2003).

Prof. Win has been actively involved in organizing and chairing a number of international conferences. He served as the Technical Program Chair for the IEEE Wireless Communications and Networking Conference in 2009, the IEEE Conference on Ultra Wideband in 2006, the IEEE Communication Theory Symposia of ICC-2004 and Globecom-2000, and the IEEE Conference on Ultra Wideband Systems and Technologies in 2002; Technical Program Vice-Chair for the IEEE International Conference on Communications in 2002; and the Tutorial Chair for ICC-2009 and the IEEE Semiannual International Vehicular Technology Conference in Fall 2001. He was the chair (2004–2006) and secretary (2002–2004) for the Radio Communications Committee of the IEEE Communications Society. He is currently an Editor for the IEEE TRANSACTIONS ON WIRELESS COMMUNICATIONS. He served as Area Editor for Modulation and Signal Design (2003–2006), Editor for Wideband Wireless and Diversity (2003–2006), and Editor for Equalization and Diversity (1998–2003), all for the IEEE TRANSACTIONS ON COMMUNICATIONS. He was Guest-Editor for the PROCEEDINGS OF THE IEEE (Special Issue on UWB Technology and Emerging Applications) in 2009 and the IEEE JOURNAL ON SELECTED AREAS IN COMMUNICATIONS (Special Issue on Ultra-Wideband Radio in Multiaccess Wireless Communications) in 2002.